Title
Engineering Metabolism for Cellulosic Biofuel Production and Carbon Conservation

Author
Lin, Po-Heng

Publication Date
2016

Peer reviewed|Thesis/dissertation

UNIVERSITY OF CALIFORNIA

Los Angeles

Engineering Metabolism for Cellulosic Biofuel Production and Carbon Conservation

A dissertation submitted in partial satisfaction of the

requirements for the degree Doctor of Philosophy

in Chemical Engineering

by

Po-Heng Lin

2016

ABSTRACT OF THE DISSERTATION

Engineering Metabolism for Cellulosic Biofuel Production and Carbon Conservation

by

Po-Heng Lin

Doctor of Philosophy in Chemical Engineering

University of California, Los Angeles, 2016

Professor James C. Liao, Chair

Biomass recalcitrance—resistance to degradation—currently limits the use of lignocellulose for biofuel production. Consolidated bioprocessing (CBP), in which cellulose hydrolysis and fermentation occur simultaneously in one pot without added cellulases, is a potential approach to improve lignocellulose utilization. Owing to its high cellulose deconstruction rate, *Clostridium thermocellum* is a promising thermophilic CBP host, which grows at 50-60^{o}C. The elevated temperature also promotes cellulose degradation, reduces contamination, and minimizes cooling cost. The method for genetic manipulation of *C. thermocellum* has not been fully developed and remains time-consuming. To expedite the progress, our first Aim was to establish the desired metabolic pathways in a related, more tractable organism, *Geobacillus thermoglucosidasius*. This Aim was accomplished by establishing a thermophilic isobutanol

pathway and demonstrating the feasibility of producing isobutanol from glucose and cellobiose at an elevated temperature using *G. thermoglucosidasius*.

Our second Aim was then to directly produce isobutanol from cellulose using the CBP organism, *C. thermocellum*. To overcome the pathway toxicity and to accelerate the promoter selection process, we cloned the essential isobutanol pathway genes under different promoters to create various plasmid constructs for isobutanol production in *C. thermocellum*. We developed a Cre-lox based gene deletion protocol to facilitate chromosomal editing. We also characterized the electron flow in the isobutanol pathway and related pathways. Specifically, we identified the Por enzyme which converts pyruvate to acetyl-CoA for ethanol and acetate production. 9.7 g/L of isobutanol was produced by the engineered *C. thermocellum* strain directly from cellulose within 100 h.

Intrinsic carbon lost from the Embden-Meyerhof-Parnas (EMP, known as glycolysis) pathway is another limitation for biofuel and biochemical production. Through glycolysis, sugar is converted to pyruvate, which is then decarboxylated to acetyl-CoA with CO_2 formation. The carbon lost from glycolysis limits the theoretical carbon atom yield to 2/3. Recently, a synthetic non-oxidative glycolysis (NOG) pathway has been engineered in an *Escherichia coli* strain to conserve all carbon from xylose (Bogorad et al., 2013). However, the engineered strain still depended on EMP pathway for xylose catabolism.

Our third Aim was to construct an *E. coli* strain that completely relies on NOG for sugar catabolism. Here we designed a rational/evolutionary strategy to allow organisms to grow based on NOG without EMP. This new type of *E. coli* strain could convert C6 or C5 sugar to C2 compound without carbon lost. At first, the EMP pathway and other potential bypass pathways

were deleted in *E. coli*. Then the cells were evolved for growth on glucose with the supplementation of acetate. Then the NOG pathway was installed and the strain was evolved first in xylose and then in glucose for growth. Finally, the strain was used for producing more than 2 molecules of C2 compound (acetate) from one molecule of glucose.

The dissertation of Po-Heng Lin is approved.

Yi Tang

Yvonne Chen

Sriram Kosuri

James C. Liao, Committee Chair

University of California, Los Angeles

2016

Table of Contents

List of Figures

List of Table

Acknowledgements

I would like to first and foremost thank the mentorship given by my advisor, Professor James C. Liao. He helped me realize my potential and exert my talents. He also shared me a lot about his philosophy in decision making and guided me to work strategically. Without his helps and suggestions, we could not achieve or even ahead to our project milestone every year.

I would thank the generous financial support from National Science Foundation (MCB-1139318), DOE BioEngery Science Center (BESC) and DOE Grant No. DE-SC0012384. This work is based upon research preformed in renovated collaborator by National Science Foundation under Grant No. 0963183, which is an award funded under the American Recovery and Reinvestment Act of 2009 (ARRA).

I have been very fortunate to have been surrounded by an amazing group of postdocs, graduate students, undergraduates and technicians. Tony knows everything in Liao lab. Luo has the best English writing skill among all of the non-native speaker I know. Jeni is one of my best friend in the U.S. She helped me improve my English a lot. Igor is another my best friend. Thanks to him for teaching me pathway design 101. Charile is my best workout partner. Thanks Candy and Xiaoqian for letting me join the "small" club. Shanshan is such a neat and nice friend and roommate. Matthew worked so hard and helped me achieve twice for BESC milestone. Sandy is a very smart Taiwanese girl, good luck to her in Wisconsin. Sawako always has full energy in the lab. Sharon is quite, but I know she is super smart. Annabel is an expert of cloning, she made 120 constructs in a month. Amy is not only a good lab tech, but a great basketball player. Maria shows her strong motivation since the day she came for interview. Joanna, Hao, Kushal, Justin and Fiona

are new, but they all very helpful. I cannot finish so much without so many people's help. Thanks for the teamwork.

I lastly like to thank my family. My parents invested their whole lives in me. They encouraged me to pursue my degree in the U.S., which is one of my best decision in my life so far. I also want to thank my brother, sister and my best friend, Tammy Hsu, for their love and mental support.

Po-Heng Lin

EDUCATION

Ph.D. candidate, Chemical Engineering, UCLA
B.S., Chemical Engineering, National Taiwan University, June 2008

FIELDS OF INTEREST

Cellulosic Biofuel and Biochemical Production, Synthetic Pathway Design,
Metabolic Engineering, Genetic Manipulation, Thermophiles

RESEARCH EXPERIENCE

Doctoral Student, *2010- 2016*
Dr. James Liao, UCLA, Department of Chemical Engineering
- Developed a consolidated bioprocessing organism *Clostridium thermocellum* to directly produce C4 alcohol from cellulose at elevated temperatures
- Utilized a Cre-lox gene manipulation strategy to improve isobutanol production yield and titer by *Clostridium thermocellum*
- Rewrote *Escherichia coli* central metabolic pathway with a synthetic pathway independent to glycolysis for efficient sugar metabolism

Research Assistant, *2009-2010*
Dr. Da-Ming Wang, National Taiwan University, Department of Chemical Engineering
- Applied mixed-matrix scaffolds to remove heavy metal ions from waste water

Undergraduate Volunteer, *2007-2008*
Dr. Da-Ming Wang, National Taiwan University, Department of Chemical Engineering
- Recovered Indium by supported liquid membrane with strip dispersion

TEACHING EXPERIENCE

Research Team Leader, ***2011-2015***
Dr. James Liao, UCLA, Department of Chemical Engineering
- Manage team of postdoctoral researchers, lab technicians and undergraduate students
- Plan and delegate member duties and responsibilities
- Mentor and tutor undergraduate students

Teaching Assistant, ***2012-2013***
Thermodynamics I, UCLA, Department of Chemical Engineering
- Teach and facilitate discussions for section of 100 students
- Evaluate student progress

PUBLICATIONS

Lemuel M.J. Soh, Wai Shun Mak, **Paul P. Lin**, Luo Mi, Frederic Y.-H. Chen, Robert Damoiseaux, Justin B. Siegel and James C. Liao. Engineering a thermostable keto acid decarboxylase using directed evolution and computationally directed protein design. ACS synthetic biology. (2016, revision)

Wei Xiong, **Paul P. Lin**, Lauren Magnusson, Lisa Warner, James C. Liao, Pin-Ching Maness and Katherine J. Chou. CO2-fixing one-carbon metabolism in a cellulose-degrading bacterium *Clostridium thermocellum*. PNAS (2016)

Paul P. Lin, Kersten S. Rabe, Jennifer L. Takasumi, Marvin Kadisch, Frances H. Arnold and James C. Liao. Isobutanol production at elevated temperatures in thermophilic *Geobacillus thermoglucosidasius*. Metabolic Engineering. (2014)

Paul P. Lin, Luo Mi, Amy H. Morioka, Kouki M. Yoshino, Sawako Konishi, Sharon C. Xu, Beth A. Papanek, Lauren A. Riley, Adam M. Guss and James C. Liao. Consolidated bioprocessing of cellulose to isobutanol using *Clostridium thermocellum*. Metabolic Engineering. (2015)

FELLOWSHIPS AND AWARDS

2014	Martin Keller Award for Excellence, 2014 BioEnergy Science Center Retreat
2012-2013	Bowei Lee Fellowship, University of California, Los Angeles and LCY Chemical Corporation
2007-2008	Presidential Award of National Taiwan University
2006-2007	Presidential Award of National Taiwan University

1. Introduction

The use of lignocellulose for biofuel production is an attractive solution to the energy problem for multiple reasons. The raw material is abundant enough to provide the quantity needed to make a significant impact. It improves net carbon and energy balances in fuel production, and avoids the food versus fuel dilemma. However, biomass recalcitrance—resistance to degradation—currently limits the use of lignocellulose. Consolidated bioprocessing (CBP) is a potential solution in which cellulose hydrolysis and fermentation occur simultaneously without added cellulases. *Clostridium thermocellum* is a promising thermophilic CBP host because of its high cellulose deconstruction rate. Also, longer-chain alcohols, such as isobutanol, offer advantages as a gasoline substitute or drop-in fuel (Atsumi et al., 2008). In this thesis, we first sought to produce isobutanol in elevated temperatures (50-60 ^{o}C) from glucose and cellobiose using *Geobacillus thermoglucosidasius*. We then implemented the strategy to a thermophilic CBP organism, *C. thermocellum* and directly produced isobutanol from cellulose.

Another problem in biofuel production is the intrinsic carbon loss though the Embden-Meyerhof-Parnas (EMP) pathway, commonly known as glycolysis, which is a fundamental metabolic pathway presents in almost all organisms to partially oxidize glucose to form pyruvate. Pyruvate is then oxidatively decarboxylated to acetyl-CoA for various biosynthetic purposes. The decarboxylation of pyruvate loses a carbon equivalent, and limits the theoretical carbon yield to only two moles of two-carbon (C2) metabolites per mole of hexose. Bogorad et al. (2013) demonstrated a cyclic pathway, termed non-oxidative glycolysis (NOG), which enables the cell to conserve all carbon and produce biofuel with additional reducing power. The authors constructed an *Escherichia coli* strain to produced 2.2 acetate per xylose consumed, approaching the maximal

theoretical yield. However, the strain still uses the EMP pathway under most conditions. To further explore the utility of NOG for carbon conservation, we sought to construct a microorganism that completely relies on NOG for sugar catabolism.

The overall goal of my Ph.D thesis is to produce isobutanol directly from cellulose using the consolidated bioprocessing (CBP) organism, *Clostridium thermocellum* and to engineer new *E. coli* strain which rely solely on NOG for sugar catabolism.

Chapter 2 discusses thermophilic isobutanol production in *Geobacillus thermoglucosidasius* (Metabolic Engineering 2014). *Geobacillus thermoglucosidasius* is a useful candidate for this initial thermophilic isobutanol production because it is a facultative anaerobic thermophile, which is capable of growth between 50 to 70 ^{o}C. In addition, a transformation protocol has been developed for this organism, enabling metabolic manipulation (Cripps et al., 2005). Thus, we chose *G. thermoglucosidasius* as a platform for testing the thermostability of enzymes involved in isobutanol biosynthesis and the feasibility of isobutanol production at high temperatures.

Chapter 3 describes consolidated bioprocessing of cellulose to isobutanol using *Clostridium thermocellum* (Metabolic Engineering 2015). Although the transformation protocol in *C. thermocellum* has been established (Argyros et al., 2011), pathway overexpression using plasmid system is still time consuming. In addition, general toxicity of pathway enzymes further limits the efficiency of genetic manipulation. To quickly and efficiently select high titer isobutanol production constructs, we proposed a stream-lined method including parallel cloning, transformation and small scale fermentation. A Cre-lox based gene deletion protocol system was

proposed to facilitate chromosomal editing. We also determined the genes responsible for ketoisovalerate decarboxylation.

Chapter 4 describes the current progress on consolidated bioprocessing of cellulose to isobutanol using *Clostridium thermocellum*. The limited step, Ahas, of isobutanol production in *C. thermocellum* was identified via an enzyme assay. The electron flow in isobutanol production and the related pathway were also characterized.

Chapter 5 discusses engineering an *Escherichia coli* strain which relies solely on non-oxidative glycolysis (NOG) for sugar catabolism. First, the EMP pathway was blocked by gene deletion. This strain was evolved to test if alternative or cryptic glycolytic pathways exist. These alternative pathways were knocked out until no EMP suppressors were detected. This glycolysis-deficient mutant was evolved to grow on glucose and acetate medium to re-route the metabolic flux from acetyl-CoA back to pyruvate using native pathways. We then expressed the NOG pathway in this evolved strain and evolved again to wean off acetate in the presence xylose, then eventually glucose. With NOG and a glucose transport pathway further overexpressed, this strain could convert glucose to acetate at more than the theoretical yield, indicating that our NOG strain relied solely on NOG for glucose catabolism. However, the strain was not able to grow in glucose minimal medium after evolution.

2. Isobutanol production at elevated temperatures in thermophilic *Geobacillus thermoglucosidasius*

Disclaimer: This chapter was originally published with the same title in *Metabolic Engineering* **24** (2014) 1-8.

2.1 Abstract

The potential advantages of biological production of chemicals or fuels from biomass at high temperatures include reduced enzyme loading for cellulose degradation, decreased chance of contamination, and lower product separation cost. In general, high temperature production of compounds that are not native to the thermophilic hosts is limited by enzyme stability and the lack of suitable expression systems. Further complications can arise when the pathway includes a volatile intermediate. Here we report the engineering of *Geobacillus thermoglucosidasius* to produce isobutanol at 50 °C. We prospected various enzymes in the isobutanol synthesis pathway and characterized their thermostabilities. We also constructed an expression system based on the lactate dehydrogenase promoter from *Geobacillus thermodenitrificans*. With the best enzyme combination and the expression system, 3.3 g/l of isobutanol was produced from glucose and 0.6 g/l of isobutanol from cellobiose in *G. thermoglucosidasius* within 48 h at 50 °C. This is the first demonstration of isobutanol production in recombinant bacteria at an elevated temperature.

2.2 Introduction

Microbial production of fuels and chemicals from plant biomass at elevated temperatures is desirable for multiple reasons. Since most cellulases have optimum temperatures of 50 to 55 °C (Liu and Xia, 2006, Lee et al., 2008, Ko et al., 2010 and Balsan et al., 2012), fermentation in that temperature range can allow for simultaneous cellulose hydrolysis and fermentation and can

reduce the loading of hydrolytic enzymes (Patel et al., 2005,Patel et al., 2006, Sun and Cheng, 2002 and Brodeur et al., 2011). In addition, high temperature fermentation minimizes the chance of contamination and reduces energy consumption for product separation and fermenter cooling (Lynd, 1989). However, high temperature fuel and chemical production faces several challenges, including limited enzyme stability and availability of suitable expression systems, volatility of pathway intermediates, and increased product toxicity. To date, thermophilic ethanol production has been reported using *Geobacillus thermoglucosidasius* (Cripps et al., 2009), *Thermoanaerobacterium saccharolyticum* (Shaw et al., 2008), and *Clostridium thermocellum* (Argyros et al., 2011). In addition, *n*-butanol production by *T. saccharolyticum* has recently been demonstrated with a final titer of about 1.05 g/l from 10 g/l xylose (Bhandiwad et al., 2013 and Bhandiwad et al.,). Moreover, 3-hydroxypropionic acid has been produced from hydrogen gas and carbon dioxide using an engineered hyperthermophile, *Pyrococcus furiosus* (Keller et al., 2013). Here, we report the engineering of a thermophile, *G. thermoglucosidasius*, for production of isobutanol.

G. thermoglucosidasius is a facultative anaerobic, rod-shaped, Gram-positive and endospore-forming bacterium (Nazina et al., 2001). Species in the *Geobacillus* genus are capable of growth between 40 °C and 70 °C and can ferment hexose and pentose sugars to generate lactate, formate, acetate and ethanol as products. However, methods for genetic modification of most *Geobacillus* spp. are underdeveloped. An exception is *G. thermoglucosidasius*, for which transformation procedures enabling metabolic manipulation have been established (Cripps et al., 2009). *G. thermoglucosidasius* was therefore chosen as a platform for investigating isobutanol production at elevated temperatures.

High-flux ethanol and isobutanol biosynthesis (Atsumi et al., 2008) both utilize a keto acid decarboxylase (KDC) to decarboxylate a keto acid (pyruvate or 2-ketoisovalerate) to the corresponding aldehyde (acetaldehyde or isobutyraldehyde), which is then reduced to the alcohol by an alcohol dehydrogenase (ADH). The acetaldehyde intermediate in ethanol production has a boiling point of 20 °C and is highly volatile at the temperatures favored by thermophilic organisms. This may explain why pyruvate decarboxylase (PDC) has been reported only in mesophiles (Ingram et al., 1999). However, one exception is pyruvate-ferredoxin oxidoreductase from the hyperthermophile *P. furiosus,* which can produce acetaldehyde from pyruvate at 90 °C (Ma et al., 1997). If the aldehyde is not reduced to the alcohol fast enough, it may escape from the cell or exert significant toxic effects (Atsumi et al., 2009). Perhaps because of this, thermophilic ethanol production has only been demonstrated by a coenzyme A (CoA)-dependent pathway, using a bifunctional aldehyde/alcohol dehydrogenase, which minimizes the loss and toxicity of the volatile aldehyde by channeling it directly to alcohol form Cripps et al. (2009)engineered two strains of *G. thermoglucosidasius* by upregulating pyruvate dehydrogenase, which increased the carbon flux through acetyl-CoA and then to ethanol, the major fermentative product. Similarly, Shaw et al. (2008) engineered *T. saccharolyticum* to produce ethanol as the only detectable product by utilizing pyruvate-ferredoxin oxidoreductase and a putative bifunctional aldehyde/alcohol dehydrogenase.

Isobutanol biosynthesis (Atsumi et al., 2008) (Fig. 2.1) shares intermediates with the valine biosynthesis pathway, which exists in most microorganisms, including *G. thermoglucosidasius*. In the pathway assembled by Atsumi et al. (2008) in *Escherichia coli*, a non-native acetolactate synthase, AlsS from *Bacillus subtilis*, was overexpressed to replace the native enzyme, as it has

specificity for pyruvate and is not end-product inhibited. In addition, the valine precursor 2-ketoisovalerate was decarboxylated using ketoisovalerate decarboxylase (Kivd) from *Lactococcus lactis*, which has 33% identity to*Zymomonas mobilis* pyruvate decarboxylase. The final step in the pathway is reduction of isobutyraldehyde by an ADH. Since isobutyraldehyde (bp 63 °C) is significantly less volatile than acetaldehyde, we reasoned that thermophilic isobutanol production should be feasible via this CoA-independent pathway using an appropriate KIVD and ADH.

Here, we investigated the thermostabilities and activities of the mesophilic pathway enzymes *B. subtilis* AlsS and *L. lactis* Kivd as well as enzymes we identified as potential thermophilic homologs. We cloned, purified, and assayed native alcohol dehydrogenases from *G. thermoglucosidasius*, identifying both NADH- and NADPH-dependent isobutanol dehydrogenases. Furthermore, we prospected promoters and designed a plasmid overexpression system to express multiple combinations of isobutanol pathway genes. We report the first example of thermophilic isobutanol production with an engineered *G. thermoglucosidasius* strain capable of producing isobutanol from glucose or cellobiose.

2.3 Material and methods

2.3.1 Bacterial strains and plasmids

G. *thermoglucosidasius* DSM 2542^{T} was used as the host for isobutanol production. *E. coli* XL1-Blue was used as the host for plasmid construction, and *E. coli* BL21 (DE3) was used for protein expression and purification. Strains and plasmids used in this study are listed in Table 2.1. Primers used in this study are listed in Table 2.2.

All plasmids were constructed by DNA assembly techniques with a modified ligation-independent cloning (LIC) protocol (Machado et al., 2012). In our modified LIC procedure, both

vector and inserts (target genes) were amplified by PCR using Phusion High-Fidelity DNA polymerase. PCR products were purified by a PCR purification Kit (Zymo Research, Irvine, CA). Then, the vector and insert were mixed (1:1 mol ratio) in 10 μl 1X NEB Buffer 2 (New England Biolabs, Ipswich, MA) containing 1 unit of T4 DNA polymerase. This reaction was incubated at room temperature for 10 min and followed by the transformation procedures of Z-competent cells (Zymo Research). The presence of correctly cloned inserts was determined by colony PCR and DNA sequencing (Laragen, Culver City, CA).

2.3.2 Chemicals and reagents

All chemicals were acquired from Sigma-Aldrich (St. Louis, MO) or Thermo Scientific (Hudson, NH). Phusion High-Fidelity DNA polymerase, T4 polymerase and restriction enzymes were purchased from New England Biolabs.

2.3.3 Media and cultivation

All *E. coli* strains were grown in LB medium containing appropriate antibiotics at 37 °C on a rotary shaker (250 rpm). Antibiotics were used at the following concentrations: ampicillin, 200 μg/ml; kanamycin, 30 μg/ml; chloramphenicol, 20 μg/ml.

All *G. thermoglucosidasius* strains were grown in TGP medium (Cripps et al., 2009) at 50 °C at 250 rpm except for isobutanol production. TGP medium contains the following components: tryptone (17 g), soytone (3 g), glucose (2.5 g), NaCl (5 g), K_2HPO_4 (2.5 g), glycerol (4 ml) and sodium pyruvate (4 g) per liter of deionized water. 15 g of agar was added to 1 l of TGP medium prior to autoclaving for solid media. For *G. thermoglucosidasius* cultures, antibiotics were used at the following concentration: chloramphenicol, 15 μg/ml.

To examine isobutanol production, engineered *G. thermoglucosidasius* DSM 2542^{T} was grown in modified ASYE medium (M9 medium, 0.2 M glucose or 0.1 M cellobiose, 0.5% yeast extract, 2 mM $MgSO_4$, 0.1 mM $CaCl_2$, 1000X dilution of Trace Metal Mix A5 (2.86 g H_3BO_3, 1.81 g $MnCl_2 \cdot 4H_2O$, 0.222 g $ZnSO_4 \cdot 7H_2O$, 0.39 g $Na_2MoO_4 \cdot 2H_2O$, 0.079 g $CuSO_4 \cdot 5H_2O$, 49.4 mg $Co(NO_3)_2 \cdot 6H_2O$ per liter water), 0.01 g/l thiamin, 2 mM citric acid, 100 µM $FeSO_4 \cdot 7H_2O$, 16.85 µM $NiCl_3 \cdot 6H_2O$, 12.5 µM biotin and 0.2 M HEPES buffer). Production of isobutanol was carried out in sealed 50 ml Falcon tubes with 10 ml of modified ASYE medium at pH 7.0, 50 °C with 250 rpm shaking. Cultures were inoculated by a 10% dilution of aerobically grown cultures (in TGP medium) which have an optical density (600 nm) between 1.0 and 1.6.

Stock cultures of *G. thermoglucosidasius* were maintained at −80 °C in 13% (v/v) glycerol.

2.3.4 *G. thermoglucosidasius* transformation

G. thermoglucosidasius transformation was conducted as described (Cripps et al., 2009). Briefly, *G. thermoglucosidasius* DSM 2542^{T} strains were grown in 50 ml of TGP medium at 50 °C and 250 rpm with a 1% inoculation from an overnight culture to exponential phase (OD_{600}, 1.0 to 1.6). The culture was chilled on ice for 10 min, and cells were collected by centrifugation in 50 ml Falcon tubes at 4 °C and 4000 rpm in a Beckman Coulter Allegra X-14 centrifuge for 15 min. The resulting pellets were washed twice with 25 ml of cold Milli-*Q* water and once with 25 ml of cold electroporation buffer (0.5 M mannitol, 0.5 M sorbitol and 10% (v/v) glycerol), with centrifugation at 4 °C and 4000 rpm for 10 min. After the supernatant was decanted, the pellets were resuspended in 2 ml of electroporation buffer, aliquoted and stored at −80 °C for future use.

For each transformation, 60 µl of the competent cells were mixed with about 200 ng of DNA. In 1-mm-gap electroporation cuvettes (Molecular BioProducts, San Diego, CA), the cells

and plasmid DNA were electroporated (2.5 kV, 25 μF, and 48 Ω) with a Bio-Rad gene pulser apparatus (Bio-Rad Laboratories, Richmond, CA). The electroporated cells were transferred to 1 ml of fresh TGP medium. The cells were rescued for 2 h at 50 °C; then, the cell pellets were spread on TPG agar plates containing 15 μg/ml of chloramphenicol. The plates were incubated at 55 °C overnight to isolate single colonies.

2.3.5 Acetolactate synthase purification and thermostability assay

To purify potential acetolactate synthase (ALS) enzymes, *B. subtilis alsS* and three putative *alsS* genes (Geoth_3495 from *G. thermoglucosidasius* DSM 2542^T, Gtng_0348 from *G. thermodenitrificans* and Str0923 from *Streptococcus thermophilus*) were cloned into pETDuet-1 and pET-26b (+) with an N-terminal polyhisidine-tag to make plasmids pSA159, pHT194, pHT195, pHT196 (Table 2.1, Table 2.2). The *E. coli* BL21 Star™ (DE3) strains transformed with these plasmids were grown to OD_{600} of 0.4 to 0.6 in 50 ml LB medium at 37 °C at 250 rpm, and induced with 1 mM IPTG. Protein overexpression was performed at room temperature for 4 h. The cells were centrifuged, resuspended in 2 ml of His-binding buffer (His-Spin Protein Miniprep™ Kit, Zymo Research) and lysed at 30 Hz for 6 min by a Tissue Lyser II (Qiagen, Valencia, CA). To separate soluble and insoluble proteins, the samples were centrifuged for 20 min (15,000 rpm, 4 °C). The putative enzymes were purified using a His-Spin Protein Miniprep™ Kit. Purified protein concentrations were measured by Pierce BCA Protein Assay (Thermo Scientific).

To assess the thermostability of different ALS enzymes, purified proteins were incubated at varying temperatures (30 °C to 90 °C) for 10 min. The heat-treated ALS enzymes were assayed as described (Yang et al., 2000), with the exception that the reaction mixture contained 20 mM pyruvate, 100 mM MOPS buffer (pH=7.0), 1 mM $MgCl_2$ and 100 μM TPP. *B. subtilis* AlsS was

assayed at 37 °C and ALS from *G. thermoglucosidasius*, *G. thermodenitrificans* and *S. thermophilus* were assayed at 50 °C. The concentration of acetoin produced was determined by a standard curve created using pure acetoin.

2.3.6 Kivd purification and thermostability assay

To purify *L. lactis* Kivd, two Kivd variants (CAG34226 and LLKF_1386) were cloned into pET-22b (+) (Table 2.1, Table 2.2; Invitrogen, Carlsbad, CA). These enzymes were overexpressed in *E. coli* BL21 Star™ (DE3) strains (Invitrogen). 10 ml of an overnight culture grown at 37 °C in LB containing 100 μg/ml of ampicilin were used to inoculate a 1 l culture. After 4 h of growth at 37 °C and 250 rpm, the temperature was decreased to 25 °C and protein production was induced with 0.1 mM Isopropyl β-D-1-thiogalactopyranoside (IPTG). After 16 h of induction, the cells were harvested by centrifugation at 5000*g* and 4 °C for 20 min. The cell pellets were resuspended in 20 mM Na_3PO_4 (pH7.5), 500 mM NaCl, 20 mM imidazole and frozen at −20 °C overnight. The cell pellets were then thawed, 700 μg/ml of lysozyme and 25 μg/ml of DNaseI were added, and the cells were incubated for 30 min at 37 °C and then lysed by sonication. The lysate was cleared by centrifugation at 25,000*g* for 30 min and filtering through a 0.2 μm filter. Since the enzymes were polyhistidine-tagged, the soluble fraction of the cell lysate was passed through a Ni-NTA column and washed with 20 mM Na_3PO_4 (pH=7.5), 500 mM NaCl, 20 mM imidazole. The proteins were eluted from the column using a linear gradient running up to 20 mM Na_3PO_4 (pH=7.5), 500 mM NaCl, 500 mM imidazole. The fractions containing protein were pooled and the buffer was exchanged to 10 mM Tris pH7.5, 10 mM NaCl, 2.5 mM $MgSO_4$ and 0.1 mM thiamine pyrophosphate (TPP). The protein concentration was determined by the Bradford

assay and purity was confirmed by SDS-PAGE. The proteins were then aliquoted, frozen on dry ice and stored at −80 °C until further use.

To test enzyme thermostability, 600 ng of *L. lactis* Kivd was incubated at different temperatures with 100 µl of 10 mM Tris (pH=7.5), 10 mM NaCl, 2.5 mM $MgSO_4$, 0.1 mM TPP, 1 µM Aaci_0153 (thermostable ADH), 500 µM NADH and 10 mM 2-ketoisovalerate in a 96-well PCR plate for 20 min. The PCR plate was placed on ice and 50 µl of the reaction mixture were transferred to a multi-well plate and the reaction was stopped by addition of guanidinium hydrochloride up to an end concentration of 3.5 M to a total volume of 100 µl. The NADH consumption was determined by fluorescence (excitation 340 nm, emission 440 nm) using a Tecan Infinite M200 PRO.

2.3.7 ADH purification, characterization and thermostability assay

To purify ADH enzymes from *G. thermoglucosidasius* DSM 2542^T, fourteen putative *adh*genes were cloned into pET-26b (+) (Invitrogen) with C-terminal polyhistidine-tags to make plasmids pHT109 to pHT126 (Table 2.1, Table 2.2). Enzyme overexpression and protein purification procedures were as described in the acetolactate synthase purification and thermostability assay section.

Activity (isobutyraldehyde formation) was determined by monitoring the oxidation of NADH by a decrease in absorbance at 340 nm. The assay mixture contained 50 mM MOPS buffer (pH=7.0), 0.25 mM NADH and varying concentrations of isobutyraldehyde (0.05 mM to 20 mM). The 600 µl of samples were incubated at 50 °C for 10 min, the reaction was initiated by adding 2 µg to 5 µg purified enzymes, and the reaction was monitored using a Beckman Coulter DU800 spectrophotometer.

To assess the thermostability of ADH from *G. thermoglucosidasius* DSM 2542^{T}, 500 ng/ml of protein was incubated at different temperature (30 °C to 90 °C) with 100 µl of 50 mM MOPS buffer (pH=7.0) for 10 min. After heat treatment, the ADH enzyme was assayed with 20 mM isobutyraldehyde, 50 mM MOPS buffer (pH=7.0) and 0.25 mM NADH (final volume is 200 µl) at 50 °C using a BioTek PowerWave HT microplate spectrophotometer.

2.3.8 Promoter identification

To establish an efficient expression system, the thermostable *lacZ* gene from*Geobacillus stearothermophilus* was used as a reporter gene for analysis of promoter strength in *G. thermoglucosidasius*. Different promoters from *G. thermoglucosidasius*and *G. thermodenitrificans* were cloned to drive the expression of thermostable β-galactosidase. The recombinants were grown in TGP medium with antibiotic. Promoter strength was measured by β-galactosidase activity of whole *G. thermoglucosidasius*cells as reported previously (Guarente, 1983), except that the incubation temperature of the enzyme was adjusted to 50 °C.

2.4 Results

2.4.1 Prospecting thermostable ALS

The synthesis of acetolactate from two pyruvate molecules can be catalyzed by either an acetohydroxy acid synthase (AHAS) or an ALS. AHAS enzymes are used in branched-chain amino acid biosynthesis; the heterotetrameric enzyme contains a large catalytic subunit and a small regulatory subunit and is typically regulated by end products (Gollop et al., 1989 and Weinstock et al., 1992). ALS is a single subunit enzyme belonging to the acetoin biosynthesis pathway. Gollop et al. (1990) reported that the catabolic *B. subtilis*AlsS is highly specific for acetolactate formation. Atsumi et al. (2008) used the *B. subtilis*AlsS instead of the native

biosynthetic enzymes to improve the isobutanol titer in *E. coli*. Unlike most AHAS enzymes, ALS, is not regulated by feedback inhibition. However, ALS-like enzymes from thermophiles have not yet been reported. After searching for homologs of *B. subtilis alsS* in thermophiles, we cloned and purified three putative enzymes: Geoth_3495 from *G. thermoglucosidasius*, Gtng_0348 from *G. thermodenitrificans*, and Str0923 from *S. thermophilus*. Of these, only *S. thermophilus*Str0923 showed ALS activity, which was 3% that of the *B. subtilis* AlsS at 37 °C.

The *S. thermophilus* (*ST*) Str0923 was tested for thermostability along with *B. subtilis*AlsS. Fig. 2.2 shows the ALS specific activities of the two enzymes after heat treatment at different temperatures for 10 min. These two enzymes showed similar thermostabilities, but the specific activity of the *B. subtilis* AlsS was higher than the thermophilic enzyme. We therefore chose AlsS from *B. subtilis* for thermophilic isobutanol production.

2.4.2 Prospecting thermostable KIVD enzymes

The decarboxylation of 2-ketoisovalerate to isobutyraldehyde is the key enzymatic step to divert flux from the native valine biosynthesis pathway to isobutanol production. To identify a suitable KIVD, we first determined the thermostabilities of two *L. lactis* Kivd variants that were previously characterized for the decarboxylation of 2-ketoisovalerate to isobutyraldehyde (named according to their accession numbers, CAG34226 and LLKF_1386) (Plaza et al., 2004 and Atsumi et al., 2010). Although the two proteins differ by only seven amino acids, their T_{50} (the temperature at which the enzyme loses half of its activity upon a 20-min. incubation) are 45 °C for CAB34226 and 57 °C for LLKF_1386 (Fig. 2.3A and B). The more thermostable Kivd, LLKF_1386, has been used previously for isobutanol biosynthesis (Atsumi et al., 2008, Atsumi et al., 2009, Smith et al., 2010,Higashide et al., 2011 and Li et al., 2012).

Since acetolactate synthase (encoded by *alsS*) from *B. subtilis* has been shown to also catalyze the decarboxylation of 2-ketoisovalerate to isobutyraldehyde (Atsumi et al., 2009), we also analyzed homologous genes that have been annotated *als* in different*Geobacillus* species. We excluded putative biosynthetic-type genes, based on the presence of a small regulatory subunit gene downstream, as these enzymes are usually highly regulated. The remaining enzymes (Table 2.3) were cloned and purified with an N-terminal (Geoth_3495, Gtng_0348 and Gtng_0651) or a C-terminal (Gtng_1810 and Gtng_1891) his-tag attached. Two purified enzymes displayed Kivd activity at 60 °C *in vitro*: *G. thermoglucosidasius* Geoth_3495 and *G. thermodenitrificans* Gtng_0348, which share 67% similarity in amino acid sequence. The corresponding enzymes exhibit respective k_{cat} of 1.1 s^{-1} and 0.4 s^{-1}. However, the k_{cat} of *L. lactis* Kivd was reported by Plaza et al. (2004) as 120 s^{-1}, which is at least 100 fold higher. We also assayed the KIVD specific activity following a 20 min heat-treatment for Gtng_0348 (Fig. 2.3C). The KIVD specific activity of LLKF_1386 is 87-fold higher than Gtng_0348 when pre-incubated at 50 °C (Fig. 2.3B and C). Thus, we chose the *L. lactis* Kivd, LLKF_1386, for thermophilic isobutanol production.

2.4.3 Identification of an isobutanol dehydrogenase from *G. thermoglucosidasius*

The last step in the isobutanol production pathway is the conversion of isobutyraldehyde to isobutanol catalyzed by an isobutanol dehydrogenase. Isobutanol was detected in the culture medium of wild-type *G. thermoglucosidasius* when it was supplemented with isobutyraldehyde (results not shown), indicating that an isobutanol-producing ADH exists in this organism. Since the genome sequence of this strain, *G. thermoglucosidasius* DSM 2542^T, is not available, we used the genome sequence of a related strain, *G. thermoglucosidasius* C56-YS93, to search for potential

isobutanol dehydrogenases. Seventeen putative *adh* genes are annotated in *G. thermoglucosidasius* C56-YS93, but none had been previously characterized for isobutanol dehydrogenase activity. Among the 17 putative enzymes, one (Geoth_3897) is a potential bifunctional aldehyde/alcohol dehydrogenase, and was excluded. Two *adh* genes (Geoth_1917 and Geoth_3108) could not be PCR-amplified from the *G. thermoglucosidasius* DSM 2542^{T} genomic DNA. The remaining 14 enzymes were cloned and overexpressed in *E. coli* with a His-tag and purified.

Among these ADH enzymes, Geoth_3237, Geoth_3554 and Geoth_3823 showed significant NADH-dependent activity for converting isobutyraldehyde to isobutanol (Fig. 2.4A). In addition, Geoth_0611 and Geoth_3823 showed significant NADPH-dependent isobutanol dehydrogenase activity (Fig. 2.4A). We rename Geoth_3237, *adhA*. This enzyme showed weak activity on isobutyraldehyde with NADPH as a cofactor. The preference for NADH was consistent with the presence of the Gly-X-Gly-X-X-Gly (where X is any amino acid) sequence that is the highly conserved in many NADH-binding domains (Scrutton et al., 1990). Using purified enzyme, we determined the kinetic parameters of *G. thermoglucosidasius* AdhA: K_M=5.9 mM, k_{cat}=9.5 s^{-1} with NADH;K_M=0.87 mM, k_{cat}=0.81 s^{-1} with NADPH (Fig. 2.4B) at room temperature, comparable to the *L. lactis* AdhA (K_M=9.1 mM, k_{cat}=6.6 s^{-1}) (Atsumi et al., 2010). We also characterized Geoth_3823. Fig. 2.4C shows the kinetic parameters: K_M=0.89 mM, k_{cat}=7.0 s^{-1} with NADH; K_M=3.0 mM, k_{cat}=12 s^{-1} with NADPH.

To test the thermostability of AdhA from *G. thermoglucosidasius*, purified enzyme was pre-incubated at different temperatures and assayed at 50 °C as described in Materials and Methods. Fig. 2.4D shows that this enzyme has a T_{50} of about 72 °C.

2.4.4 Promoter prospecting

Having identified thermostable enzymes for the isobutanol pathway, we needed a strong promoter to express the genes in G. thermoglucosidasius. We employed a thermostablelacZ gene isolated from G. stearothermophilus as a reporter for testing different promoters. Several promoters, including most of the native glycolytic promoters (glk, pgi pfkA, gap, pgk, gpm, eno), were selected to drive this lacZ gene. We also included *ldh* (Gtng_0487) and *glpD* (Gtng_2098) promoters from G. thermodenitrificans and the P43 promoter from B. subtilis, which is a constitutive promoter. The DNA fragments (200–300 b.p.) upstream of the start codon of the corresponding gene were PCR-amplified from genomic DNA and assembled in plasmids to express the thermostable lacZ gene. Fig. 2.5 shows that the ldh promoter from G. thermodenitrificans was the strongest among all tested. Thus, we selected the ldh promoter to drive the expression of pathway genes for isobutanol production in *G. thermoglucosidasius*.

2.4.5 Isobutanol production

With appropriate thermostable enzymes identified and the expression system established, we proceeded to establish isobutanol production in *G. thermoglucosidasius*. We first cloned *kivd* from *L. lactis* under the control of the *ldh* promoter from *G. thermodenitrificans* into the pNW33N (Table 2.1) backbone, resulting in plasmid pHT79 (Fig. 2.6A). Isobutanol was not detected when only Kivd was overexpressed *in G. thermoglucosidasius* using ASYE media. However, when 2-ketoisovalerate was added to the medium, isobutanol was detected, indicating

that Kivd was expressed and functional. This result suggested that the native metabolic flux from pyruvate to 2-ketoisovalerate was insufficient to produce isobutanol in *G. thermoglcosidasius* at 50 °C.

When *B. subtilis alsS* was overexpressed along with *kivd* (Fig. 2.6A, pHT13), 0.2 g/l of isobutanol was produced in two days at 50 °C from glucose. However, 0.4 g/l of 2,3-butanediol was also produced. 2,3-butanediol is a reduced form of acetoin (Fig. 2.1), which could be produced from acetolactate through spontaneous cleavage at elevated temperature (Xiao et al., 2012). This result indicates that the flux from acetolactate to 2,3-dihydroxy-isovalerate is insufficient, and suggests that overexpressing KARI may help isobutanol production. We thus cloned and overexpressed *kivd* and *alsS* with each of the three thermophilic *ilvC* genes: Geoth_0987 from *G. thermoglucosidasius* (Fig. 2.6A, pHT71), Aaci_2227 from *A. acidocaldarius* (Fig. 2.6A, pHT133) and Aflv_0593 from *A. flavithermus* (Fig. 2.6A, pHT134). Among these, the strain with *G. thermoglucosidasius ilvC* overexpressed (pHT71) achieved the highest isobutanol production level: 3.3 g/l of isobutanol in two days at 50 °C (Fig. 2.6A and B).

We also overexpressed *G. thermoglucosidasius ilvD* in the same operon downstream of*kivd*, *ilvC* and *alsS* (Fig. 2.6A, pHT77). Interestingly, overexpression of *ilvD* in addition to the *kivd*, *ilvC* and *alsS* had no significant effect on isobutanol production. It is possible that *ilvD* expression reduced expression of the other three enzymes due to limited transcription/translation machinery.

To test whether increasing intracellular isobutanol dehydrogenase concentration could improve the isobutanol titer, *G. thermoglucosidasius adhA* was overexpressed with *kivd*,*ilvC*, *alsS* (Fig. 2.6A, pHT208). Surprisingly, overexpression of AdhA reduced

isobutanol production (Fig. 2.6A). This result indicates that chromosomal AdhA expression was sufficient to support isobutanol production. We hypothesize that the transcription/translation machinery may be saturated with the strong *ldh* promoter from*G. thermodenitrificans*.

To test the utility of other thermostable enzymes for isobutanol production, we also tested the alternative ALS, *ST* Str0923, which was substituted for *B. subtilis* AlsS (Fig. 2.6A, pHT209). Unfortunately, no isobutanol was detected when pHT209 was used, indicating that the *ST* Str0923 activity was not enough to support isobutanol production from glucose. This is consistent with the *in vitro* enzyme assay that showed the *ST* Str0923 was significantly less active than *B. subtilis* AlsS (Fig. 2.2).

Using the best production strain (pHT71), we also tested isobutanol production from the glucose disaccharide cellobiose, which is a primary product of cellulose hydrolysis. However, only a small amount of cellobiose is consumed by *G. thermglucosidasius* in the modified ASYE medium with 0.5% yeast extract, which led us to remove yeast extract from the medium. Ultimately, 0.6 g/l of isobutanol was produced from cellobiose (without yeast extract) (Fig. 2.6C) at 50 °C.

2.5 Discussion

In this work, we have demonstrated production of isobutanol in a thermophilic organism and established *G. thermoglucosidasius* as a platform for biofuel production. Although this organism has an established transformation protocol and an integration vector system for gene replacements (Cripps et al., 2009), no expression system has been established. Here, we identified a robust promoter to drive gene expression from a plasmid, and we characterized enzymes for isobutanol biosynthesis at elevated temperature. With the best combination of enzymes (*L.*

lactis Kivd, *G. thermoglucosidasius* KARI and *B. subtilis* AlsS) and our expression system, we achieved titers of 3.3 g/l isobutanol from glucose and 0.6 g/l isobutanol from cellobiose at 50 °C. The success of thermophilic isobutanol production at 50 °C demonstrated that isobutyraldehyde volatility is not a major issue at this temperature, although we could not rule out this issue at 55 °C or higher temperatures.

Previously, Atsumi et al. (2008) showed that *E. coli* can be metabolically engineered to produce isobutanol by diverting the keto acid intermediate in the valine biosynthesis pathway toward isobutanol production. Two important foreign enzymes, *L. lactis* Kivd and *B. subtilis* AlsS, were used to establish this heterologous pathway. The same key enzymes have been used for isobutanol production in other mesophiles (Atsumi et al., 2009, Smith et al., 2010, Higashide et al., 2011 and Li et al., 2012).

To produce isobutanol in a thermophile, we identified Gtng_0348 from *G. thermodenitrificans* for high temperature Kivd activity. We also identified several ALS enzymes from thermophiles. Interestingly, the mesophilic *L. lactis* Kivd and *B. subtilis*AlsS were found to be the most active enzymes at 50 °C.

The system also produced isobutanol at 55 °C, but inconsistently and at lower titers, possibly due to the instability of Kivd, which has a T_{50} value of about 56.7 °C (Fig. 2.3B). A highly thermostable Kivd has not been reported. Also, because Kivd-homologs have not been found in thermophiles, either new enzyme identification or protein engineering may be required for production above 55 °C. Although Gtng_0348 showed Kivd activity *in vitro*, the activity is about 100 times lower than *L. lactis* Kivd.

One of the key features of high titer fuel production is growth-independent production (Atsumi et al., 2008). However, the *G. thermoglucosidasius* cells enter the death phase (lysis) under micro-aerobic conditions after 34 h (i.e., the OD_{600} dropped significantly due to cell lysis and sometimes aggregation). Therefore, the isobutanol production stopped at 3.3 g/l in this system. Tang et al. (2009) also reported a similar phenomenon. Increasing production titers may be achieved by extending the stationary phase of the *G. thermoglucosidasius* cells.

With our established thermophilic isobutanol production strain, we have demonstrated the feasibility of producing higher-density liquid fuels at a high temperature, essential for producing next-generation cellulosic biofuels using simultaneous saccharification and fermentation.

2.6 Figures

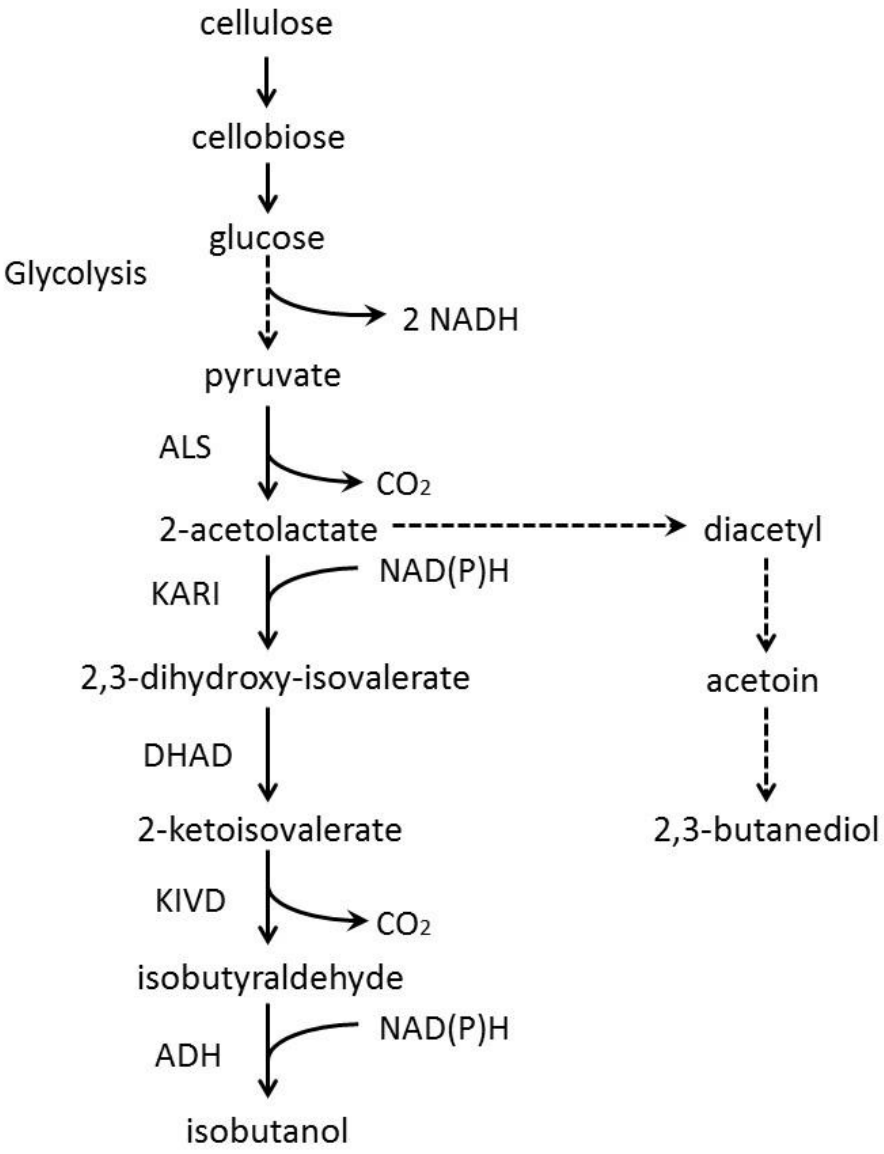

Figure 2-1. Isobutanol pathway.

Enzyme abbreviations are: ALS, acetolactate synthase; KARI, ketol-acid reductoisomerase; DHAD, dihydroxy acid dehydratase; KIVD, 2-ketoisovalerate decarboxylase; ADH, alcohol dehydrogenase

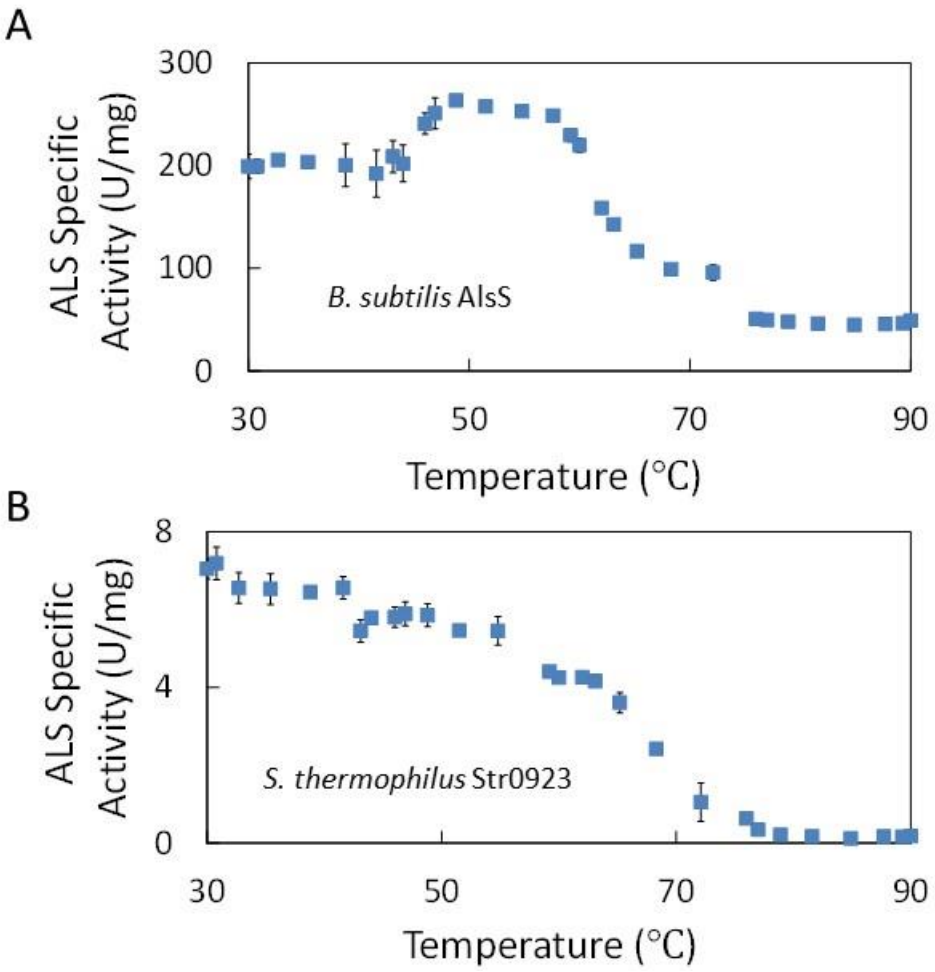

Figure 2-2. ALS specific activity.

(A) *B. subtilis* AlsS and (B) *S. thermophilus* Str0923 after a 10 minute heat treatment at different temperatures. Enzyme unit, U, is defined as the amount of the enzyme that catalyzes the conversion of 1 micromole of pyruvate per minute. Error bars represent standard deviation, n = 3.

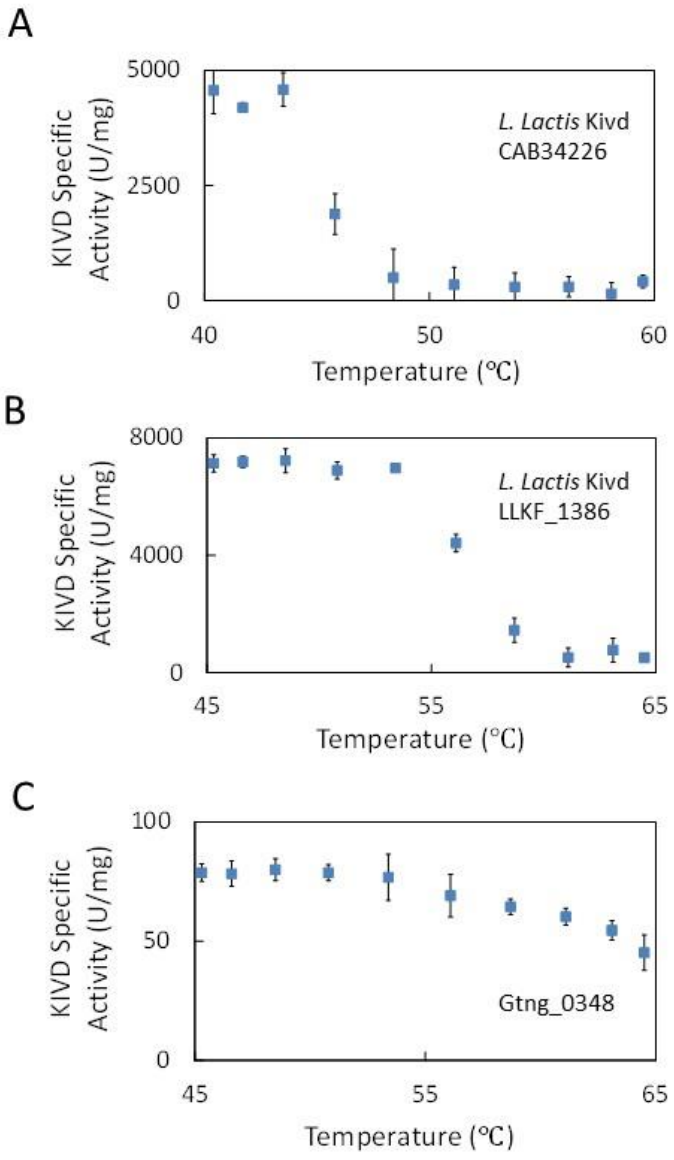

Figure 2-3. KIVD specific activity.

(A) *L. lactis* Kivd (CAB34226) (B) *L. lactis* Kivd (LLKF_1386) and (C) Gtng_0348 after a 20 minute heat treatment at different temperatures. Enzyme unit, U, is defined as the amount of the enzyme that catalyzes the conversion of 1 micromole of 2-ketoisovalerate per minute. Error bars represent standard deviation, n = 3.

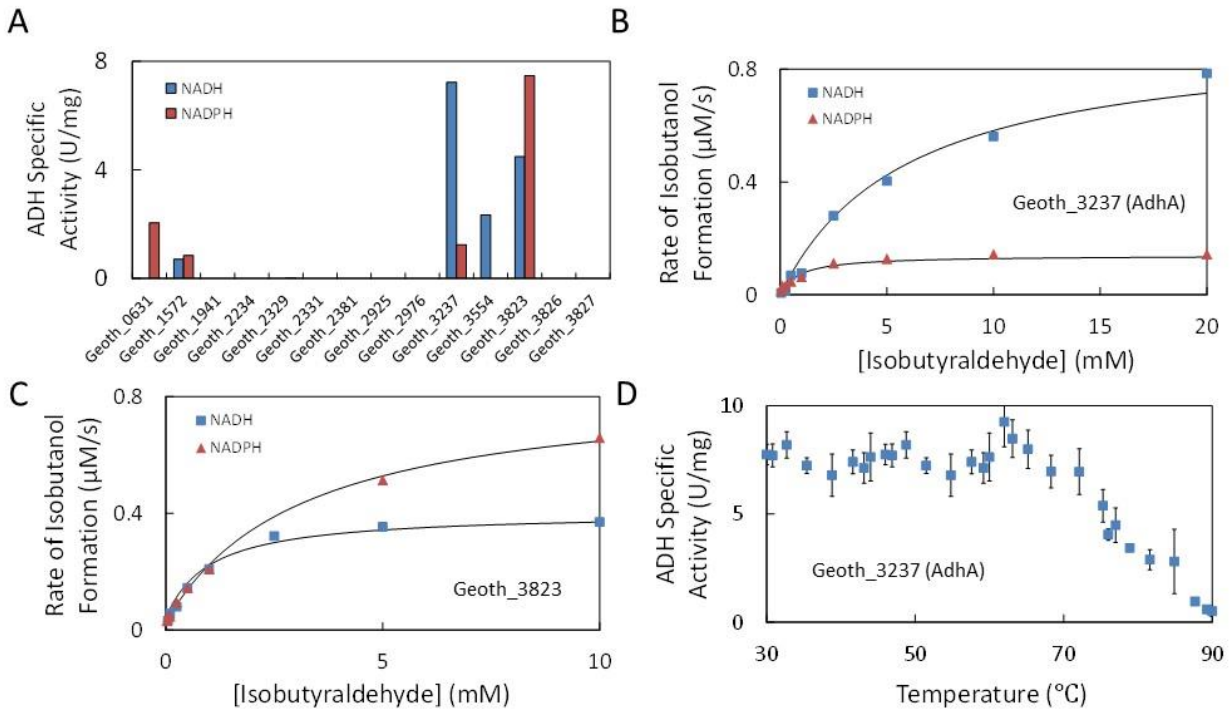

Figure 2-4. ADH specific activity for isobutyraldehyde reduction of putative alcohol dehydrogenases from *G. thermoglucosidasius*.

Blue bars represent the enzyme activity using NADH as the cofactor. Red bars represent the enzyme activity using NADPH as the cofactor. Enzyme unit, U, is defined as the amount of the enzyme that catalyzes the conversion of 1 micromole of isobutyraldehyde per minute. Michaelis–Menten plots of (B) G. thermoglucosidasius AdhA (Geoth_3237) and (C) G. thermoglucosidasius Geoth_3823 using NADH or NADPH as cofactor at room temperature. (D) ADH specific activity of G. thermoglucosidasius AdhA after a 10 minute treatment at different temperatures. Error bars represent standard deviation, n = 3.

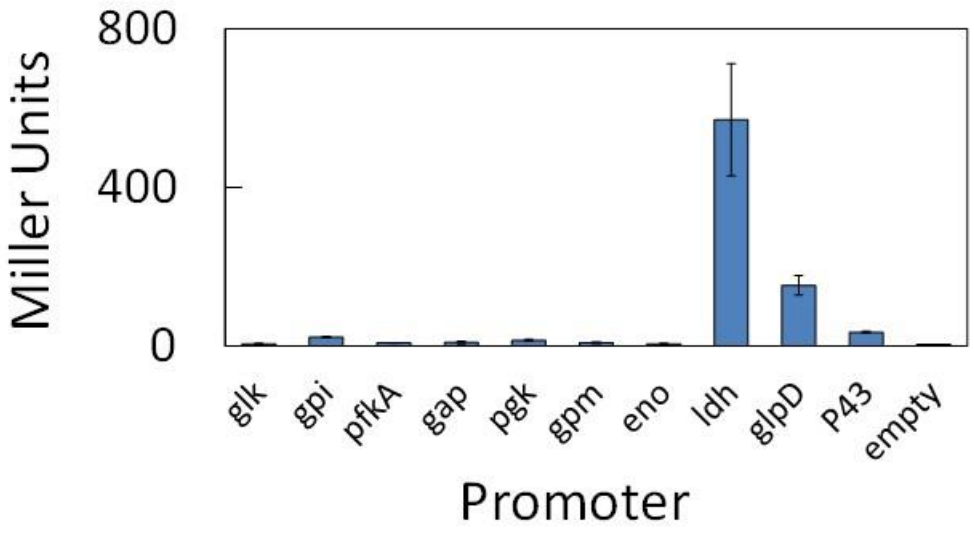

Figure 2-5. Promoter characterization.

Promoters were PCR-amplified and used to drive the expression of the thermostable *G. stearothermophilus lacZ* gene. *G. thermoglucosidasius* strains harboring these plasmids were assayed for promoter strength with a β-galactosidase assay at 50 ^{o}C. Promoter abbreviations are: *glk*, glucose kinase; *gpi*, glucose phosphate isomerase; *pfkA*, phosphofructokinase; *gap*, glyceraldehyde phosphate dehydrogenase; *pgk*, phosphoglycerate kinase; *gpm*, phosphoglycerate mutase; *eno*, enolase; *ldh*, lactate dehydrogenase; *glpD*, glycerol-3-phosphate dehydrogenase. Error bars represent standard deviation, n = 3.

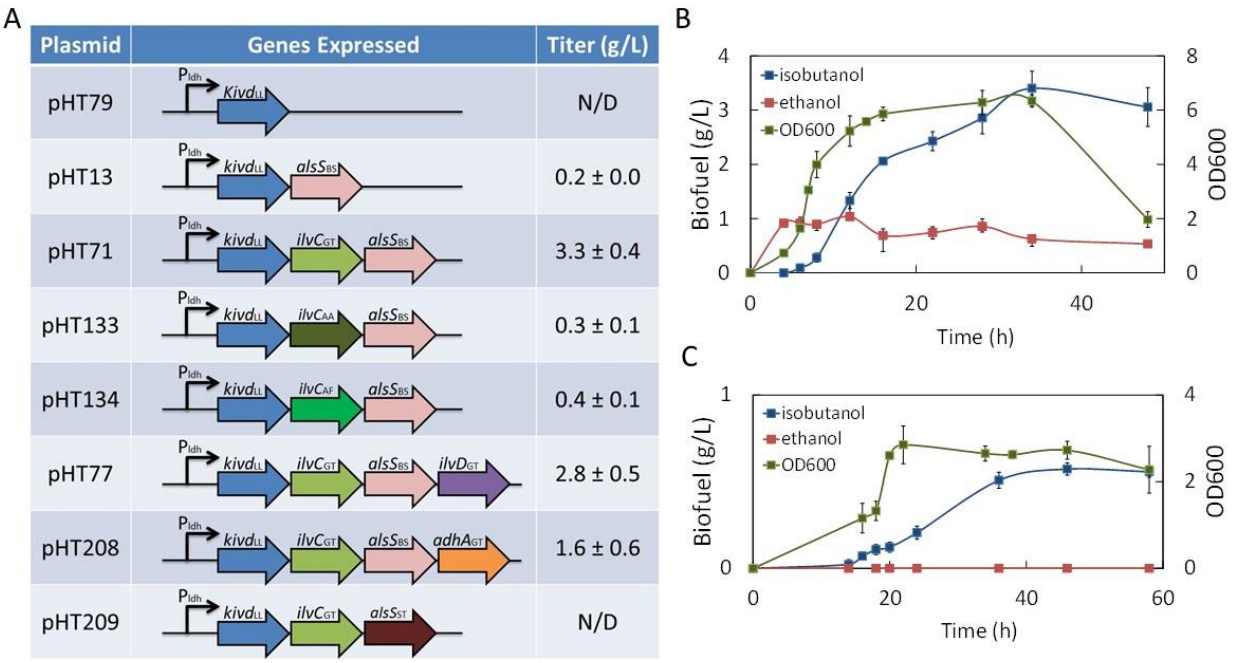

Figure 2-6. Plasmid constructs and isobutanol production titers at 50 ºC from glucose and cellobiose over two days.

(A) Plasmid constructs and isobutanol titer. In gene symbols, subscripts indicate the source of the gene: GS, *Geobacillus stearothermophilus*; LL, *Lactococcus lactis*; BS, *Bacillus subtilis*; GT, *Geobacillus thermoglucosidasius*; AA, *Alicyclobacillus acidocaldarius*; AF, *Anoxybacillus flavithermus;* ST, *Streptococcus thermophiles*; GD, *Geobacillus thermodenitrificans*. Biofuel production and optical density of pHT71 in *G. thermoglucosidasius* from (B) glucose (C) cellobiose. Error bars represent standard deviation, n = 3.

2.7 Tables

Table 2-1. List of strains and plasmids used in this study.

Strain or plasmid	Description[a]	Reference
Strains		
E. coli XL1-Blue	F´ *pro*AB l*ac*IqZΔM15 Tn10 Tet^r	Stratagene
E. coli BL21(DE3)	E. coli B dcm ompT hsdS($r_B^-m_B^-$) gal	Invitrogen
G. thermoglucosidasius	DSM 2542^T	*Bacillus* Genetic Stock Center
G. thermodenitrificans	DSM 465^T/ BGSC 94A1	*Bacillus* Genetic Stock Center
Plasmid		
pDL	Source of thermostable *lacZ*$_{GS}$	*Bacillus* Genetic Stock Center
pNW33N	ColE1 and pBC1 *ori*; Cm^R; *E. coli-Bacillus* shuttle vector	*Bacillus* Genetic Stock Center
pHT01	ColE1 and pBC1 *ori*; Cm^R; *lacZ*$_{GS}$ without promoter	This study
pHT13	ColE1 and pBC1 *ori*; Cm^R; P$_{ldh}$::*kivd*$_{LL}$-*alsS*$_{BS}$	This study

pHT71	ColE1 and pBC1 *ori*; Cm^R; P_{ldh}::$kivd_{LL}$-$ilvC_{GT}$-$alsS_{BS}$	This study
pHT77	ColE1 and pBC1 *ori*; Cm^R; P_{ldh}::$kivd_{LL}$-$ilvC_{GT}$-$alsS_{BS}$-$ilvD_{GT}$	This study
pHT79	ColE1 and pBC1 *ori*; Cm^R; P_{ldh}::$kivd_{LL}$	This study
pHT112	Derivative of pET-26b (+) with putative *adh* (Geoth_3237)	This study
pHT114	Derivative of pET-26b (+) with putative *adh* (Geoth_3823)	This study
pHT133	ColE1 and pBC1 *ori*; Cm^R; P_{ldh}::$kivd_{LL}$-$ilvC_{AA}$-$alsS_{BS}$	This study
pHT134	ColE1 and pBC1 *ori*; Cm^R; P_{ldh}::$kivd_{LL}$-$ilvC_{AF}$-$alsS_{BS}$	This study
pHT194	Derivative of pET-26b (+) with putative *alsS* (Geoth_3495)	This study
pHT195	Derivative of pET-26b (+) with putative *alsS* (Gtng_0348)	This study
pHT196	Derivative of pET-26b (+) with putative *alsS* (Str0923)	This study
pHT208	ColE1 and pBC1 *ori*; Cm^R; P_{ldh}::$kivd_{LL}$-$ilvC_{GT}$-$alsS_{BS}$-$adhA_{GT}$	This study

pHT209	ColE1 and pBC1 *ori*; Cm^R; P_{ldh}::$kivd_{LL}$-$ilvC_{GT}$-$alsS_{ST}$	This study
pKSR124	Derivative of pET-22b (+) with Gtng_0348	This study
pSA65	Source of $kivd_{LL}$	
pSA69	Source of $alsS_{BS}$	
pSA159	Derivative of pETDuet-1 with $alsS_{BS}$	

[a] In plasmid descriptions, subscripts indicate the source of the gene as follows: GS, *Geobacillus stearothermophilus*; LL, *Lactococcus lactis*; BS, *Bacillus subtilis*; GT, *Geobacillus thermoglucosidasius*; AA, *Alicyclobacillus acidocaldarius*; AF, *Anoxybacillus flavithermus*; ST, *Streptococcus thermophilus* ;GD, *Geobacillus thermodenitrificans*

2.8 Supplementary

Table 2-2. List of primers used in this study

Primer	Sequence (5' to 3')	Template	Plasmid
HT01_TBGF	ACCATGATTACGCCAAGCTTATGAATGTGTTATCCTCAAT	pDL	pHT01
HT01_TBGR	AACCAGCCAGCCCGAGAATTCCTAAACCTTCCCGGCTTCA		
HT01_BBF	GAATTCTCGGGCTGGCTGGT	pNW33N	
HT01_BBR	AAGCTTGGCGTAATCATGGTCAT		
HT79_kivdF	AATAAGAAGGGAGAATAGTGATGTATACAGTAGGAGATTA	pSA65	HT79
HT79_kivdR	TTATGATTTATTTTGTTCAG	pSA65	
HT79_BBF	CTGAACAAAATAAATCATAAGAATTCTCGGGCTGGCTGGT	pHT01	
HT79_BBR	CACTATTCTCCCTTCTTATTATTG	pHT01	
HT13_AlsF	AAATAAATCATAATAAGGAGGAACTACTTTGACAAAAGCAACAAAAGAACAAAAATCCC	pSA69	HT13

	TCAGCAATAAACCAGCCAGC		
HT13_AlsR	CCGAGAATTCTTAGAGAGCTT TCGTTTTCATGAGTTCC	pSA69	
HT13_BBF	GAATTCTCGGGCTGGCTGGT CTTTTGTCAAAGTAGTTCCTC	HT79	
HT13_BBR	CTTATTATGATTTATTTTGTTC AGCAAATAGTTTGCCC	HT79	
	CATAATAAGGAGGAACTACT		
HT71_ilvCF	ATGGCAAAAGTTTACTATAA CGG	*G. thermoglucosidasius*	HT71
	TGCTTTTGTCAAAGTAGTTCC		
HT71_ilvCR	TCCTTATTAATTTTTCTCACTC GTAACC		
HT71_BBF	GAACTACTTTGACAAAAGCA	HT13	
HT71_BBR	AGTAGTTCCTCCTTATTATG		
HT77_ilvDF	CCGTTCCCAATTCCACATTGC A	*G. thermoglucosidasius*	HT77
HT77_ilvDR	TAAGGAGGAACTACTATGTT GGGAAAACTTCGCAG		
HT77_BBF	TGCAATGTGGAATTGGGAAC GG	HT71	

HT77_BBR	AGTAGTTCCTCCTTATTAATT TTTCTCACTCGTAA		
HT112_AdhF	TAAGGAGGAACTACTATGAA AGCACTTACATACCTAGGG	*G. thermoglucosidasius*	HT112
HT112_AdhF	CCAGCCCGAGAATTCTTAACT GTTGGAAATAATGACTTTTAA CG		
HT112_BBF	CACCACCACCACCACCACTG	pET-26b (+)	
HT112_BBR	CGGATCCGAATTAATTCCGAT ATCCATGGC		
HT133_ilvCF	TAAGGAGGAACTACTATGGA GAAAATTTATTACGACGC	*A. acidocaldarius*	HT71
HT133_ilvCR	CAAAGTAGTTCCTCCTTATTA AGCCCGATCCGCGGTGG		
HT133_BBF	GTCGTAATAAATTTTCTCCAT AGTAGTTCCTCCTTATTATGA TTTATTTTGTTCAGCAA	HT71	
HT133_BBR	TAAGGAGGAACTACTTTGAC AAAAGCAACAAAAGAACA		

	TAAGGAGGAACTACTATGGT		
HT134_ilvCF	AAAAGTATATTACAATGGCG	*A. flavithermus*	HT71
	A		
HT134_ilvCR	CAAAGTAGTTCCTCCTTATTA ATTTTTCGCACCGACCGT		
	ATTGTAATATACTTTTACCAT		
HT134_BBF	AGTAGTTCCTCCTTATTATGA	HT71	
	TTTATTTTGTTCAGCAA		
HT134_BBR	TAAGGAGGAACTACTTTGAC AAAAGCAACAAAAGAACA		
	AATTCGGATCCGCACCACCAC		
HT194_AlsF	CACCACCACATGAAACAGAC	*G. thermoglucosidasius*	HT194
	CATCCGCAATATCAGC		
	CTTTCGGGCTTTGTTAGCAGC		
HT194_AlsR	CGGATCTCACCGAGAATTCG		
	AGCGCTTTCG		
HT194_BBF	TGAGATCCGGCTGCTAACAA AGC	pET-26b (+)	
HT194_BBR	GTGGTGGTGGTGGTGGTGC		

HT195_AlsF	AATTCGGATCCGCACCACCACCACCACCACATGGGAGGGACGGCCATG	*G.thermodenitrificans*	HT195
HT195_AlsR	CTTTCGGGCTTTGTTAGCAGCCGGATCTCATCATCTGTCTGACAGTCTCATCGTCA		
HT195_BBF	TGAGATCCGGCTGCTAACAAAGC	pET-26b (+)	
HT195_BBR	GTGGTGGTGGTGGTGGTGC		
HT196_AlsF	TCGGATCCGCACCACCACCACCACCACGTGTTCATGTCAGAAGAAAAGCAATTGTATGG	*S. thermophilus*	HT196
HT196_AlsR	TTCGGGCTTTGTTAGCAGCCGGATCTCAGTAAAATTCATCTGGCAAAATAGTTTCGCCG		
HT196_BBF	TGAGATCCGGCTGCTAACAAAGC	pET-26b (+)	
HT196_BBR	GTGGTGGTGGTGGTGGTGC		
HT208_AdhF	CCGTTCCCAATTCCACATTGCA	HT112	HT208

HT208_AdhR	TAAGGAGGAACTACTATGAAAGCACTTACATACCTAGGG		
HT208_BBF	TGCAATGTGGAATTGGGAACGG	HT71	
HT208_BBR	TTCATAGTAGTTCCTCCTTATTAGAGAGCTTTCGTTTTCA		
HT209_AlsF	AGTGAGAAAAATTAATAAGGAGGAACTACTGTGTTCATGTCAGAAGAAAAGCAATTGT	HT196	HT209
HT209_AlsR	CAGCAATAAACCAGCCAGCCCGAGAATTCGTAAAATTCATCTGGCAAAATAGTTTCGCC		
HT209_BBF	GAATTCTCGGGCTGGCTGGT	HT71	
HT209_BBR	AGTAGTTCCTCCTTATTAATTTTTCTCACTCGTAA		
KSR124_UP	GATATACATATGCACCACCACCACCACCACGGAGGGACGGCCATG	*G.thermodenitrificans*	KSR124
KSR124_DN	CTTTGTTAGCAGCCGGATCTCATCATCTGTCTGACAGTCTCATCG		

KSR123_UP	TGAGATCCGGCTGCTAACAAAG	pET-22b (+)	
KSR123_DN	GTGGTGGTGGTGGTGGTGCATATGTATATCTCCTTCTTAAAGTTAAACAAAATTATTTC		
KSR238-UP	TTAACTTTAAGAAGGAGATATACATATGTATACAGTAGGAGATTACCTATTAGACCG		KSR238
KSR238-DN	GGGCTTTGTTAGCAGCCGGATCTCAGTGGTGGTGGTGGTGGTGTGATTTATTTTGTTCAGCAAATAGTTTGCCC	*L. lactis*	
KSR201_UP	TGAGATCCGGCTGCTAACAAAGC	pET-22b (+)	
KSR201_DN	ATGTATATCTCCTTCTTAAAGTTAAACAAAATTATTTCTAGAGGGG		

Table 2-3. Kivd activity of purified putative decarboxylases from thermophiles.

Organism	Gene locus	His-tag location	K_{cat} (s^{-1})
G. thermoglucosidasius	Geoth_3495	N- terminus	1.1
G. thermodenitrificans	Gtng_0348	N- terminus	0.4
	Gtng_0651	N- terminus	0.1
	Gtng_1810	C- terminus	ND
	Gtng_1891	C- terminus	ND

2.9 Reference

Argyros, D.A., Tripathi, S.A., Barrett, T.F., Rogers, S.R., Feinberg, L.F., Olson, D.G., Foden, J.M., Miller, B.B., Lynd, L.R., Hogsett, D.A., others, 2011. High ethanol titers from cellulose using metabolically engineered thermophilic, anaerobic microbes. Applied and Environmental Microbiology 77, 8288-8294.

Atsumi, S., Hanai, T., Liao, J.C., 2008. Non-fermentative pathways for synthesis of branched-chain higher alcohols as biofuels. Nature 451, 86–89.

Atsumi, S., Higashide, W., Liao, J.C., 2009. Direct photosynthetic recycling of carbon dioxide to isobutyraldehyde. Nat Biotech 27, 1177–1180.

Atsumi, S., Li, Z., Liao, J.C., 2009. Acetolactate synthase from *Bacillus subtilis* serves as a 2-ketoisovalerate decarboxylase for isobutanol biosynthesis in *Escherichia coli*. Applied and Environmental Microbiology 75, 6306.

Atsumi, S., Wu, T.Y., Eckl, E.M., Hawkins, S.D., Buelter, T., Liao, J.C., 2010. Engineering the isobutanol biosynthetic pathway in *Escherichia coli* by comparison of three aldehyde reductase/alcohol dehydrogenase genes. Applied microbiology and biotechnology 85, 651–657.

Balsan, G., Astolfi, V., Benazzi, T., Meireles, M., Maugeri, F., Di Luccio, M., Dal Prá, V., Mossi, A., Treichel, H., Mazutti, M., 2012. Characterization of a commercial cellulase for hydrolysis of agroindustrial substrates. Bioprocess and Biosystems Engineering 35, 1229–1237.

Bhandiwad, A., Guseva, A., Lynd, L., 2013. Metabolic engineering of *Thermoanaerobacterium thermosaccharolyticum* for increased *n*-Butanol production. Advances in Microbiology 2013, 3, 46-51

Bhandiwad, A., Joe Shaw, A., Guss, A., Guseva, A., Bahl, H., Lynd, L.R. Metabolic engineering of *Thermoanaerobacterium saccharolyticumfor n*-butanol production. Metabolic Engineering 21, 17–25.

Brodeur, G., Yau, E., Badal, K., Collier, J., Ramachandran, K.B., Ramakrishnan, S., 2011. Chemical and physicochemical pretreatment of lignocellulosic biomass: A Review. Enzyme Research 2011.

Cripps, R.E., Eley, K., Leak, D.J., Rudd, B., Taylor, M., Todd, M., Boakes, S., Martin, S., Atkinson, T., 2009. Metabolic engineering of *Geobacillus thermoglucosidasius* for high yield ethanol production. Metabolic Engineering 11, 398–408.

Gollop, N., Damri, B., Barak, Z., Chipman, D.M., 1989. Kinetics and mechanism of acetohydroxy acid synthase isozyme III from Escherichia coli. Biochemistry 28, 6310–6317.

Gollop, N., Damri, B., Chipman, D.M., Barak, Z., 1990. Physiological implications of the substrate specificities of acetohydroxy acid synthases from varied organisms. J Bacteriol 172, 3444–3449.

Guarente, L., 1983. Yeast promoters and lacZ fusions designed to study expression of cloned genes in yeast. Meth. Enzymol. 101, 181–191.

Higashide, W., Li, Y., Yang, Y., Liao, J.C., 2011. Metabolic engineering of *Clostridium cellulolyticum* for production of isobutanol from cellulose. Applied and Environmental Microbiology 77, 2727.

Ingram, L.O., Aldrich, H.C., Borges, A.C.C., Causey, T.B., Martinez, A., Morales, F., Saleh, A., Underwood, S.A., Yomano, L.P., York, S.W., Zaldivar, J., Zhou, S., 1999. Enteric bacterial catalysts for fuel ethanol production. Biotechnol. Prog. 15, 855–866.

Keller, M.W., Schut, G.J., Lipscomb, G.L., Menon, A.L., Iwuchukwu, I.J., Leuko, T.T., Thorgersen, M.P., Nixon, W.J., Hawkins, A.S., Kelly, R.M., Adams, M.W.W., 2013. Exploiting microbial hyperthermophilicity to produce an industrial chemical, using hydrogen and carbon dioxide. PNAS 201222607.

Ko, C.-H., Tsai, C.-H., Lin, P.-H., Chang, K.-C., Tu, J., Wang, Y.-N., Yang, C.-Y., 2010. Characterization and pulp refining activity of a *Paenibacillus campinasensis* cellulase expressed in Escherichia coli. Bioresour. Technol. 101, 7882–7888

Lee, Y.-J., Kim, B.-K., Lee, B.-H., Jo, K.-I., Lee, N.-K., Chung, C.-H., Lee, Y.-C., Lee, J.-W., 2008. Purification and characterization of cellulase produced by *Bacillus amyoliquefaciens* DL-3 utilizing rice hull. Bioresour. Technol. 99, 378–386.

Li, H., Opgenorth, P.H., Wernick, D.G., Rogers, S., Wu, T.Y., Higashide, W., Malati, P., Huo, Y.X., Cho, K.M., Liao, J.C., 2012. Integrated electromicrobial conversion of CO_2 to higher alcohols. Science 335, 1596–1596.

Liu, J., Xia, W., 2006. Purification and characterization of a bifunctional enzyme with chitosanase and cellulase activity from commercial cellulase. Biochemical Engineering Journal 30, 82–87.

Lynd, L., 1989. Production of ethanol from lignocellulosic materials using thermophilic bacteria: Critical evaluation of potential and review, in: lignocellulosic materials, advances in biochemical engineering/biotechnology. Springer Berlin / Heidelberg, pp. 1–52.

Ma, K., Hutchins, A., Sung, S.-J.S., Adams, M.W.W., 1997. Pyruvate ferredoxin oxidoreductase from the hyperthermophilic archaeon, *Pyrococcus furiosus*, functions as a CoA-dependent pyruvate decarboxylase. PNAS 94, 9608–9613.

Machado, H.B., Dekishima, Y., Luo, H., Lan, E.I., Liao, J.C., 2012. A selection platform for carbon chain elongation using the CoA-dependent pathway to produce linear higher alcohols. Metabolic Engineering 14, 504–511.

Nazina, T.N., Tourova, T.P., Poltaraus, A.B., Novikova, E.V., Grigoryan, A.A., Ivanova, A.E., Lysenko, A.M., Petrunyaka, V.V., Osipov, G.A., Belyaev, S.S., Ivanov, M.V., 2001. Taxonomic study of aerobic thermophilic bacilli: Descriptions of *Geobacillus subterraneus* Gen. Nov., Sp. Nov. and *Geobacillus uzenensis* Sp. Nov. from petroleum reservoirs and transfer of *Bacillus stearothermophilus*, *Bacillus thermocatenulatus*, *Bacillus thermoleovorans*, *Bacillus kaustophilus*, *Bacillus thermodenitrificans* to *Geobacillus* as the New Combinations *G. stearothermophilus*, G. Th. Int. J. Syst. Evol. Microbiol. 51, 433–446.

Patel, M.A., Ou, M.S., Harbrucker, R., Aldrich, H.C., Buszko, M.L., Ingram, L.O., Shanmugam, K.T., 2006. Isolation and characterization of acid-tolerant, thermophilic bacteria for effective fermentation of biomass-derived sugars to lactic acid. Applied and Environmental Microbiology 72, 3228–3235.

Patel, M.A., Ou, M.S., Ingram, L.O., Shanmugam, K.T., 2005. Simultaneous saccharification and co-fermentation of crystalline cellulose and sugar cane bagasse hemicellulose hydrolysate to lactate by a thermotolerant acidophilic *Bacillus sp.* Biotechnology Progress 21, 1453–1460.

Plaza, M., Fernández de Palencia, P., Peláez, C., Requena, T., 2004. Biochemical and molecular characterization of α-ketoisovalerate decarboxylase, an enzyme involved in the formation of aldehydes from amino acids by *Lactococcus lactis*. FEMS microbiology letters 238, 367–374.

Scrutton, N.S., Berry, A., Perham, R.N., 1990. Redesign of the coenzyme specificity of a dehydrogenase by protein engineering. Nature 343, 38–43.

Shaw, A.J., Podkaminer, K.K., Desai, S.G., Bardsley, J.S., Rogers, S.R., Thorne, P.G., Hogsett, D.A., Lynd, L.R., 2008. Metabolic engineering of a thermophilic bacterium to produce ethanol at high yield. PNAS 105, 13769–13774.

Smith, K.M., Cho, K.-M., Liao, J.C., 2010. Engineering *Corynebacterium glutamicum* for isobutanol production. Applied microbiology and biotechnology 87, 1045–1055.

Sun, Y., Cheng, J., 2002. Hydrolysis of lignocellulosic materials for ethanol production: a review. Bioresour. Technol. 83, 1–11.

Tang, Y.J., Sapra, R., Joyner, D., Hazen, T.C., Myers, S., Reichmuth, D., Blanch, H., Keasling, J.D., 2009. Analysis of metabolic pathways and fluxes in a newly discovered thermophilic and ethanol-tolerant Geobacillus strain. Biotechnology and Bioengineering 102, 1377–1386.

Weinstock, O., Sella, C., Chipman, D.M., Barak, Z., 1992. Properties of subcloned subunits of bacterial acetohydroxy acid synthases. Journal of bacteriology 174, 5560.

Xiao, Z., Wang, X., Huang, Y., Huo, F., Zhu, X., Xi, L., Lu, J.R., 2012. Thermophilic fermentation of acetoin and 2,3-butanediol by a novel *Geobacillus* strain. Biotechnology for Biofuels 5, 88.

Yang, Y. T., M. Peredelchuk, G. N. Bennett, and K. Y. San., 2000. Effect of variation of *Klebsiella pneumoniae* acetolactate synthase expression on metabolic flux redistribution in *Escherichia coli*. Biotechnol. Bioeng. 69:150–159.

3. Consolidated bioprocessing of cellulose to isobutanol using *Clostridium thermocellum*

Disclaimer: This chapter was originally published with the same title in Metabolic Engineering 31 (2015) 44-52.

3.1 Abstract

Consolidated bioprocessing (CBP) has the potential to reduce biofuel or biochemical production costs by processing cellulose hydrolysis and fermentation simultaneously without the addition of pre-manufactured cellulases. In particular, *Clostridium thermocellum* is a promising thermophilic CBP host because of its high cellulose decomposition rate. Here we report the engineering of *C. thermocellum* to produce isobutanol. Metabolic engineering for isobutanol production in *C. thermocellum* is hampered by enzyme toxicity during cloning, time-consuming pathway engineering procedures, and slow turnaround in production tests. In this work, we first cloned essential isobutanol pathway genes under different promoters to create various plasmid constructs in *Escherichia coli*. Then, these constructs were transformed and tested in *C. thermocellum.* Among these engineered strains, the best isobutanol producer was selected and the production conditions were optimized. We confirmed the expression of the overexpressed genes by their mRNA quantities. We also determined that both the native ketoisovalerate oxidoreductase (KOR) and the heterologous ketoisovalerate decarboxylase (KIVD) expressed were responsible for isobutanol production. We further found that the plasmid was integrated into the chromosome by single crossover. The resulting strain was stable without antibiotic selection pressure. This strain produced 5.4 g/L of isobutanol from cellulose in minimal medium at 50 °C within 75 h, corresponding to 41% of theoretical yield.

3.2 Introduction

Lignocellulose instead of sugar as the raw material for biofuel and biochemicals production can potentially provide the quantity needed to make a significant impact, improve net carbon and energy balances, lower production cost, and avoid the food vs. fuel dilemma (Lynd et al., 2005 and Lynd et al., 2008). However, biomass recalcitrance—resistance to degradation—currently limits the use of lignocellulose. Consolidated bioprocessing (CBP) is a potential solution in which cellulose hydrolysis and fermentation occur simultaneously without added cellulase. *Clostridium thermocellum* is a promising thermophilic CBP host because of its high cellulose deconstruction rate. Recent studies of metabolic features of *C. thermocellum* (Zhou et al., 2013) and advances in genetic modification tools (Tyurin et al., 2004, Tripathi et al., 2010 and Argyros et al., 2011) for *C. thermocellum* make the CBP organism an attractive platform for biofuel or biochemical production.

Longer-chain alcohols offer advantages as a gasoline substitute or drop-in fuel (Atsumi et al., 2008). In particular, isobutanol received significant attention because it can be used as fuel or a feedstock chemical. Isobutanol can be dehydrated to form isobutene, which can then be oligomerized to C8 then C12 alkenes to be use as jet fuel. The C8 alkene can also be dehydrocyclized to form p-xylene Peters et al., (2011), which can then be oxidized to form terephthalic acid as a monomer for the common plastic polyethylene terephthalate (PET). Microbial production of isobutanol from renewable sources has been demonstrated in multiple engineered organisms (Atsumi et al., 2008, Atsumi et al., 2009, Smith et al., 2010, Higashide et al., 2011, Li et al., 2012 and Lin et al., 2014), indicating the flexibility of the pathway. Isobutanol production from cellulose has also been demonstrated using a cellulolytic organism, *Clostridium*

cellulolyticum (Higashide et al., 2011). However, this organism has a low cellulolytic rate and a long doubling time, and is not suitable for CBP. *C. thermocellum* offers much higher cellulose decomposition rate and has the ability to grow at elevated temperatures (50–60 ◦C), which facilitate cellulose degradation and reduce the chance of contamination compared to the case at mesophilic temperatures. Here, we seek to produce isobutanol directly from cellulose to achieve high titer using *C. thermocellum*.

C. thermocellum genetic tools (Tripathi et al., 2010, Argyros et al., 2011, Guss et al., 2012 and Deng et al., 2013) and isobutanol pathway at elevated temperatures (Lin et al., 2014) have been previously reported. In addition, selected *C. thermocellum* promoters have been characterized (Olson et al., 2015). However, the apparent toxicity of the isobutanol pathway genes severely limits the applicability of these genetic systems. Thus, we developed a strategy to overcome this problem and screened for appropriate promoter combinations to express the necessary genes for the pathway, and constructed various strains for isobutanol production using the available plasmid-based system (Argyros et al., 2011, Guss et al., 2012 and Deng et al., 2013). We then characterized the strains constructed, determined the gene copy number, identified native enzymes potentially involved in isobutanol biosynthesis, and optimized the production conditions.

3.3 Methods

3.3.1 Bacterial strains and plasmids

C. thermocellum DSM 1313 Δ*hpt* was a gift from Katherine Chou from the National Renewable Energy Laboratory. We referred *C. thermocellum* DSM 1313 Δ*hpt* as the wild type strain in this study because the Δ*hpt* is used for the sole purpose of counter-selection when needed, and has no effect on growth and fermentation. *Escherichia coli*BL21 (New England Biolabs,

Ipswich, MA) and MDS™42 LowMut Δ*recA* (Pósfai et al., 2006) (SCARAB genomics, Madison, WI) were used as host for plasmid construction. Strains and plasmids used in this study are listed in Table 3.1.

All plasmids were constructed by DNA assembly techniques. Both vector and inserts (target genes) were amplified by PCR using Phire Hot Start II DNA polymerase (Thermo Scientific, Hudson, NH). PCR products were purified by a PCR purification Kit (Zymo Research, Irvine, CA). The vector and insert were mixed with Gibson Assembly Master Mix (New England Biolabs, Ipswich, MA) and incubated at 50 °C for 1 h. Then the assembly product was transformed to BL21 or MDS™42 LowMut Δ*recA* strain. The presence of correctly cloned inserts was determined by colony PCR and DNA sequencing (Retrogen, San Diego, CA).

3.3.2 Chemicals and reagents

All chemicals unless otherwise specified were acquired from Sigma-Aldrich (St. Louis, MO) or Thermo Scientific. Phire Hot Start II DNA polymerase was purchased from New England Biolabs.

3.3.3 Media and cultivation

All *E. coli* strains were grown in LB or TB medium containing appropriate antibiotics at 37 °C on a rotary shaker (250 rpm). Antibiotics were used at the following concentrations: ampicillin, 200 μg/ml; kanamycin, 50 μg/ml; chloramphenicol, 20 μg/ml.

Except for small scale isobutanol production, all *C. thermocellum* strains were cultured inside a Coy anaerobic chamber (Coy Laboratory Products, Grass Lake, MI) in a modified CTFuD medium (Tripathi et al., 2010) at 50 °C incubation . CTFuD medium contains the following components: 3 g/L of sodium citrate tribasic dehydrate, 1.3 g/L ammonium sulfate, 1.43 g/L

potassium phosphate monobasic, 1.37 g/L potassium phosphate dibasic, 0.5 g/L cysteine-HCl, 21 g/L MOPS, 6 g/L glycerol-2-phospate disodium, 5 g/L cellobiose, 4.5 g/L yeast extract, 0.01 g/L calcium chloride, 0.011 g/L magnesium chloride, 0.0006 g/L ferrous sulfate heptahydrate, 0.01 g/L thiamin, and 0.001 g/L resazurin. Antibiotics were used at the following concentrations: thiamphenicol 20 ug/ml. In addition, 2.5 g/L sodium bicarbonate was used to enhance *C. thermocellum*growth.

Stock cultures of *E. coli* were maintained at −80 °C in 13% (v/v) glycerol. Stock cultures of *C. thermocellum* were maintained at −80 °C directly.

3.3.4 *C. thermocellum* transformation

C. thermocellum electro-competent cells were freshly prepared as described (Guss et al., 2012). Briefly, *C. thermocellum* DSM 1313 Δ*hpt* was grown in CTFuD medium at 50 °C inside a Coy anaerobic chamber till OD_{600} =0.4–1. The culture was chilled on ice for 10 min, and cells were collected by centrifugation in a 500 ml corning bottle at 4 °C and 6000 g for 40 min. Then supernatants were removed aerobically. To minimize disturbance, cell pellets were washed with 400 ml ice MilliQ water (MQ) twice, and centrifuged at 4 °C and 6000*g* for 25 min. Lastly, pellets were resuspended with 200–500 µl electroporation buffer (250 mM sucrose and 10% glycerol) in the anaerobic chamber.

For each transformation, 25 µl of the competent cells were mixed with about 200–1000 ng of DNA in 1-mm-gap pre-chilled electroporation cuvettes (Molecular BioProducts, San Diego, CA). The mixtures were electroporated (1.2 kV, 1.5 m s square pulse) with a BioRad GenePulser XCell (BioRad Laboratories, Hercules, CA). Cells were immediately resuspended in 1 ml pre-warmed CTFuD medium, then plated by mixing with 25 ml molten CTFuD medium (0.8% agar)

containing 20 μg/ml thiamphenicol without recovery period. The plates were incubated at 50 °C anaerobically for up to one week.

3.3.5 Screening isobutanol production strain from *C. thermocellum* recombinants

To screen for our isobutanol producing strain, 2 ml of engineered *C. thermocellum* DSM 1313 Δ*hpt* cultures were grown until stationary phase (OD_{600}=0.9–1.2) and centrifuged in 2 ml tubes at 6000*g* at 25 °C for 10 min. The pellets were resuspended in 1 ml CTFuD medium containing 100 g/L cellulose and 20 ug/ml thiamphenicol. The production was performed at 50 °C. Isobutanol was measured by gas chromatography after 24 h.

3.3.6 Optimization of production condition using small scale fermentation

Low-carbon minimal growth medium (LC medium) (Holwerda et al., 2012) was the starting point for optimizing isobutanol production. Optimization was studied using recombinant CT24*(CT24 strain with two point mutations on *kivd*, but no significant difference in isobutanol production compared to CT24). A small scale fermentation process was used in order to have faster experiment turnover rate. First, CT24* was pre-cultured in 50–250 ml of CTFuD medium till log phase (OD_{600}=0.2–0.6) or stationary phase (OD_{600}=0.9–1.2). Then, the culture was concentrated to 3 ml LC medium with 100 g/L cellulose at OD_{600}=3.3 or 16 with varying medium composition to start isobutanol production. During the production, pH was checked by pH strip (EMD Millipore, Billerica, MA) and titrated every 2 h by 45% KOH. Cells and cellulose were vigorous mixed every 2 h.

3.3.7 Isobutanol production

To examine isobutanol production, engineered *C. thermocellum* DSM 1313 Δ*hpt* cultures were grown till stationary phase (OD_{600}=0.9–1.2) and centrifuged at 4300 rpm at 40 °C for 30 min.

Supernatant was removed and pellets were resuspended in LC medium. LC medium contains the following constituents: 100 g/L cellulose, 0.4 g/L urea, 5 g/L cellobiose, 21 g/L MOPS, 2 g/L potassium phosphate monobasic, 3 g/L potassium phosphate dibasic, 0.1 g/L cysteine-HCl, 0.05 g/L calcium chloride, 0.2 g/L magnesium chloride, 0.0035 g/L ferrous sulfate heptahydrate, 2.5 g/L sodium bicarbonate, 0.02 g/L pyridoxamine dihydrochloride, 0.004 g/L PABA, 0.002 g/L biotin, 0.002 g/L B12, and 0.01 g/L thiamin. For *C. thermocellum* cultures, antibiotics were used at the following concentration: thiamphenicol 20 ug/ml. Production of isobutanol was carried out in 5 mL centrifuge tubes with 3 mL of LC medium at pH 7.5, and 50 °C anaerobic incubation. Samples were maintained at pH=7.5 in 2 h intervals.

3.3.8 Cellulose measurement

Quantitative saccharification assay (Sluiter et al., 2008) was used for cellulose concentration measurement. First, 100 µL homogeneous medium solution were aliquoted into 1.5 mL microcentrifuge tubes and spun down for 2 min at 15,000 rpm. The supernatant was removed and the cellulose pellet was resuspended and vortexed in 1 mL of MQ twice. Following the last wash, samples were incubated overnight at 55 °C to dry pellets. Then, the dried samples were added to 143 µL of 72% H_2SO_4 and incubated samples for 1 h at 30 °C on an Eppendorf Thermomixer (Eppendorf, Hauppauge, NY) until the cellulose was completely dissolved. The solubilized samples were transferred to 5 ml centrifuge tubes with 4 mL of MQ and autoclaved for 1 h. Then, 500 µL autoclaved sample was then filtered to a 2 ml vial. Lastly, cellulose concentration was measured by first degrading to glucose, which was quantitatively measured via high-performance liquid chromatography (Agilent, Hanover, NH) with Aminex HPX-87 column (Biorad Laboratories, Hercules, CA).

3.3.9 Measuring gene transcription using quantitative real-time PCR (qRTPCR)

C. thermocellum cell samples were prepared using the same procedure as in isobutanol fermentation process. At the predetermined time point, 300 µl cell culture ($1.6x10^{10}$ cfu/ml) was collected and immediately mixed with 2 volumes of Qiagen RNAprotect bacteria agent to stabilize intracellular RNA. The cells were lysed with proteinase K and 15 mg/ml lysozyme in Tris buffer at pH 8.0 for 2 h. Total mRNA was subsequently extracted using Qiagen RNeasy Mini kit following the manufacturer′s protocol. RNase-free DNase (Qiagen) was further used to treat the RNA column to minimize the genomic DNA contamination.

The qRTPCR reaction was carried out using iScript Reverse Transcription Supermix (BioRad) following the manufacturer′s protocol. A typical reaction of 20 µl contains 10 µl iScript RT Supermix solution, 300 nM of each primer, 500 ng RNA sample, and 0.25 µl reverse transcriptase. The reactions were carried out in a 96-well plate using BioRad CFX96 Real Time System. The qRTPCR results were analyzed with the ΔC_T method using *recA* as the reference gene. The list of primers used in qRTPCR is listed in Table 3.2.

3.3.10 Measuring plasmid copy number using quantitative real-time PCR

C. thermocellum cell samples were grown in CTFuD rich medium to reach the stationary phase. The cells were subsequently washed with MQ through two cycles of centrifugation and resuspension. The concentrated cell suspensions were then subject to 98 °C for 4 min in a thermal cycler. The insoluble *C. thermocellum* cell debris was removed from the heat-treated samples after centrifugation, and the supernatant that contains *C. thermocellum* cell total DNA was collected for plasmid copy number analysis.

The qRTPCR reaction and the subsequent data analysis to determine plasmid copy number was carried out following the sample procedure as in the previous measurement of gene transcription, except no reverse transcriptase was added in the reaction mixture.*recA* was used as the reference gene in *C. thermocellum* genomic DNA, and *repB* was used as the plasmid-specific gene to determine the plasmid copy number.

3.3.11 Isobutanol dehydrogenase enzyme assay

The isobutanol dehydrogenase enzyme assay was carried out at 50 °C using an Agilent 8453 UV–vis spectrophotometer. The reaction mixture contains 40 mM Tris–Cl at pH 7.0, 5 mM dithiothreitol (DTT), 300 µM NADH/NADPH, 20 mM isobutaldehyde and crude extract. The reaction was initiated with the addition of isobutaldehyde. The rate of the enzymatic reaction was monitored with the decrease of absorption at 340 nm, corresponding to the consumption of NADH/NADPH. The total protein concentration was quantified using Bradford assay (BioRad).

3.3.12 Ketoisovalerate ferrodoxin-dependent reductase (KOR) enzyme assay

The KOR enzyme assay procedure was adapted from a previously reported protocol (Heider et al., 1996). The assay was carried out at 50 °C using the Agilent 8453 UV–vis spectrophotometer under strict anaerobic condition. The reaction mixture contained 200 mM potassium phosphate at pH 7.0, 5 mM thiamine pyrophosphate (TPP), 10 mM methyl viologen, 10 mM DTT, 2 mM $MgCl_2$, 2 mM coenzyme A, 6 mM KIV, if indicated, and crude extract. The reaction was initiated with the addition of *C. thermocelllum* crude extract. The rate of the enzymatic reaction was monitored with the increase of absorption at 604 nm, corresponding to the reduction of methyl viologen. The total protein concentration was quantified using Bradford assay (BioRad).

3.3.13 Strain stability assay

The *C. thermocellum* CT24 was prepared by freshly inoculating antibiotic-free CTFuD rich media from strain freeze stock. Then, the *C. thermocellum* culture at late exponential or early stationary phase (OD_{600}=0.8–1.5) was used for 10% inoculation to a fresh antibiotic-free CTFuD medium. The CT24 culture sample was taken at each cell passage and plated onto CTFuD agar with or without 20 µg/ml thiamphenicol. The difference in the number of colonies subsequently formed is used to determine the percentage of cells that retained the gene integration.

3.4 Results and discussion

3.4.1 Toxicity of acetohydroxyacid synthase

Our previous work using *Geobacillus thermoglucosidasius* (Lin et al., 2014) confirms that the isobutanol pathway enzymes, specifically, *Bacillus subtilis* acetolactate synthase (AlsS) and *L. lactis* KIVD, are functional *at an elevated temperature* (50 °C). This result suggests that the pathway should work in *C. thermocellum*. In addition, various genes have been expressed by native glyceraldehyde-3-phosphate dehydrogenase (*gapDH*), cellobiose phosphorylase (*cbp)* and enolase promoters (Tripathi et al., 2010 and Deng et al., 2013) in *C. thermocellum*. Based on these results, we began by overexpressing *L. lactis kivd* and *B. subtilis alsS* driven by the *gapDH* promoter. However, *C. thermocellum*transformation of the plasmids containing *gapDH* driven *L. lactis kivd* or *B. subtilis alsS*were unsuccessful after repeated attempts. A similar phenomenon was also observed in*C. cellulolyticum* when transforming a plasmid to express *B. subtilis* AlsS (Higashide et al., 2011). Cloning of genes having the same activity, such as *ilvBN* from various organisms, encountered similar difficulty (Li and Liao, 2015). During the cloning process, the *E. coli* host recognized the foreign promoters used and expressed the gene in an uncontrolled fashion. The

metabolic changes then upset the host and resulted in either no colonies or colonies with inactivated genes. Interestingly, the *ilvB* clones almost always contain an insertion sequence IS10 (Fig. 3.1) at specific positions (956, 1078, and 1315 bp). Kovarík et al. (2001) reported an IS10 transposition event which occurred incidentally during gene cloning. Use of the Clean Genome® strain (Pósfai et al., 2006) alleviated the insertion problem and facilitated plasmid construction.

3.4.2 Selection of appropriate promoters for expressing isobutanol pathway genes in *C. thermocellum*

Insufficient expression of the pathway genes cannot produce high titers of isobutanol, while excessive expression may cause toxicity. Therefore, we had to select for a set of appropriate promoters to express the isobutanol pathway in *C. thermocellum* without compromising cell growth.

We started by applying the prevailing strategy (Fig. 3.2A) for prospecting promoters in *C. thermocellum* using a thermostable *lacZ as a reporter*. Promoters of various strengths were chosen to overexpress enzymes in the isobutanol pathway. However, the success of individual promoters does not necessarily translate to a functional pathway when combined, particularly because of the metabolic imbalance issue that may lead to toxicity. Therefore, we applied an alternative strategy (Fig. 3.2B) to directly screen for isobutanol production. We cloned all of the necessary genes (*kivd* from *L. lactis*, *alsS* from *B. subtilis* or *ilvBN* from *C. thermocellum*, and *ilvCD* from *C. thermocellum*) for isobutanol production under varying promoters to create different constructs. We included *C. thermocellum* AHAS (coded by *ilvBN*) as the enzyme to catalyze the first step in the isobutanol pathway, because this enzyme is relatively insensitive to feedback inhibition. These

constructs excluded alcohol dehydrogenase (Fig. 3.3A) because the enzyme activity (NADPH-dependent) is present in *C. thermocellum* crude extract (Fig. 3.9).

However, cloning remains challenging due to the toxicity of overexpressing enzymes in the isobutanol pathway. All target plasmids containing the *alsS* gene driven by *C. thermocellum* promoters were unable to be constructed. We constructed 120 different plasmids using various promoters at the P1 and P2 positions and the native *ilvD* promoter for the P3 position (Table 3.3 and Table. 3.4 and 3.5) (Fig. 3.3A). 21 plasmids were sequence-verified and transformed into *C. thermocellum*. Then, these engineered *C. thermocellum* strains were tested in the rich CTFuD medium at 50 ^{o}C for isobutanol production. The best strain (CT24) produced 0.6 g/L of isobutanol within 24 h in the un-optimized condition (Fig. 3.3B).

We tested the effect of overexpressing isobutanol dehydrogenase. Two thermostable isobutanol dehydrogenase enzymes from *G. thermoglucosidasius,* one NADH-dependent (Geoth_3237) and one NADPH-dependent (Geoth_3823) (Lin et al., 2014), were cloned onto the pCT24 backbone to make pCT228 and pCT229. These plasmids were transformed to *C. thermocellum* to make strains CT228 and CT229. However, both CT228 and CT229 had no significant effect on isobutanol production compared to CT24 strain (Fig. 3.5). This suggests isobutanol dehydrogenase is not the limiting step in isobutanol production of our recombinant strain CT24.

3.4.3 Optimization of production conditions from cellulose

Although many defined minimal growth medium for *C. thermocellum* have been previously reported (Fleming and Quinn, 1971, Johnson et al., 1981 and Holwerda et al., 2012), medium composition has not been optimized for isobutanol production. We chose the LC medium

(Holwerda et al., 2012) with Avicel cellulose as the starting point for optimizing isobutanol production. To accelerate the turnover rate of the experiment and explore better production conditions, we developed a small scale high density fermentation as mentioned previously. Initially, the target strain was grown in CTFuD medium for the fast growth rate. Then, the culture was concentrated to higher density to achieve higher productivity and to mimic industrial processes.

We varied the medium composition (vitamin, bicarbonate, urea and pH). Lower urea concentration (from 7.5 g/L to 1 g/L) improved isobutanol production titer 2.4 fold (Fig. 3.4A), but had no significant effect on ethanol production (Fig. 3.4B). High urea concentration favored valine production, while low urea shifted the product to isobutanol, as expected (Fig. 3.11). Further, we focused on optimizing the pre-culture condition and density (OD_{600}) after suspension. Fig. 3.12 shows that cell harvesting at the stationary phase (OD_{600}=1.1) increased both isobutanol and ethanol production almost twofold as a result of less valine and lactate production. Pre-culture with cellulose and mixing during production had no significant effect on isobutanol production (Fig. 3.12A), yet increased density (OD_{600}=3.3–16) enhanced isobutanol production fivefold (Fig. 3.12A), as expected.

With the improved procedure, we tested isobutanol production from cellulose in LC medium using CT24. The strain was grown in CTFuD medium to OD_{600}=1–1.5, then concentrated to LC medium (80 g/L cellulose, pH=7.5, urea=0.4 g/L) at OD_{600}=16. Under this production protocol, 5.4 g/L of isobutanol was produced during 75 h (Fig. 3.5A). Since the initial cellulose concentration was 80 g/L, and the final concentration of cellulose was 46.4 g/L with 1.6 g/L glucose left in the medium, the yield roughly 41% of the theoretical maximum. The major byproducts during the CT24 fermentation were lactate, acetate and ethanol (Fig. 3.5B). The wild-

type control produced about 1.5 g/L of isobutanol, with a significant amount of valine (0.54 g/L for WT, 1.1 g/L for CT24) produced.

3.4.4 Confirming pathway overexpression with qRTPCR

In order to ascertain that the observed boost in isobutanol titer from our best production strain CT24 was a direct result of isobutanol pathway overexpression, quantitative real-time PCR (qRTPCR) was performed to measure the relative transcription level of five genes (*ilvB*, *ilvN*, *ilvC*, *ilvD* and *kivd*) constituting this pathway. The *recA* gene was selected as the reference in qRTPCR following previous studies (Stevenson and Weimer, 2005 and Wei and Fu, 2014). Under the optimized fermentation condition (Fig. 3.6A), a significant increase in mRNA levels was detected for all genes of interest (Fig. 3.6B). The most pronounced change, approximately fivefold increase in comparison to parental*C. thermocellum*, was observed for *ilvB*, *ilvN* and *ilvC*, all of which were under the control of native phosphoenolpyruvate carboxykinase (*pck*) promoter. Furthermore, the successful transcription of the non-native gene *kivd* was also confirmed in this experiment. A similar transcriptional pattern was observed for CT24 during the growth phase (Fig. 3.13, CTFuD medium and OD_{600}=1 medium cell density) . Taken together, these results indicate that the isobutanol pathway overexpression was responsible for the increase in isobutanol titer.

3.4.5 Enzymes catalyzing KIV decarboxylation

Ketoisovalerate (KIV) is the divergent point between valine biosynthesis and isobutanol production. As reported previously Holwerda et al. (2014), we also found that *C. thermocellum* wild type strain without genetic engineering is capable of producing detectable amounts of isobutanol (Fig. 3.5A) indicates that a KIVD-independent native pathway exists in this

organism to convert KIV to isobutanol. Examination of *C. thermocellum* DSM 1313 genome points to ketoisovalerate ferrodoxin-dependent reductase (KOR) as the most likely native enzyme to carry out the KIV decarboxylation reaction in the wild type strain (Fig. 3.7A). KOR had been previously reported in several anaerobic thermophiles (Heider et al., 1996). Three putative KOR genes (Clo1313_0020-0023, Clo1313_0382-0385 and Clo1313_1353-1356) were also annotated in *C. thermocellum* genome.

To verify that *C. thermocellum* has functional KOR to decarboxylate KIV to isobutyryl-CoA using coenzyme-A as a cofactor, we performed an anaerobic KOR enzyme assay following a previously reported protocol using wild type crude extract (Heider et al., 1996). The methyl viologen-based end point assay showed the presence of oxygen-sensitive KOR in *C. thermocellum* crude extract. This KOR enzyme activity was quantified in a subsequent kinetic assay to be 2.4 µmol/min/mg (Fig. 3.7 B and C).

The confirmation of native KOR activity naturally led us to consider whether KIVD overexpression is indeed needed for isobutanol production in CT24. In order to answer this question, we constructed a *C. thermocellum* strain to overexpress *ilvB, ilvN, ilvC and ilvD* using the same promoters as in CT24 while leaving out *kivd*. The resulting strain, termed CT242, showed an isobutanol titer measurably higher than wild type strain but significantly lower than CT24 (Fig. 3.5A and Fig. 3.14). Presumably, the overexpression of*ilvB, ilvN, ilvC and ilvD* was able to increase the flux to ketoisovalerate and the native KOR diverts this intermediate to isobutanol production in CT242. These results demonstrated that the KIV decarboxylation step in CT24 was carried out by a combined contribution from both KOR and KIVD.

3.4.6 Genome integration and strain stability

To determine the copy number of the plasmid in CT24, qRTPCR was used to quantify the gene copy number of *recA* (genome specific), *repB* (plasmid specific) and *ilvC* (exist both on genome and plasmid) using *C. thermocellum* CT24 total DNA (Skulj et al. 2008). The resulting ratio of *recA*:*repB*:*ilvC*=1:1:2 (Fig. 3.8A) indicates that, regardless of its DNA form, the plasmid exists as a single copy inside the cell. This result suggests that the plasmid may be integrated into the chromosome by single crossover. PCR was then used to amplify CT24 *ilvBNC* and *ilvHD* operons. As these two operons share sequence similarity with the plasmid, they are the potential sites for homologous recombination. The PCR products were then sequenced and the results conclusively showed that the plasmid expressing isobutanol pathway was integrated into the *ilvBNC* operon in the *C. thermocellum* genome via a single crossover (Fig. 3.8B).

Interestingly, this single-crossover genome insertion was observed in our study to be very stable even without antibiotic selection (Fig. 3.8C). Furthermore, genetically engineered CT24 strain was found to outcompete wild type *C. thermocellum* in a prolonged semi-continuous mixed culture using antibiotic-free CTFuD rich medium (data not shown), which suggested that the overexpression of isobutanol pathway may increase *C. thermocellum* fitness under certain growth conditions. This finding was further confirmed by growth measurement (Fig. 3.8D). This result also attests to the practical applicability of this strain and single crossover as a strain construction strategy.

3.5 Conclusion

In this work, we engineered *C. thermocellum* to produce isobutanol directly from cellulose. We first addressed the cloning difficulty in *E. coli* caused by an IS10 insertion which occurred due

to the enzyme toxicity of acetohydroxyacid synthase (encoded as*ilvBN*). Then we applied a strategy to select the best isobutanol producing engineered strain without compromising cell growth. The successful pathway overexpression was subsequently verified with qRTPCR. The activity of the native ketoisovalerate oxidoreductase (KOR), a key enzyme in the native isobutanol pathway, was also demonstrated. We further discovered that the plasmid in the best production strain was chromosomally integrated by a single crossover event. However, this strain was stable without the antibiotic selection pressure. The best engineered strain produced 5.4 g/L of isobutanol from cellulose in optimized minimal medium at 50 °C within 75 h, corresponding to 41% of theoretical yield. The success of this strain demonstrates that *C. thermocellum* is a promising CBP organism for isobutanol production from cellulose.

3.6 Figures

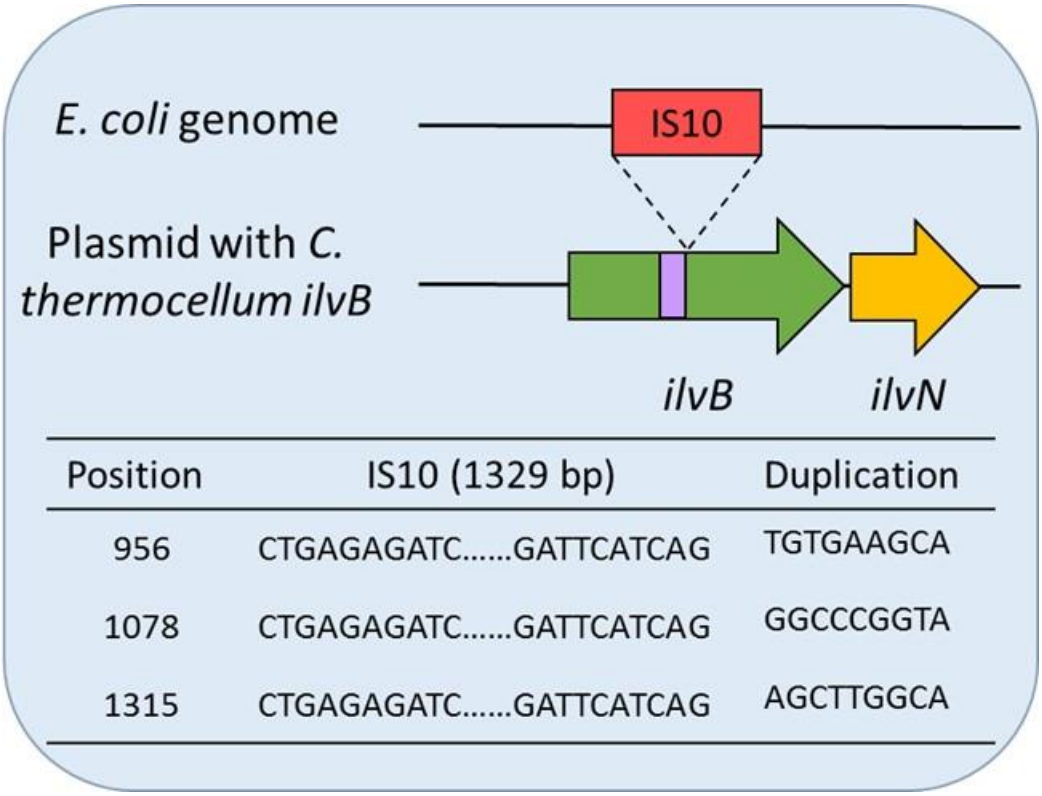

Position	IS10 (1329 bp)	Duplication
956	CTGAGAGATC……GATTCATCAG	TGTGAAGCA
1078	CTGAGAGATC……GATTCATCAG	GGCCCGGTA
1315	CTGAGAGATC……GATTCATCAG	AGCTTGGCA

Figure 2-7. Scheme of inactivated *C. thermocellum ilvB* with *E. coli* IS10 during cloning.

IS10 commonly inserts C. thermocellum ilvB at 956, 1078 and 1315 bp. Insertion starts at the end of the duplication sequence (represented here in purple).

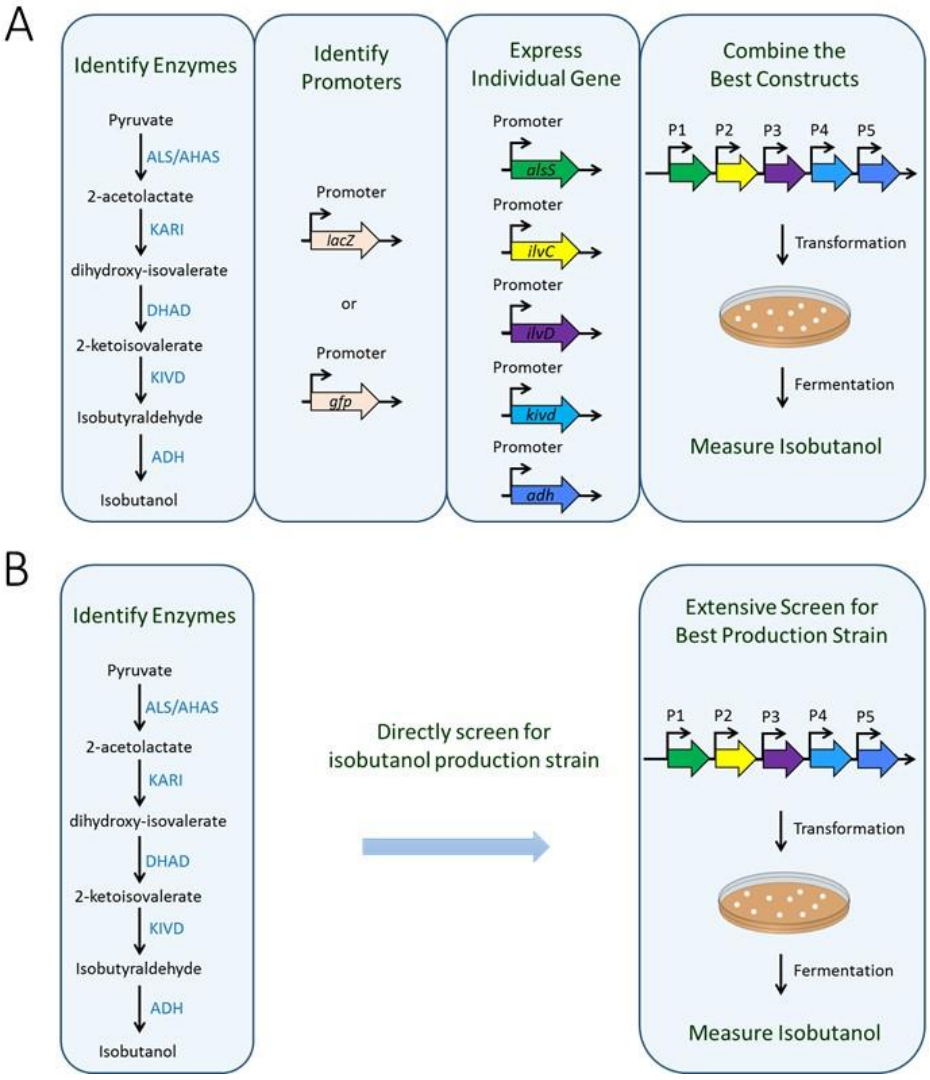

Figure 2-8. A streamline approach to direct screen isobutanol production in *C. thermocellum*. (A) Current metabolic approach for constructing isobutanol pathway in *C. thermocellum.* (B) An alternative approach to directly screen for best *C. thermocellum* isobutanol production recombinant.

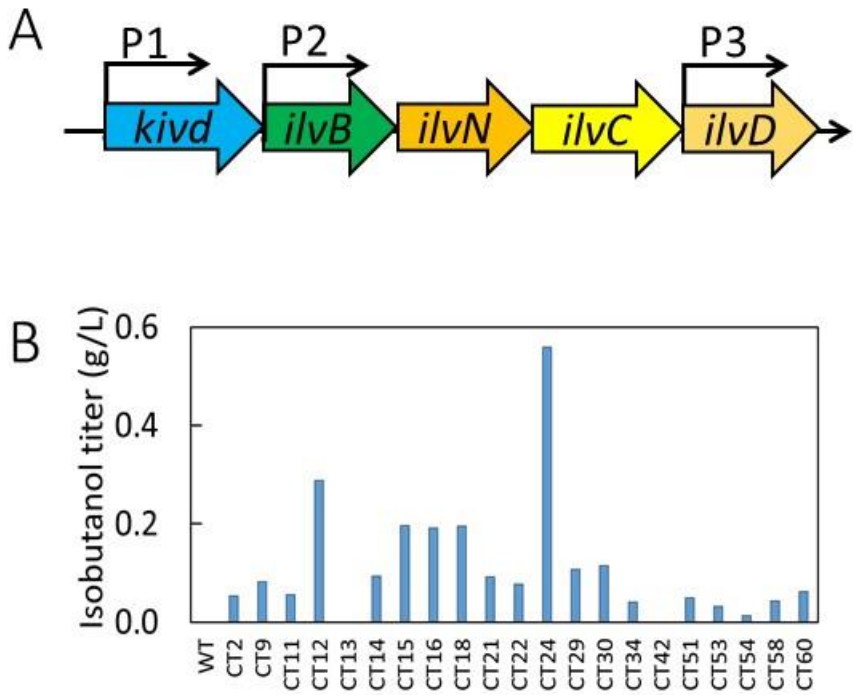

Figure 2-9. Plasmid construction configuration and isobutanol production titer in the engineered *C. thermocellum* strains.

(A) Plasmid constructs for overexpressing isobutanol pathway in *C. thermocellum*. P1, P2 represent individual promoter and P3 is the native *C. thermocellum ilvD* promoter. (B) Screening of isobutanol production from engineered *C. thermocellum* in CTFuD medium within 24 h. Recombinant strains were grown in CTFuD medium to OD_{600} = 1, then concentrated to CTFuD medium with 100 g/L cellulose at OD_{600} = 2.

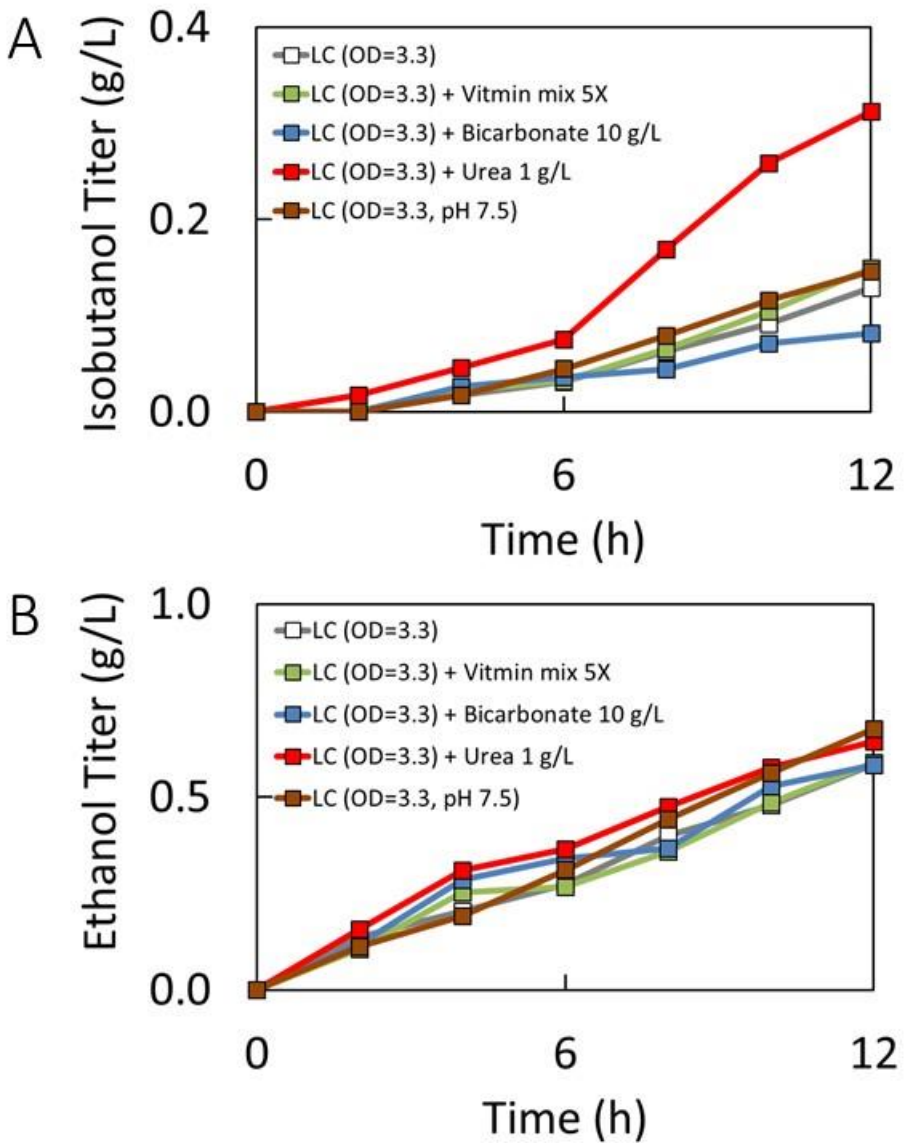

Figure 2-10. LC medium optimization for isobutanol production at 50 ^{o}C.

CT24* strain (CT24 strain with two point mutations on kivd, but no significant difference in isobutanol production compared to CT24) was grown in CTFuD medium to OD_{600} = 0.2, then concentrated to LC medium with 100 g/L cellulose at OD = 3.3.

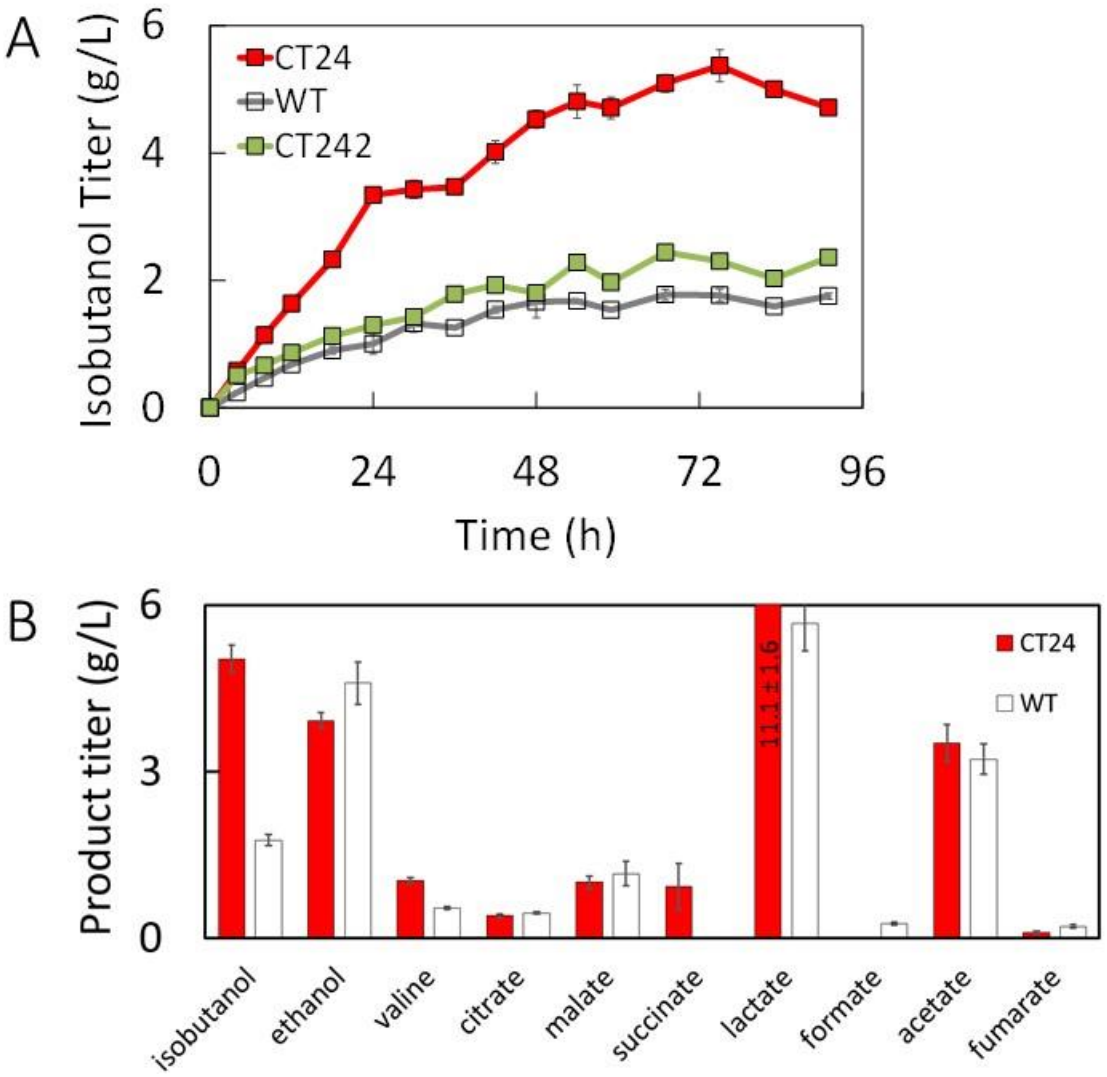

Figure 2-11. Isobutaol production and fermentation products formation during 75 h in LC medium.

Wild type, CT24 and CT242 strains were grown in CTFuD medium to OD_{600} = 1 - 1.2, then concentrated to LC medium (0.4 g/L urea) with 80 g/L cellulose at OD_{600} = 16 Error bar represents the standard deviation (n = 3).

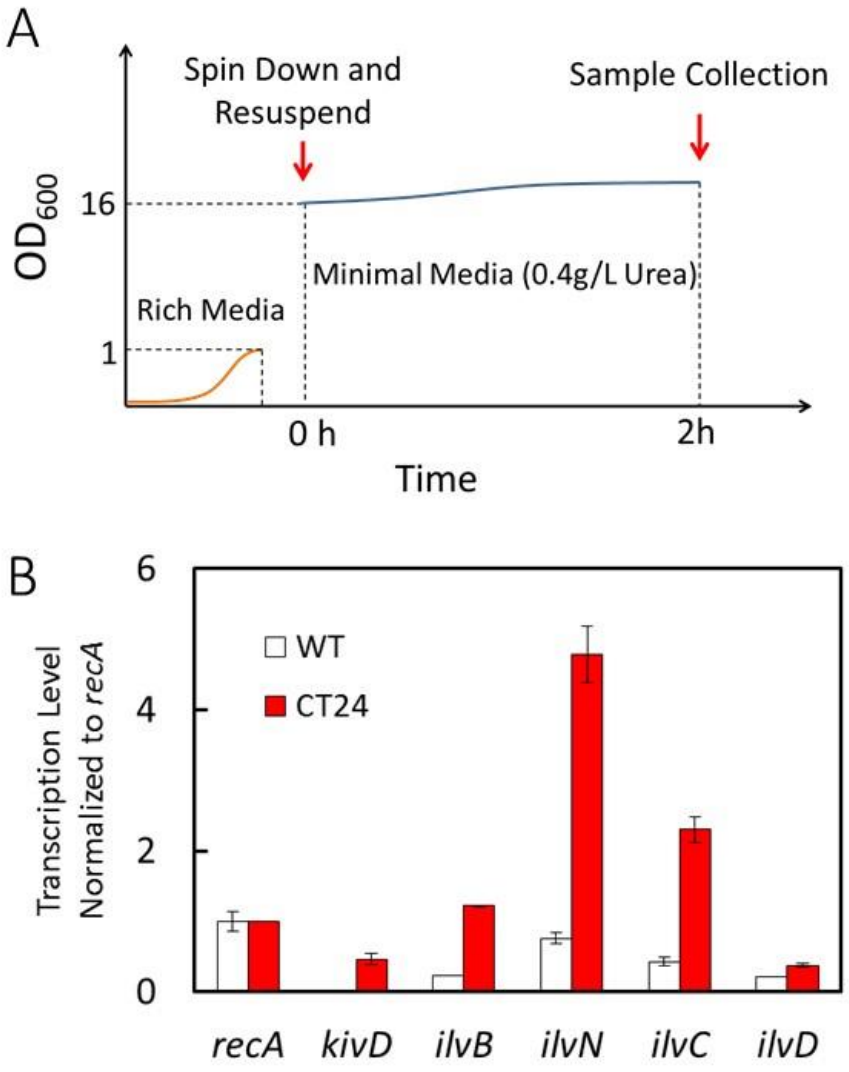

Figure 2-12. qRTPCR for gene transcription comparison between wild type *C. thermocellum* and isobutanol production strain (CT24) during fermentation.

(A) Scheme for collecting qRTPCR samples under isobutanol fermentation condition (B) Gene transcription comparison between wild type *C. thermocellum* and isobutanol production strain (CT24) during fermentation. *recA* was used as the reference gene in all samples. Error bar represents the standard deviation (n = 3).

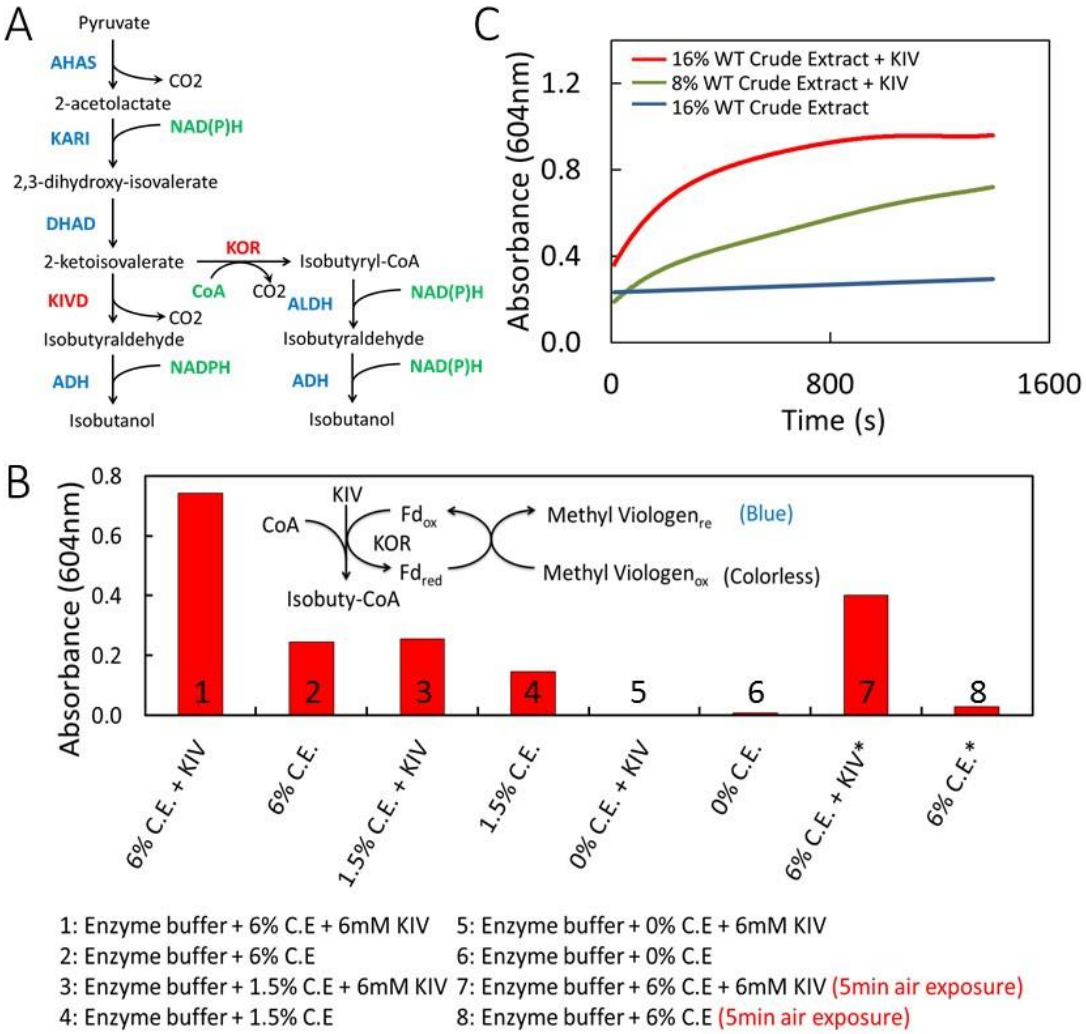

Figure 2-13. Identify the existing of KOR activity in *C. thermocellum* for isobutanol production.

(A) Two conversion routes of 2-ketoisovalerate to isobutanol in engineered *C. thermocellum* isobutanol production strain. (B) Anaerobic end point enzyme assay of native KOR enzyme activity using wild type *C. thermocellum* crude extract. (C) Anaerobic kinetic enzyme assay of native KOR enzyme activity using wild type *C. thermocellum* crude extract.

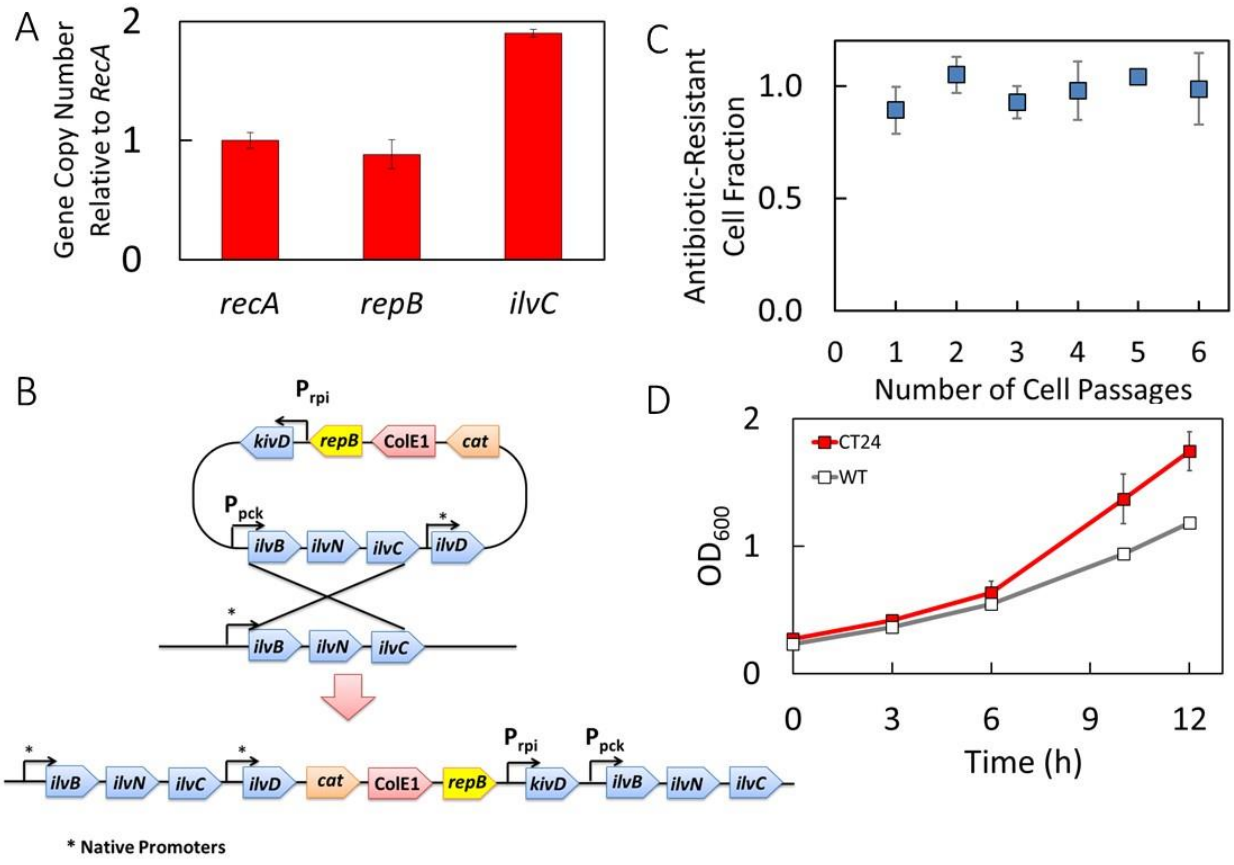

Figure 2-14. Plasmid integration and growth advantage in CT24.

(A) Determination of gene DNA copy number in CT24 using qRTPCR. Error bar represents the standard deviation (n = 3). (B) Sequencing verified plasmid genome integration after a single crossover in CT24. (C) Strain stability measured by the retention of antibiotics marker after growth and passage in antibiotic-free rich media. (D) Growth curve of CT24 and wild type strain in CTFuD medium without antibiotic pressure.

3.7 Tables

Table 2-4. List of strains and plasmids used in this study.

Name	Description[a]	Reference
Strain		
E. coli BL21	*fhuA2 [lon] ompT gal [dcm] ΔhsdS*	New England Biolabs
MDS™42 LowMut ΔrecA	MG1655 multiple-deletion strain (1) ΔdinB ΔpolB ΔumuDC (2) ΔIS609 ΔpatD ΔydcV ΔydcU ΔydcT ΔydcS ΔydcR ΔhicA ΔhicB ΔyncJ ΔydcP ΔydcN ΔydcO ΔydcM ΔrecA (1819) The *recA* 1819 mutation is a deletion of *recA*	SCARAB genomics
C. thermocellum Δhpt	DSM 1313^{T} *Δhpt*[b]	National Renewable Energy Laboratory[d]
CT24	Δhpt *ilvBN*:: P_{rpi}::*kivd*$_{LL}$- P_{pck}::*ilvBNC*$_{CT}$- P_{ilvD}::*ilvD*$_{CT}$	This study

CT24*	Strain CT24 with two point mutation on *kivd*[c]	This study
CT242	Δhpt *ilvBN*:: P_{pck}::*ilvBNC*$_{CT}$- P_{ilvD}::*ilvD*$_{CT}$	This study
Plasmid		
pDL	Source of thermostable *lacZ*$_{GS}$	*Bacillus* Genetic Stock Center
pNW33N	ColE1 and pBC1 *ori*; Cm^R; *E. coli-Bacillus* shuttle vector	*Bacillus* Genetic Stock Center
pCT24	ColE1 and pBC1 *ori*; Cm^R; P_{rpi}::*kivd*$_{LL}$- P_{pck}::*ilvBNC*$_{CT}$- P_{ilvD}::*ilvD*$_{CT}$	This study
pCT228	ColE1 and pBC1 *ori*; Cm^R; P_{rpi}::*kivd*$_{LL}$::RBS:: Geoth_3237 - P_{pck}::*ilvBNC*$_{CT}$- P_{ilvD}::*ilvD*$_{CT}$	This study
pCT229	ColE1 and pBC1 *ori*; Cm^R; P_{rpi}::*kivd*$_{LL}$::RBS:: Geoth_3823 - P_{pck}::*ilvBNC*$_{CT}$- P_{ilvD}::*ilvD*$_{CT}$	This study
pCT24*	ColE1 and pBC1 *ori*; Cm^R; P_{rpi}::*kivd*$_{LL}$(m2)[c] - P_{pck}::*ilvBNC*$_{CT}$- P_{ilvD}::*ilvD*$_{CT}$	This study
pCT242	ColE1 and pBC1 *ori*; Cm^R; P_{pck}::*ilvBNC*$_{CT}$- P_{ilvD}::*ilvD*$_{CT}$	This study

[a] In plasmid descriptions, subscripts indicate the source of the gene as follows: GS, *Geobacillus stearothermophilus*; LL, *Lactococcus lactis*; CT, *Clostridium thermocellum*

[b] *C. thermocellum* DSM 1313 Δ*hpt* as wild type strain in this study because the Δ*hpt* is used for the sole purpose of counter-selection, and has no effect on growth and fermentation

[c] CT24* contains a *kivd* gene with two point mutations. However, there is no significant difference in isobutanol production between strains with CT24 and CT24*

[d] *C. thermocellum* DSM 1313 Δ*hpt* was given by Katherine Chou from National Renewable Energy Laboratory

Table 2-5. Primer sequences used in qRTPCR

Gene name	Primer sequence
recA	f: CTTATTGTTTCCCAGCCGGATACC
	r: CTGAAGACCTACATGGGAATCTCC
kivD	f: CAATTGGATATACATTCCCAGC
	r: CTAATTCTTGCACCGTAAGTTG
ilvB	f: TTATGGTTTCAAGGGCAGGAG
	r: TCCGACAGCATCTCTTTCAAC
ilvN	f: AAGCATACTTTATCGGTCCTGG
	r: GCTGTCAATGTTAAATCCCCTC
ilvC	f: GTTCTTGCTTTTGCCCACG
	r: ACACCTTTTCCCTCCACATAC
ilvD	f: CAGGTATCAGAATGGCAGGAG
	r: CATTCCCGTATGACCCATCG
repB	f: ACAGTTCGTTGGTTGTTTCTCAC
	r: CCGTTGCACGCATAAAACCA

Table 2-6. List of plasmid constructs tested in *C. thermocellum* for isobutanol production.

Plasmid name	Promoter for *kivd*	Promoter for *ilvBNC*
pCT04	clo1313_0295	clo1313_0099
pCT09	clo1313_2131	clo1313_0099
pCT11	clo1313_1798	clo1313_0099
pCT12	clo1313_1616	clo1313_0099
pCT13	clo1313_0184	clo1313_0099
pCT14	clo1313_1983	clo1313_0099
pCT15	clo1313_2092	clo1313_0099
pCT16	clo1313_2093	clo1313_0099
pCT18	clo1313_1717	clo1313_0099
pCT21	clo1313_1616	clo1313_0099
pCT22	clo1313_0184	clo1313_1616
pCT24	clo1313_0184	clo1313_0415
pCT29	clo1313_1616	clo1313_1983
pCT30	clo1313_1616	clo1313_2131
pCT34	clo1313_1616	clo1313_1364
pCT42	clo1313_0184	clo1313_1717
pCT51	clo1313_0184	clo1313_1983
pCT53	clo1313_1983	clo1313_2092

pCT54	clo1313_1983	clo1313_2942
pCT58	clo1313_1798	clo1313_1616
pCT60	clo1313_1798	clo1313_1818

Table 2-7. List of promoters used for various plasmid constructions at P1 position.

P1 (drive *kivd)*
Alcohol Dehydrogenase (clo1313_2131)
Alcohol Dehydrogenase (clo1313_1798)
PFOR (clo1313_1616)
Ribulose-5-P Isomerase (clo1313_0184)
GAPDH (clo1313_2095)
Triosephosphate Isomerase (clo1313_2093)
Pyruvate Formate Lyase (clo1313_1717)
carbohydrate binding family protein (clo1313_1983)
Transketolase (clo1313_0295)

Table 2-8. List of promoters used for various plasmid constructions at P2 position.

P2 (drive *ilvBNC*)
AHAS (clo1313_0099)
Ribulose-5-P Isomerase (clo1313_0184)
PFOR (clo1313_1616)
Phosphoglycerate mutase (clo1313_2903)
Pyruvate Formate Lyase (clo1313_1717)
PEP carboxykinase (clo1313_0415)
Transketolase (clo1313_0295)
carbohydrate binding family protein (clo1313_1983)
Alcohol dehydrogenase (clo1313_1827)
RNA polymerase, sigma 28 subunit, SigI (clo1313_1818)
branched-chain amino acid aminotransferase (clo1313_1364)

3.8 Supplementary

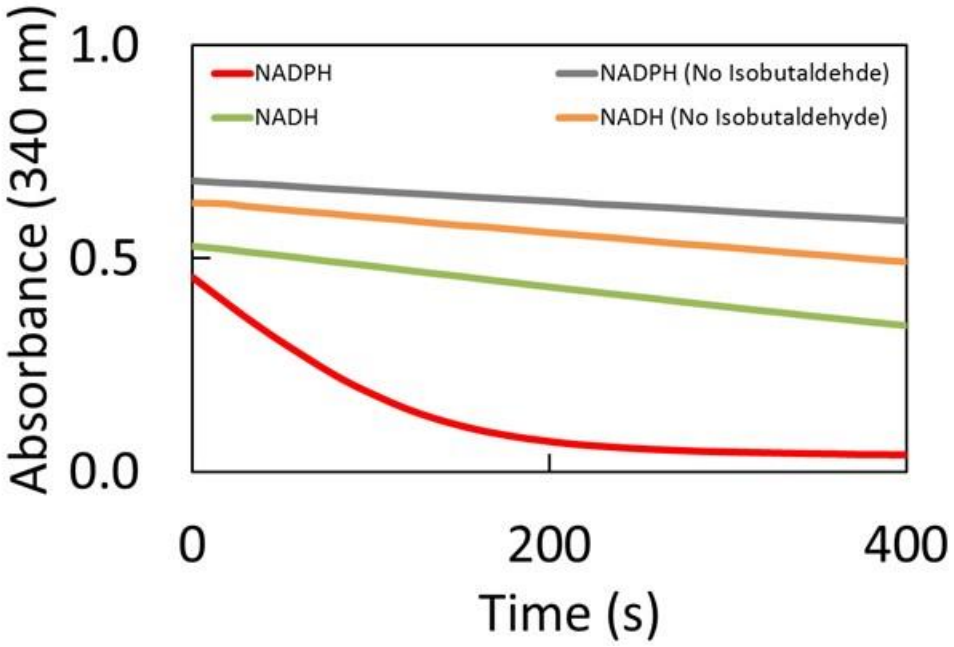

Figure 2-15. Native isobutanol dehydrogenase in *C. thermocellum*.

Enzyme activity was measured by depletion of isobutyraldehyde using cell crude extract.

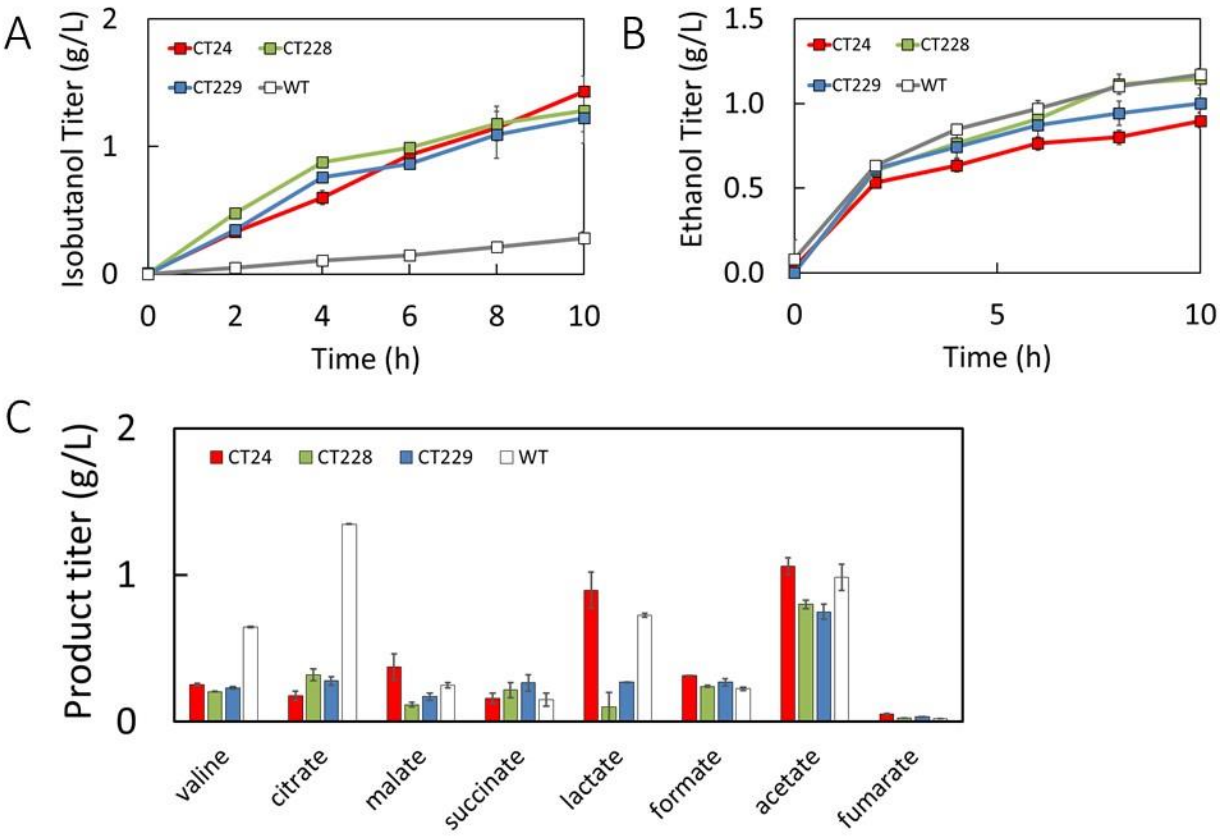

Figure 2-16. Effect of alcohol dehydrogenase overexpression.

(A) Isobutanol production, (B) ethanol production and (C) byproducts formation. Wild type, CT24, CT228 and CT229 strains were grown in CTFuD medium to OD_{600} = 1 - 1.2, then concentrated to LC medium (0.4 g/L urea) with 80 g/L cellulose at OD_{600} = 16. Error bar represents the standard deviation (n = 3).

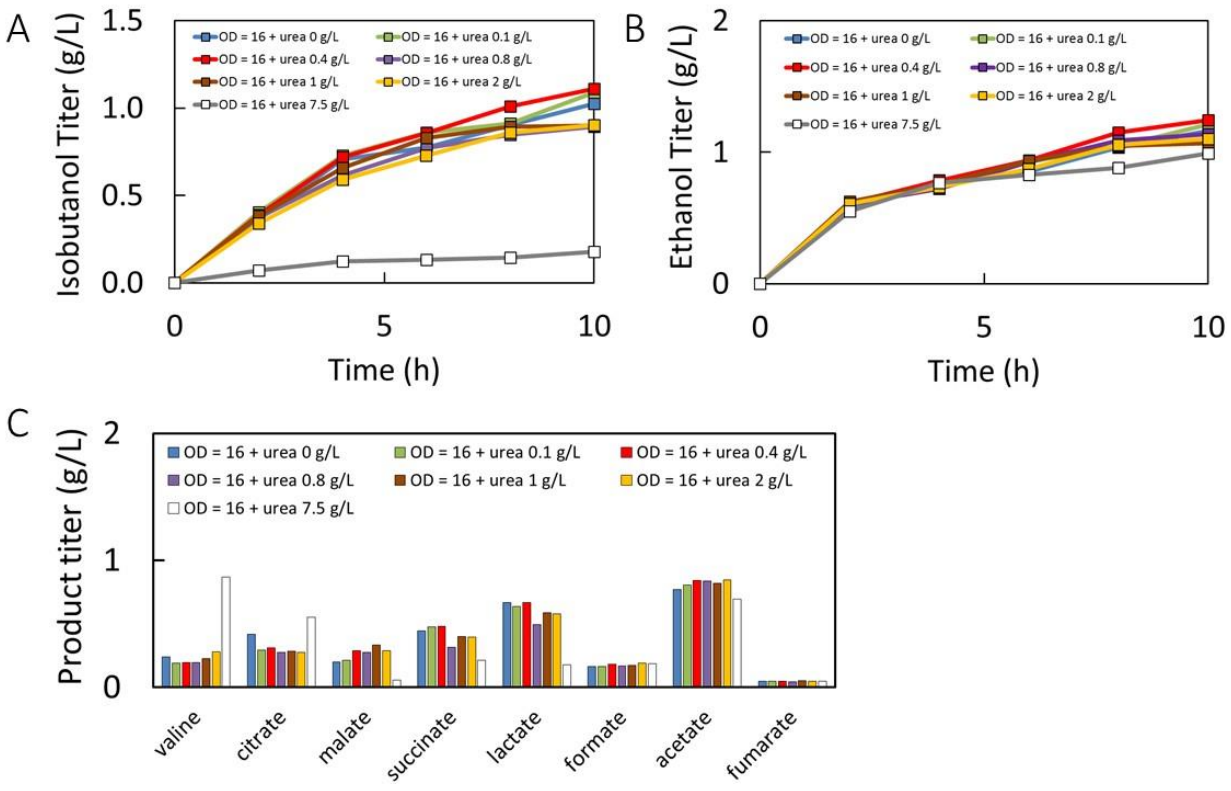

Figure 2-17. LC medium optimization for isobutanol production at 50 ^{o}C.

(A) Isobutanol, (B) Ethanol and (C) Byproducts production under different urea concentration in LC medium. CT24* strain was grown in CTFuD medium to OD_{600} = 1.1 with 1 g/L cellulose, then concentrated to LC medium (with different urea concentration) with 80 g/L cellulose at OD_{600} = 16.

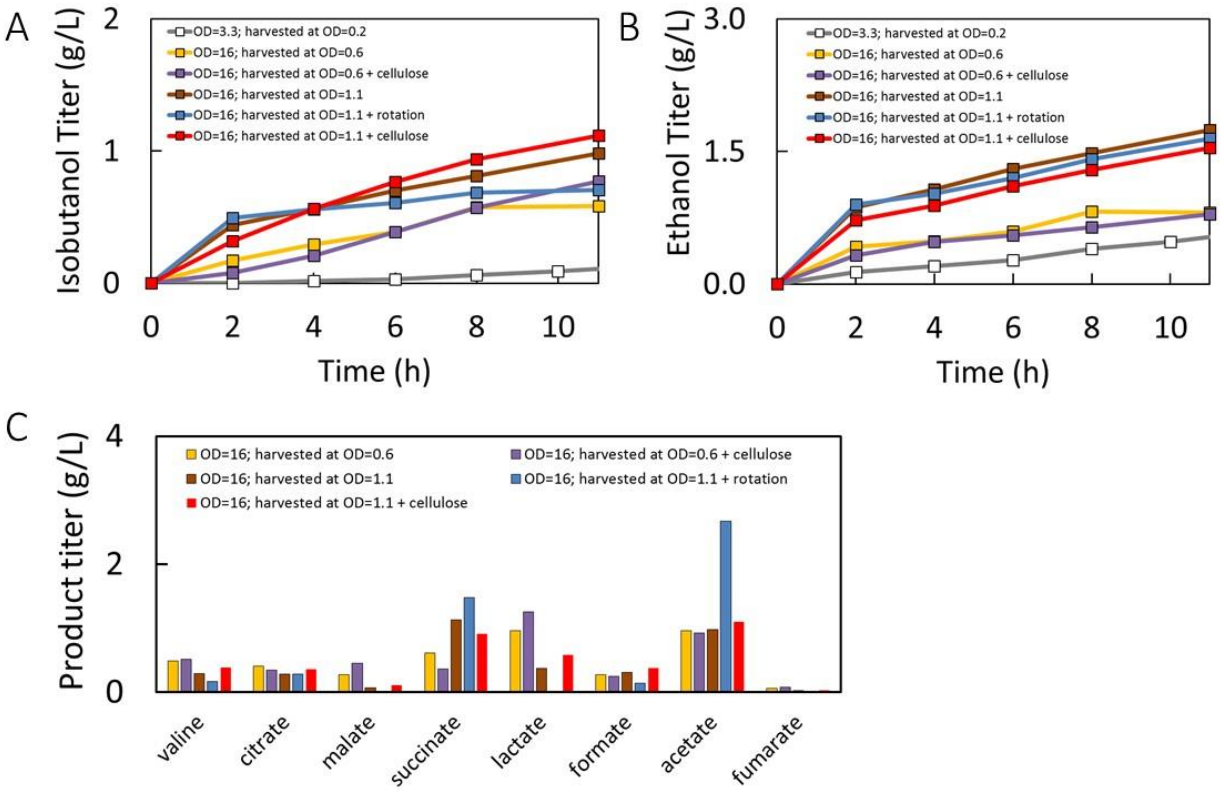

Figure 2-18. *C. thermocellum* production condition optimization for isobutanol production at 50 ^{o}C.

(A) Isobutanol, (B) Ethanol and (C) Byproducts production under different pre-culture and production condition. CT24* strain was grown in CTFuD medium to OD_{600} = 0.6 or 1.1 either with or without 1 g/L cellulose, then concentrated to LC medium (1 g/L urea) with 80 g/L cellulose at OD_{600} = 16**.**

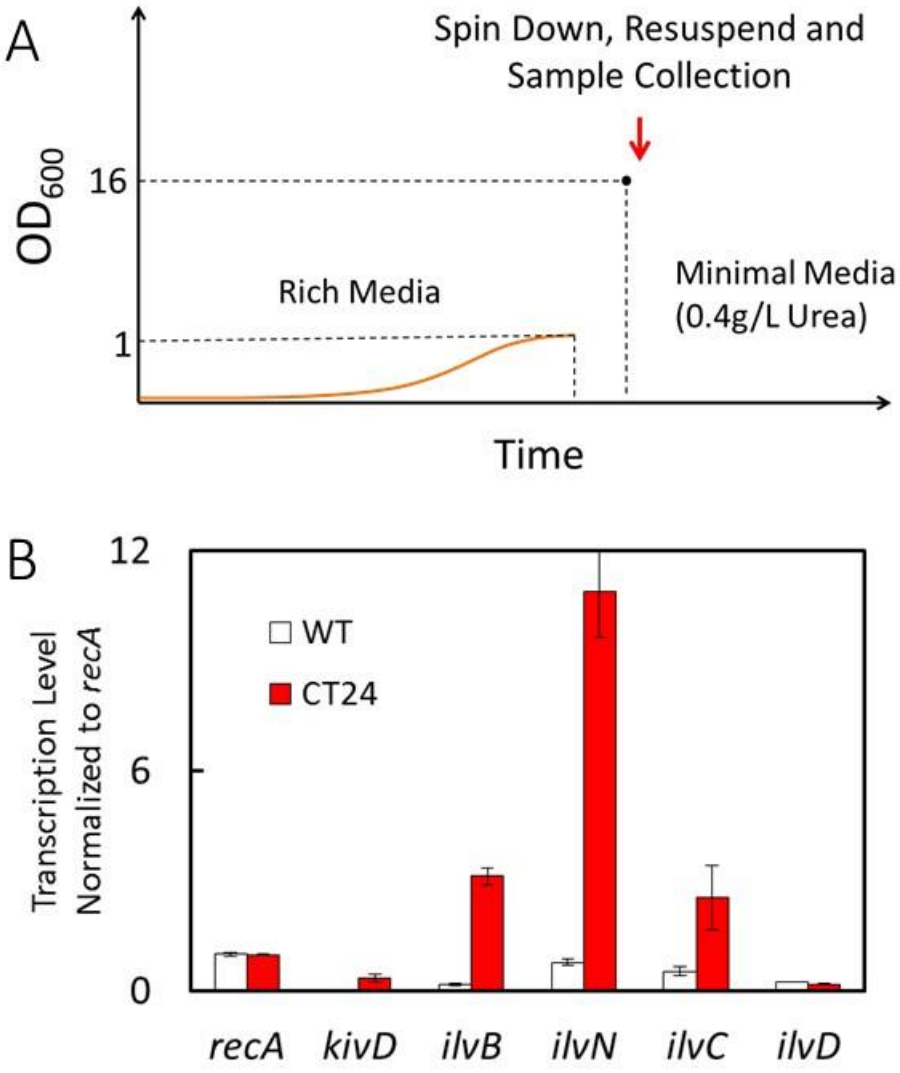

Figure 2-19. qRTPCR for gene transcription comparison between wild type *C. thermocellum* and isobutanol production strain (CT24) before fermentation.

(A) Scheme for collecting qRTPCR samples prior to fermentation initiation (B) Gene transcription comparison between wild type *C. thermocellum* and isobutanol production strain (CT24) prior to fermentation initiation. *recA* was used as the reference gene in all samples.

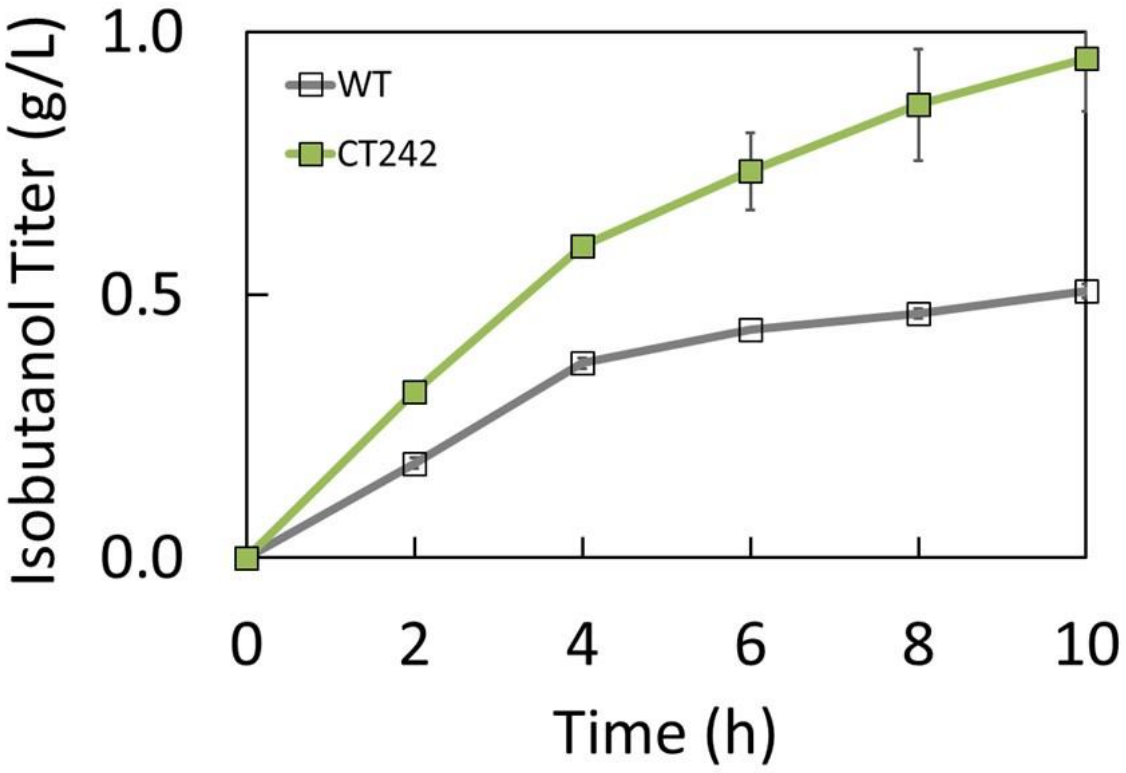

Figure 2-20. Isobutanol production during 10 h in LC medium.

Wild type and CT242 strains were grown in CTFuD medium to OD_{600} = 1 - 1.2, then concentrated to LC medium (0.4 g/L urea) with 80 g/L cellulose at OD_{600} = 16 Error bar represents the standard deviation (n = 3).

3.9 Reference

Argyros, D.A., Tripathi, S.A., Barrett, T.F., Rogers, S.R., Feinberg, L.F., Olson, D.G., Foden, J.M., Miller, B.B., Lynd, L.R., Hogsett, D.A., others, 2011. High Ethanol Titers from Cellulose using Metabolically Engineered Thermophilic, Anaerobic Microbes. Appl.Environ.Microbiol.77, 8288–8294.

Atsumi, S., Hanai, T., Liao, J.C., 2008. Non-fermentative pathways for synthesis of branched-chain higher alcohols as biofuels. Nature 451, 86–89.

Atsumi, S., Higashide, W., Liao, J.C., 2009. Direct photosynthetic recycling of carbon dioxide to isobutyraldehyde. Nat Biotech 27, 1177–1180.

Deng, Y., Olson, D.G., Zhou, J., Herring, C.D., Joe Shaw, A., Lynd, L.R., 2013. Redirecting carbon flux through exogenous pyruvate kinase to achieve high ethanol yields in *Clostridium thermocellum*. Metab. Eng. 15, 151–158.

Fleming, R.W., Quinn, L.Y., 1971. Chemically Defined Medium for Growth of *Clostridium thermocellum*, a Cellulolytic Thermophilic Anaerobe. Appl. Microbiol 21, 967.

Guss, A.M., Olson, D.G., Caiazza, N.C., Lynd, L.R., 2012. Dcm methylation is detrimental to plasmid transformation in *Clostridium thermocellum*. Biotechnology for Biofuels 5, 30.

Heider, J., Mai, X. and Adams, A. W. 1996 Characterization of 2-ketoisovalerate ferredoxin oxidoreductase, a new and reversible coenzyme A-dependent enzyme involved in peptide fermentation by hyperthermophilic archaea. J. Bacteriol. 178, 780-787.

Higashide, W., Li, Y., Yang, Y., Liao, J.C., 2011. Metabolic Engineering of *Clostridium cellulolyticum* for Production of Isobutanol from Cellulose. Appl.Environ.Microbiol 77, 2727.

Holwerda, E.K., Hirst, K.D., Lynd, L.R., 2012. A defined growth medium with very low background carbon for culturing *Clostridium thermocellum*. J. Ind. Microbiol. Biotechnol. 39, 943–947.

Holwerda, E.K., Thorne, P.G., Olson, D.G., Amador-Noguez, D., Engle, N.L., Tschaplinski, T.J., Dijken, J.P. van, Lynd, L.R., 2014. The exometabolome of Clostridium thermocellum reveals overflow metabolism at high cellulose loading. Biotechnology for Biofuels 7, 155.

Johnson, E.A., Madia, A., Demain, A.L., 1981. Chemically Defined Minimal Medium for Growth of the Anaerobic Cellulolytic Thermophile *Clostridium thermocellum*. Appl.Environ.Microbiol 41, 1060–1062.

Kovarík, A., Matzke, M.A., Matzke, A.J., Koulaková, B., 2001. Transposition of IS10 from the host *Escherichia coli* genome to a plasmid may lead to cloning artefacts. Mol. Genet. Genomics 266, 216–222.

Li, H., Opgenorth, P.H., Wernick, D.G., Rogers, S., Wu, T.Y., Higashide, W., Malati, P., Huo, Y.X., Cho, K.M., Liao, J.C., 2012. Integrated Electromicrobial Conversion of CO2 to Higher Alcohols. Science 335, 1596–1596.

Li, H., Liao, J.C., 2015. A Synthetic Anhydrotetracycline-Controllable Gene Expression System in *Ralstonia eutropha* H16. ACS Synth. Biol. 4, 101–106. doi:10.1021/sb4001189

Lin, P.P., Rabe, K.S., Takasumi, J.L., Kadisch, M., Arnold, F.H., Liao, J.C., 2014. Isobutanol production at elevated temperatures in thermophilic *Geobacillus thermoglucosidasius*. Metab. Eng. 24, 1–8.

Lynd, L. R., W. H. van Zyl, J. E. McBride, and M. Laser. 2005. Consolidated bioprocessing of cellulosic biomass: an update. Curr. Opin. Biotechnol. 16:577–583.

Lynd, L.R., Laser, M.S., Bransby, D., Dale, B.E., Davison, B., Hamilton, R., Himmel, M., Keller, M., McMillan, J.D., Sheehan, J., Wyman, C.E., 2008. How biotech can transform biofuels. Nat Biotech 26, 169–172.

Olson, D.G., Maloney, M., Lanahan, A.A., Hon, S., Hauser, L.J., Lynd, L.R., n.d. Identifying promoters for gene expression in *Clostridium thermocellum*. Metab. Eng. Communications.

Peters, M.W., Taylor, J.D., Jenni, M., Manzer, L.E., Henton, D.E., 2011. Integrated Process to Selectively Convert Renewable Isobutanol to P-Xylene. US20110087000 A1.

Pósfai, G., Plunkett, G., Fehér, T., Frisch, D., Keil, G.M., Umenhoffer, K., Kolisnychenko, V., Stahl, B., Sharma, S.S., de Arruda, M., Burland, V., Harcum, S.W., Blattner, F.R., 2006. Emergent properties of reduced-genome *Escherichia coli*. Science 312, 1044–1046.

Skulj, M., Okrslar, V., Jalen, Spela., Jevsevar, S., Slanc, P., Strukelj, B. and Menart, V. 2008. Improved determination of plasmid copy number using quantitative real-time PCR for monitoring fermentation processes. Microb. Cell Fact. 7, 6.

Sluiter A, Hames B, Ruiz R, Scarlata C, Sluiter J, Templeton D, Crocker D. 2008. Determination of structural carbohydrates and lignin in biomass. NREL Laboratory Analytical Procedures (LAPs). NREL/TP-510-42618.

Smith, K.M., Cho, K.-M., Liao, J.C., 2010. Engineering *Corynebacterium glutamicum* for isobutanol production. Appl Microbiol Biotechnol 87, 1045–1055.

Stevenson, D. M., Weimer, P. J. 2005 Expression of 17 genes in *Clostridium thermocellum* ATCC 27405 during fermentation of cellulose or cellobiose in continuous culture. Appl. Environ. Microbiol. 71, 4672-4678.

Tripathi, S.A., Olson, D.G., Argyros, D.A., Miller, B.B., Barrett, T.F., Murphy, D.M., McCool, J.D., Warner, A.K., Rajgarhia, V.B., Lynd, L.R., others, 2010. Development of pyrF-based genetic system for targeted gene deletion in *Clostridium thermocellum* and creation of a pta mutant. Appl.Environ.Microbiol.76, 6591.

Tyurin M, Desai S, Lynd L. 2004. Electrotransformation of *Clostridium thermocellum*. Appl. Environ. Microbiol. 70:883-890.

Wei, H., Fu, Y., et al. 2014 Comparison of transcriptional profiles of *Clostridium thermocellum* grown on cellobiose and pretreated yellow poplar using RNA-Seq. Front Microbiol. 5, 142.

Zhou, J., Olson, D.G., Argyros, D.A., Deng, Y., van Gulik, W.M., van Dijken, J.P., Lynd, L.R., 2013. Atypical glycolysis in *Clostridium thermocellum*. Appl. Environ. Microbiol. 79, 3000–3008.

4. High titer isobutanol production in *C. thermocellum*

4.1 Introduction

Lignocellulosic biofuel and biochemical production has several advantages including: improve net carbon and energy balances, lower production cost, and avoid the food vs. fuel dilemma (Lynd et al., 2005 and Lynd et al., 2008). To date, lignocellulose utilization is mainly limited biomass recalcitrance. Consolidated bioprocessing (CBP), cellulose hydrolysis and fermentation occur simultaneously without added cellulose, provides a potential solution. *Clostridium thermocellum* is a promising thermophilic CBP host because it has high cellulose deconstruction rate. Recent studies of metabolic features of *C. thermocellum* (Zhou et al., 2013) and advances in genetic modification tools (Tyurin et al., 2004, Tripathi et al., 2010 and Argyros et al., 2011 and Guss et al., 2012) for *C. thermocellum* make the CBP organism an attractive platform for biofuel or biochemical production.

Longer-chain alcohols offer advantages as a gasoline substitute or drop-in fuel (Atsumi et al., 2008). In particular, isobutanol received significant attention because it can be used as fuel or a feedstock chemical. Isobutanol can be dehydrated to form isobutene, which can then be oligomerized to C8 then C12 alkenes to be used as jet fuel. The C8 alkene can also be dehydrocyclized to form p-xylene (Peters et al., (2011)), which can then be oxidized to form terephthalic acid as a monomer for the common plastic polyethylene terephthalate (PET). Microbial production of isobutanol from renewable sources has been demonstrated in multiple engineered organisms (Atsumi et al., 2008, Atsumi et al., 2009, Smith et al., 2010, Higashide et al., 2011, Li et al., 2012, Lin et al., 2014 and Higashide et al., 2011) including *C. thermocellum* (Lin et al., 2015).

Through our streamlined working flow to screen promoters for pathway overexpression in C. thermocellum, 5.4 g/L of isobutanol has been produced directly from cellulose within 72 h (Lin et al., 2015), roughly 41% yield. To meet the criteria for industrial production, we sought to further improve the production titer and yield. We first identified Ahas is the most limiting enzyme in the isobutanol pathway in our engineered *C. thermocellum* strain, CT24. We tried to overexpress the both Ahas isoenzymes, IlvB and IlvI, by replacing the native promoter with other stronger promoters. The best strain PL208 produced 9.7 g/L isobutanol within 120 h. We also identified the major pyruvate ferredoxin oxidoreductase (Por), which attributes the most activity for converting pyruvate to Acetyl-CoA, precursor for acetate and ethanol production. Knockout Por on PL208 strain should increase isobutanol production titer and yield further.

4.2 Methods

4.2.1 Bacterial strains and plasmids

C. thermocellum DSM 1313 Δ*hpt* was a gift from Katherine Chou from the National Renewable Energy Laboratory. We referred *C. thermocellum* DSM 1313 Δ*hpt* as the wild type strain in this study because the Δ*hpt* is used for the sole purpose of counter-selection when needed, and has no effect on growth and fermentation. *Escherichia coli*BL21 (New England Biolabs, Ipswich, MA) and MDS™42 LowMut Δ*recA* (Pósfai et al., 2006) (SCARAB genomics, Madison, WI) were used as host for plasmid construction. Strains and plasmids used in this study are listed in Table 3.1.

All plasmids were constructed by DNA assembly techniques. Both vector and inserts (target genes) were amplified by PCR using Phire Hot Start II DNA polymerase (Thermo Scientific, Hudson, NH). PCR products were purified by a PCR purification Kit (Zymo Research, Irvine, CA).

The vector and insert were mixed with Gibson Assembly Master Mix (New England Biolabs, Ipswich, MA) and incubated at 50 °C for 1 h. Then the assembly product was transformed to BL21 or MDS™42 LowMut Δ*recA* strain. The presence of correctly cloned inserts was determined by colony PCR and DNA sequencing (Laragen, Culver City, CA).

4.2.2 Chemicals and reagents

All chemicals unless otherwise specified were acquired from Sigma-Aldrich (St. Louis, MO) or Thermo Scientific. Phire Hot Start II DNA polymerase was purchased from New England Biolabs.

4.2.3 Media and cultivation

All *E. coli* strains were grown in LB medium containing appropriate antibiotics at 37 °C on a rotary shaker (250 rpm). Antibiotics were used at the following concentrations: ampicillin, 200 μg/ml; kanamycin, 50 μg/ml; chloramphenicol, 20 μg/ml.

Except for small scale isobutanol production, all *C. thermocellum* strains were cultured inside a Coy anaerobic chamber (Coy Laboratory Products, Grass Lake, MI) in a modified CTFuD medium (Tripathi et al., 2010) at 50 °C incubation . CTFuD medium contains the following components: 3 g/L of sodium citrate tribasic dehydrate, 1.3 g/L ammonium sulfate, 1.43 g/L potassium phosphate monobasic, 1.37 g/L potassium phosphate dibasic, 0.5 g/L cysteine-HCl, 21 g/L MOPS, 6 g/L glycerol-2-phospate disodium, 5 g/L cellobiose, 4.5 g/L yeast extract, 0.01 g/L calcium chloride, 0.011 g/L magnesium chloride, 0.0006 g/L ferrous sulfate heptahydrate, 0.01 g/L thiamin, and 0.001 g/L resazurin. Antibiotics were used at the following concentrations: thiamphenicol 20 ug/ml. In addition, 2.5 g/L sodium bicarbonate was used to enhance *C. thermocellum*growth.

Stock cultures of *E. coli* were maintained at −80 °C in 13% (v/v) glycerol. Stock cultures of *C. thermocellum* were maintained at −80 °C directly.

4.2.4 Isobutanol dehydrogenase enzyme assay

The isobutanol dehydrogenase enzyme assay was carried out at 50 °C using an Agilent 8453 UV–vis spectrophotometer. The reaction mixture contains 40 mM Tris–Cl at pH 7.0, 5 mM dithiothreitol (DTT), 300 µM NADH/NADPH, 20 mM isobutaldehyde and crude extract. The reaction was initiated with the addition of isobutaldehyde. The rate of the enzymatic reaction was monitored with the decrease of absorption at 340 nm, corresponding to the consumption of NADH/NADPH. The total protein concentration was quantified using Bradford assay (BioRad).

4.2.5 Ketoisovalerate ferrodoxin-dependent reductase (KOR) enzyme assay

The KOR enzyme assay procedure was adapted from a previously reported protocol (Heider et al., 1996). The assay was carried out at 50 °C using the Agilent 8453 UV–vis spectrophotometer under strict anaerobic condition. The reaction mixture contained 200 mM potassium phosphate at pH 7.0, 5 mM thiamine pyrophosphate (TPP), 10 mM methyl viologen, 10 mM DTT, 2 mM $MgCl_2$, 2 mM coenzyme A, 6 mM KIV, if indicated, and crude extract. The reaction was initiated with the addition of *C. thermocelllum* crude extract. The rate of the enzymatic reaction was monitored with the increase of absorption at 604 nm, corresponding to the reduction of methyl viologen. The total protein concentration was quantified using Bradford assay (BioRad).

4.2.6 *C. thermocellum* transformation

C. thermocellum electro-competent cells were freshly prepared as described (Guss et al., 2012). Briefly, *C. thermocellum* DSM 1313 Δ*hpt* was grown in CTFuD medium (total 400 ml) at

50 °C inside a Coy anaerobic chamber till OD_{600} =0.4–1. The culture was chilled on ice for 10 min, and cells were collected by centrifugation in several 50 ml Falcon tubes at 4 °C and 6500 g for 60 min. Then supernatants were removed aerobically. Cell pellets were resuspeneded with 10 ml ice 10% glycercol, and centrifuged at 4 °C and 6000*g* for 30 min twice. Lastly, pellets were resuspended with 1 ml 10% glycercol.

For each transformation, 50 µl of the competent cells were mixed with about 200–1000 ng of DNA in 1-mm-gap pre-chilled electroporation cuvettes (Molecular BioProducts, San Diego, CA). The mixtures were electroporated (1.2 kV, 1.5 m s square pulse) with a BioRad GenePulser XCell (BioRad Laboratories, Hercules, CA). Cells were immediately resuspended in 1 ml pre-warmed CTFuD medium, and rescued at 50 °C for 3 h. Then cells were plated by mixing with 25 ml molten CTFuD medium (0.8% agar) containing 20 µg/ml thiamphenicol. The plates were incubated at 50 °C anaerobically for up to one week.

4.2.7 Isobutanol production

To examine isobutanol production, engineered *C. thermocellum* DSM 1313 Δ*hpt* cultures were grown till stationary phase (OD_{600}=0.9–1.2) and centrifuged at 6500 rpm at 40 °C for 30 min. Supernatant was removed and pellets were resuspended in LC medium. LC medium contains the following constituents: 100 g/L cellulose, 0.4 g/L urea, 5 g/L cellobiose, 21 g/L MOPS, 2 g/L potassium phosphate monobasic, 3 g/L potassium phosphate dibasic, 0.1 g/L cysteine-HCl, 0.05 g/L calcium chloride, 0.2 g/L magnesium chloride, 0.0035 g/L ferrous sulfate heptahydrate, 2.5 g/L sodium bicarbonate, 0.02 g/L pyridoxamine dihydrochloride, 0.004 g/L PABA, 0.002 g/L biotin, 0.002 g/L B12, and 0.01 g/L thiamin. For *C. thermocellum* cultures, antibiotics were used at the following concentration: thiamphenicol 20 ug/ml. Production of isobutanol was carried out

in 5 mL centrifuge tubes with 3 mL of LC medium at pH 7.5, and 50 °C anaerobic incubation. Samples were maintained at pH=7.5 in 2 h intervals.

4.3 Results

4.3.1 Identified limiting enzyme in *C. thermocellum* isobutanol production

Through our streamlined working flow to screen promoters for pathway overexpression in *C. thermocellum*, 5.4 g/L of isobutanol has been produced directly from cellulose within 72 h (Lin et al., 2015) using the engineered strain CT24. Isobutanol productivity significantly decreased after 48 h (Fig. 3.5A). To further improve the production titer, we first sought to identify the limiting enzyme in the current isobutanol pathway. We measured activity of six different enzymes in isobutanol pathway at 2 h and 48 h during the production. Within 48 h, acetohydroxyacid synthase (Ahas) activity dropped more than 90% (Fig. 4-1) while other five enzymes maintained at least more than 60% activity.

4.3.2 Overexpression Ahas activity to improve isobutanol production

After identifying Ahas as the most limiting step, we then tried to further overexpress the Ahas activity. There are two Ahas isoenzymes annotated in *C. thermocellum* genome. We replaced the native promoters of two different Ahas isoenzymes, IlvI and IlvBN individually, with stronger promoters and tested for isobutanol production as shown in Fig. 4-2A. Isobutanol production titer was increased using most of the engineered strains with *ilvBN* and *ilvI* further overexpressed, indicating improving Ahas activity is the essential to increase the production titer. The best engineered strain, PL208 (replacing IlvI promoter by gapDH promoter), prolonged the production after 72 h and achieved 9.7 g/L of isobutanol during 100 h (Fig. 4-2B). Ahas enzyme assay also confirmed the overexpression by twofold (Fig. 4-2C). Ahas activity, although improved threefold

at 48 h, still decreased significantly within 48 h in PL208, suggesting that there is some protein degradation mechanism in *C. thermocellum* specific to Ahas enzymes. To further improve the production titer, we will keep working on maintaining the Ahas activity.

4.3.3 Characterized electron flow in isobutanol production and the related pathway in *C. thermocellum*

Ethanol, acetate and lactate are the major byproducts during isobutanol production in *C. thermocellum* (Fig. 3.5B). To improve production yield, we transformed the plasmid pCT24 (Lin et al., 2015) to an *hpt* and *ldh* double knockout strain for overexpressing isobutanol pathway. After several generations of growth, the plasmid was integrated into the transformant genome, resulting strain CT25. Lactate production was eliminated in the production using CT25, most of the fermentation products were produced similar to CT24 expect ethanol production was improved. In order to direct the carbon flux to isobutanol, we first sought to eliminate ethanol by knockout the bifunctional enzyme AdhE (Fig. 4-3), which coverts acetyl-CoA to ethanol. However, we could not attain the knockout strain after repeating efforts. A potential explanation is the NADH cannot be consumed fast enough because the two major NADH consumption steps, Ldh and AdhE, are knockout.

Acetyl-CoA is the precursor for ethanol and acetate production in *C. thermocellum* (Fig. 4-3). It is mainly produced from pyruvate through pyruvate ferredoxin oxidoreductase (POR). There are four Por or Por homologs (por-A to por-D) and one indolepyruvate oxidoreductase that have been annotated in *C. thermocellum* genome. However, none of these putative Por has been characterized. We individually deleted each of these five enzymes in the wildtype strains. Among these five knockout strains, knockout por-A strain increased isobutanol titer threefold within 6 h

and decreased ethanol titer more than twofold, suggesting that Por-A is the main enzyme converting pyruvate to acetyl-CoA for ethanol and acetate production.

4.4 Figures

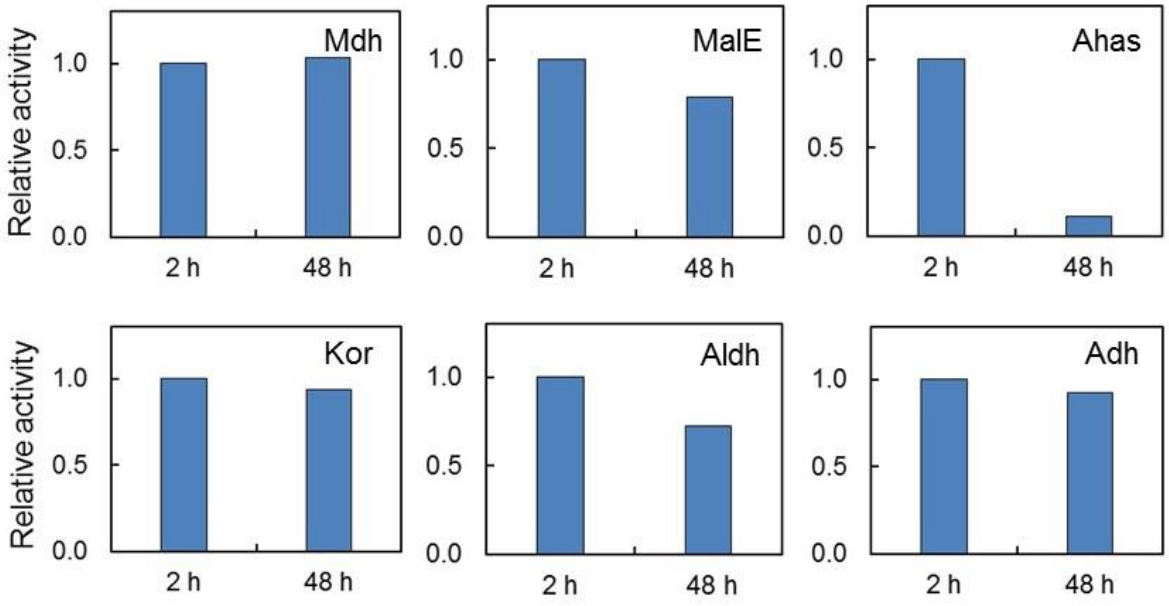

Figure 4-1. Identify limiting enzyme in isobutanol pathway in *C. thermocellum*.

CT27 strain was grown in CTFuD medium to OD_{600} = 1 - 1.2, then concentrated to LC medium (0.4 g/L urea) with 80 g/L cellulose at OD_{600} = 16. Error bar represents the standard deviation (n = 3).

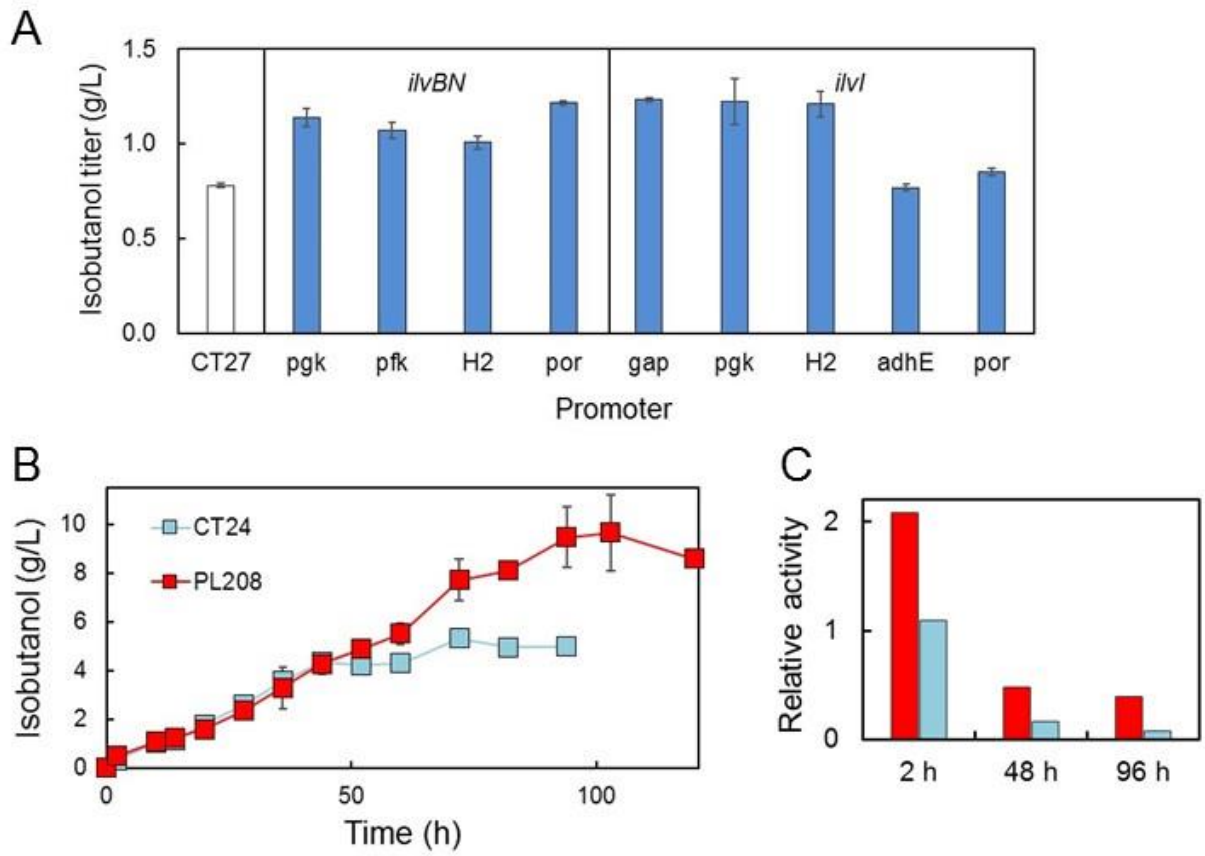

Figure 4-2. Screening of isobutanol production from Ahas overexpressed *C. thermocellum*.

Isobutanol titer within 24 h with overexpressing Ahas isoenzymes (*ilvBN* or *ilvI*) by different promoters. (B) Isobutanol production within 120h. CT24 and PL208 were grown in CTFuD medium to OD_{600} = 1, then concentrated to modified LC medium with 80 g/L cellulose at OD_{600} = 16. (C) Ahas enzyme assay of CT27 and PL208 at 2 and 48 h. Error bar represents the standard deviation (n = 3).

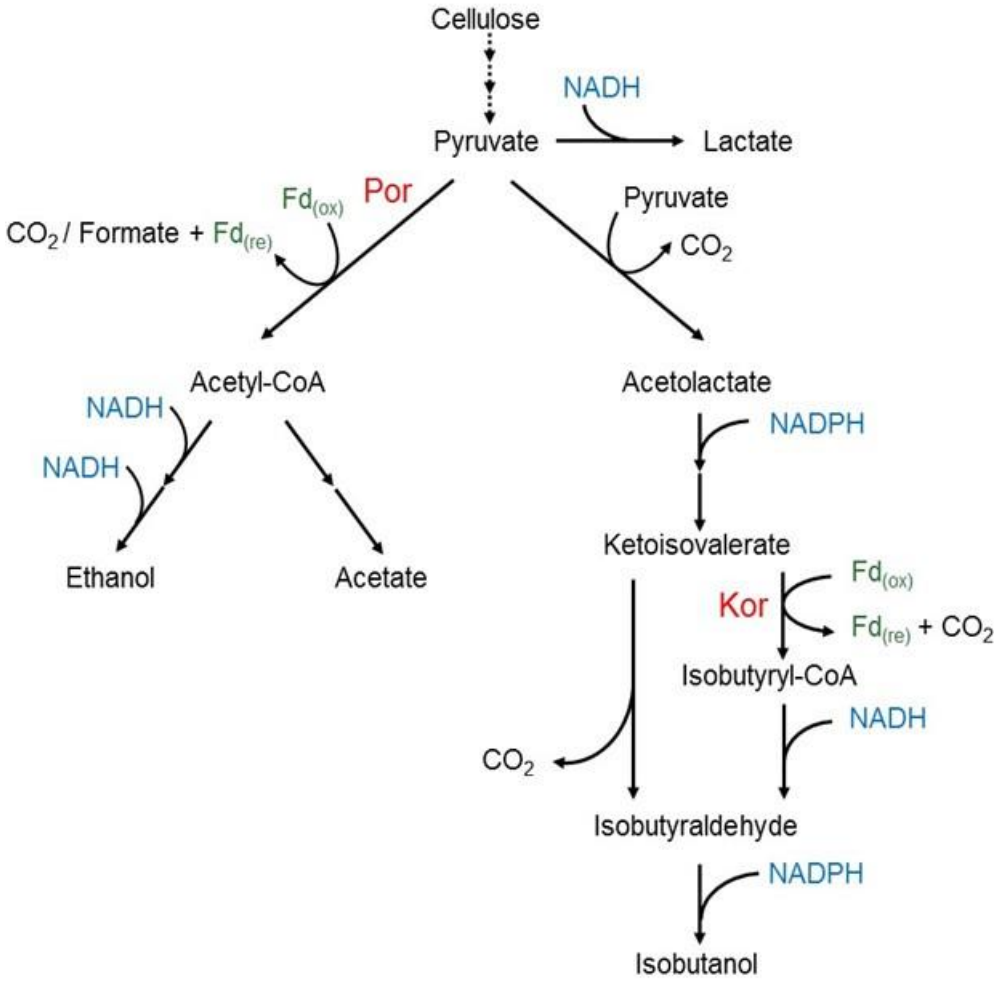

Figure 4-3. Electron flow in isobutanol production and the related pathway in *C. thermocellum*

Por, pyruvate ferredoxin oxidoreductase; Kor, ketoisovalerate ferredoxin oxidoreductase

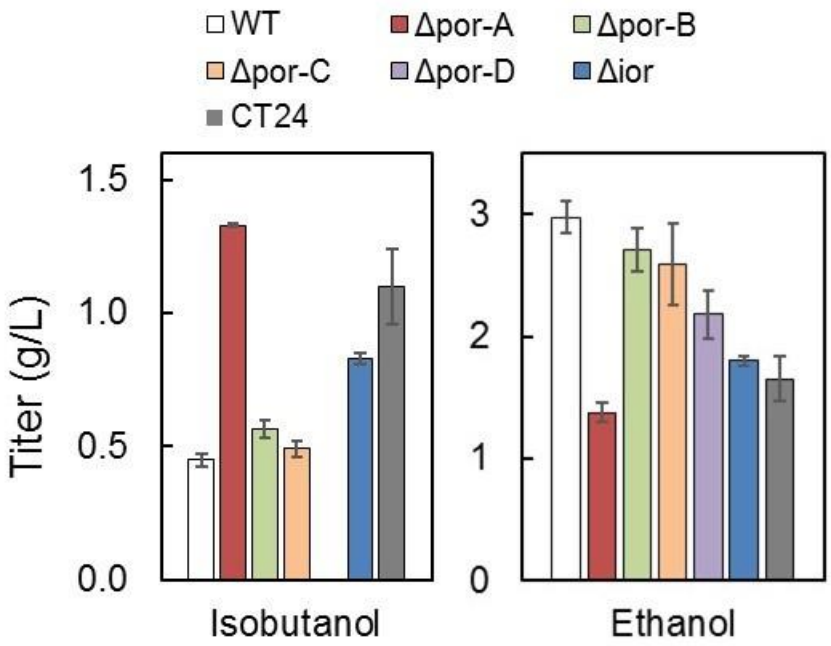

Figure 4-4. Isobutanol and ethanol production in putative Por knockout strains in modified LC medium within 6 h.

WT and knockout strains were grown in CTFuD medium to OD_{600} = 1, then concentrated to modified LC medium with 80 g/L cellulose at OD_{600} = 16. Error bar represents the standard deviation (n = 3).

4.5 Reference

Argyros, D.A., Tripathi, S.A., Barrett, T.F., Rogers, S.R., Feinberg, L.F., Olson, D.G., Foden, J.M., Miller, B.B., Lynd, L.R., Hogsett, D.A., others, 2011. High Ethanol Titers from Cellulose using Metabolically Engineered Thermophilic, Anaerobic Microbes. Appl.Environ.Microbiol.77, 8288–8294.

Atsumi, S., Hanai, T., Liao, J.C., 2008. Non-fermentative pathways for synthesis of branched-chain higher alcohols as biofuels. Nature 451, 86–89.

Atsumi, S., Higashide, W., Liao, J.C., 2009. Direct photosynthetic recycling of carbon dioxide to isobutyraldehyde. Nat Biotech 27, 1177–1180.

Guss, A.M., Olson, D.G., Caiazza, N.C., Lynd, L.R., 2012. Dcm methylation is detrimental to plasmid transformation in *Clostridium thermocellum*. Biotechnology for Biofuels 5, 30.

Heider, J., Mai, X. and Adams, A. W. 1996 Characterization of 2-ketoisovalerate ferredoxin oxidoreductase, a new and reversible coenzyme A-dependent enzyme involved in peptide fermentation by hyperthermophilic archaea. J. Bacteriol. 178, 780-787.

Higashide, W., Li, Y., Yang, Y., Liao, J.C., 2011. Metabolic Engineering of *Clostridium cellulolyticum* for Production of Isobutanol from Cellulose. Appl.Environ.Microbiol 77, 2727.

Li, H., Opgenorth, P.H., Wernick, D.G., Rogers, S., Wu, T.Y., Higashide, W., Malati, P., Huo, Y.X., Cho, K.M., Liao, J.C., 2012. Integrated Electromicrobial Conversion of CO2 to Higher Alcohols. Science 335, 1596–1596.

Lin, P.P., Mi, L., Morioka, A.H., Yoshino, K.M., Konishi, S., Xu, S.C., Papanek, B.A., Riley, L.A., Guss, A.M., Liao, J.C., 2015. Consolidated bioprocessing of cellulose to isobutanol using Clostridium thermocellum. Metabolic Engineering 31.

Lin, P.P., Rabe, K.S., Takasumi, J.L., Kadisch, M., Arnold, F.H., Liao, J.C., 2014. Isobutanol production at elevated temperatures in thermophilic *Geobacillus thermoglucosidasius*. Metab. Eng. 24, 1–8.

Lynd, L. R., W. H. van Zyl, J. E. McBride, and M. Laser. 2005. Consolidated bioprocessing of cellulosic biomass: an update. Curr. Opin. Biotechnol. 16:577–583.

Lynd, L.R., Laser, M.S., Bransby, D., Dale, B.E., Davison, B., Hamilton, R., Himmel, M., Keller, M., McMillan, J.D., Sheehan, J., Wyman, C.E., 2008. How biotech can transform biofuels. Nat Biotech 26, 169–172.

Peters, M.W., Taylor, J.D., Jenni, M., Manzer, L.E., Henton, D.E., 2011. Integrated Process to Selectively Convert Renewable Isobutanol to P-Xylene. US20110087000 A1.

Pósfai, G., Plunkett, G., Fehér, T., Frisch, D., Keil, G.M., Umenhoffer, K., Kolisnychenko, V., Stahl, B., Sharma, S.S., de Arruda, M., Burland, V., Harcum, S.W., Blattner, F.R., 2006. Emergent properties of reduced-genome *Escherichia coli*. Science 312, 1044–1046.

Smith, K.M., Cho, K.-M., Liao, J.C., 2010. Engineering *Corynebacterium glutamicum* for isobutanol production. Appl Microbiol Biotechnol 87, 1045–1055.

Tripathi, S.A., Olson, D.G., Argyros, D.A., Miller, B.B., Barrett, T.F., Murphy, D.M., McCool, J.D., Warner, A.K., Rajgarhia, V.B., Lynd, L.R., others, 2010. Development of pyrF-based genetic system for targeted gene deletion in *Clostridium thermocellum* and creation of a pta mutant. Appl.Environ.Microbiol.76, 6591.

Tyurin M, Desai S, Lynd L. 2004. Electrotransformation of *Clostridium thermocellum*. Appl. Environ. Microbiol. 70:883-890.

Zhou, J., Olson, D.G., Argyros, D.A., Deng, Y., van Gulik, W.M., van Dijken, J.P., Lynd, L.R., 2013. Atypical glycolysis in *Clostridium thermocellum*. Appl. Environ. Microbiol. 79, 3000–3008.

5. Engineer new *Escherichia coli* strain which rely solely on non-oxidative glycolysis (NOG) for sugar catabolism

5.1 Introduction

Acetyl-coenzyme A (acetyl-CoA) is a two carbon metabolite and important metabolic precursor to a variety of industrially relevant compounds including biofuels. An ultimate limitation of acetyl-CoA derived biochemical production is the inherent carbon loss when forming acetyl-CoA. Most organisms use some glycolytic variation, commonly the Embden-Meyerhof Pathway (EMP), to initially degrade sugar into pyruvate. Pyruvate, a C3 metabolite, is then decarboxylated to form acetyl-CoA, losing carbon to the environment. This decarboxylation limits the carbon yield to only two molecules of acetyl-CoA from one molecule of hexose, thus inhibiting the economics of any associated bioprocess. A synthetic sugar catabolism pathway, termed non-oxidative glycolysis (NOG) (Bogorad et al., 2013), was recently developed to address this problem, as it uses a combination of phosphoketolase dependent cleavage of sugar phosphates and a carbon rearrangement cycle to directly generate three C2 units per hexose in a redox neutral manner. To further expand the applications using NOG, an *Escherichia coli* strain was constructed to rely solely on NOG for sugar catabolism in this work. Therefore, the resulting strain offers significant potential to be engineered for the production of a variety of acetyl-CoA derived compounds. To implement NOG as a growth pathway, all native sugar degradation pathways, including the EMP, ED and methylglyoxal bypass, were removed, eliminating the cell's ability to grow on sugar as a sole carbon source. In addition, the glyxoylate shunt and gluconeogenesis pathways, which are necessary for the production of essential metabolites using NOG, were upregulated. Then, this engineered strain was evolved to grow in minimal glucose media supplemented with exogenous acetate. Under anaerobic conditions, it was verified that this strain overexpressed NOG and

glucose transporter genes and produces acetate as a major fermentation product from glucose. However, this strain did not restore the cells ability to grow on sugar as a sole carbon (glucose or xylose) source with further evolution.

5.2 Results

5.2.1 NOG strain construction in *Escherichia coli*

Figure 5.1 is the flow chart for the NOG strain construction. To construct a NOG platform strain, we first eliminated glycolysis and other possible growth pathways (Fig. 5.1 and 5.2). Glycolysis was inactive by knocking out glyceraldehyde 3-phosphate dehydrogenase (GapA). In addition, methylglyoxal was also knocked out by deleting MgsA for a potential route to provide pyruvate from glyceraldehyde 3-phosphate (Yomano et al., 2009). This double knockout strain (PHL2) could not grow in glucose minimal media and could be rescued by SGC media (M9 minimal salt with 50 mM succinate, 50 mM glycerol and 3% casamino acid) as reported in the literature (Seta et al., 1997). Then we overexpressed Xpk in PHL2 and evolved with glucose minimal medium with SGC addition. However, PHL2 could not grow in minimal medium with glucose as sorely carbon source after one month of evolution. To facilitate fast evolution rate, an *E. coli* mutataor, *mutD5* (Schaaper, 1988, 1989; Damagnez et al., 1989), was also overexpressed in PHL2. After two weeks of evolution, PHL2 strain with Xpk and MutD5 overexpressed was able to grow in glucose minimal medium. However, the evolved strain was still able to grow in minimal medium without overexpressing Xpk, indicating the growth was due to surpressor mutations. To construct a better NOG platform strain, we further eliminated glycolysis and other possible growth pathways (Fig. 5.1 and 5.2). Phosphoglycerate kinase (Pgk) and ED pathway (*zwf*, *edd* and *eda*) were knocked out in the PHL2 background. In order to prevent erythrose 4-phosphate

dehydrogenase (GapB) from rescuing GapA function (Boschi-Muller et al., 1997) the gene was also deleted, resulting strain PHL7. PHL7 with Xpk and MutD5 overexpressed failed to evolve to grow in glucose minimal medium after two months of evolution.

We further engineered the genome for adapting the cell to NOG growth. The main phosphofrutokinase (>90% activity, PfkA) was deleted to prevent a potential futile cycle. To increase the flux from acetyl-CoA to pyruvate, glyoxylate shunt (GS) and phosphophenylpyruvate carboxykinase (Pck) were upregulated. Specifically, we knocked out the GS regulator (IclR) and substituted Pck promoter by $P_{L\text{-}lacO}$ promoter. We further knockout PoxB, which converts pyruvate to acetate, to prevent a potential futile cycle.

5.2.2 Evolution of NOG strain

Xpk is required to make acetylphosphate (AcP) using NOG. However, Fpk alone failed to rescue growth in the glycolysis knockout strain. To diagnostic the limitation of NOG growth, we split the pathway into two parts: glucose to acetyl-CoA and from acetyl-CoA to pyruvate. To test the ability of Fpk enzyme activity to supply acetyl-CoA from glucose, we cloned Fpk on the plasmid pIB29n and transformed this plasmid to an acetyl-CoA auxotroph strain JCL301 (Δ*aceE* Δ*poxB* Δ*pflB*). Figure 5.3 shows Xpk overexpression can rescue JCL301, suggesting that our first part of the pathway is functional. We then integrated Xpk into our NOG strain, resulting PHL13 (Δ*gapA* Δ*mgsA* Δ*zwf* Δ*pgk-gapB* Δ*pfkA* Δ*iclR* Δ*edd-eda*::$P_{L\text{-}lacO}$::Fpk ΔP_{pgk}::$P_{L\text{-}lacO}$). PHL13 could not grow on glucose minimal medium.

We first adapted PHL13 to be able to grow on glucose minimal medium with extra acetate (Fig. 5.4A). PHL13*-9 and PHL PHL13*-10 (Fig. 5.5A) were isolated from the evolved culture. The amount of acetate strictly limited the growth (OD_{600} at stationary phase) of the PHL13*-9 and

PHL PHL13*-10 (Fig. 5.5B), resulting acetyl-CoA auxotroph strains. We continued to carry out the evolution carried out using serial dilutions with decreasing acetate concentrations. However, we could not evolve these two strains grown on M9 + glucose medium.

5.2.3 Elucidating pitfalls in NOG growth

After the failure of evolution, we sought to determine the imitating steps for growth. One particular problem observed was the glucose uptake. HPLC analysis showed that there was no significant sugar utilization while acetate was consumed completely during the growth on glucose + acetate. This phenomenon could be attributed to either an inactive sugar transportation system or to bottlenecks in the pathway from glucose to AcP.

PTS system might be dysfunctional in our NOG strain because of insufficient phosphoenolpyruvate (PEP) supply. On the other hand, *E. coli* hexose transporter galactose permease (GalP) and hexokinase gluc okinase (Glk) have already been shown to restore the glucose uptake in *ptsI* knockout strain (Fig. 5.6).

In addition, to identify where are the bottlenecks in the pathway, we developed an *in vitro* pathway assay using PHL12 (Δ*gapA* Δ*mgsA* Δ*zwf* Δ*pgk-gapB* Δ*pfkA* Δ*iclR* Δ*edd-eda*::$P_{L\text{-}lacO}$::Fpk ΔP_{pgk}::$P_{L\text{-}lacO}$ Δ*ack*) strain. This assay measures AcP formation from fructose 6-phosphate (F6P). First, we hypothesized that the pentose phosphate pathway were limiting so we overexpressed Tal, Tkt and Rpe in addition to Fbp using pPL94. Using PHL12/pPL94 crude extra, we were able to identify Fpk as the most limiting enzyme for AcP production by addition all eight NOG purified enzymes individually (Fig. 5.7). However, PHL13*/pIB29/ pPL103 (overexpressed Xpk, GalP and Glk) still could not grow on glucose minimal medium. For the NOG strain to grow on glucose, Xpk activity is essential. However, enzyme overexpression sometimes compromised the cell

growth (Li and Liao, 2015). Therefore, we cloned a RBS library to express Xpk (pPL157 library) in PHL13. Few colonies could grow in glucose minimal medium with additional ethanol. However, with two months of evolution, these colonies still could not grow on glucose minimal medium.

5.3 Figures

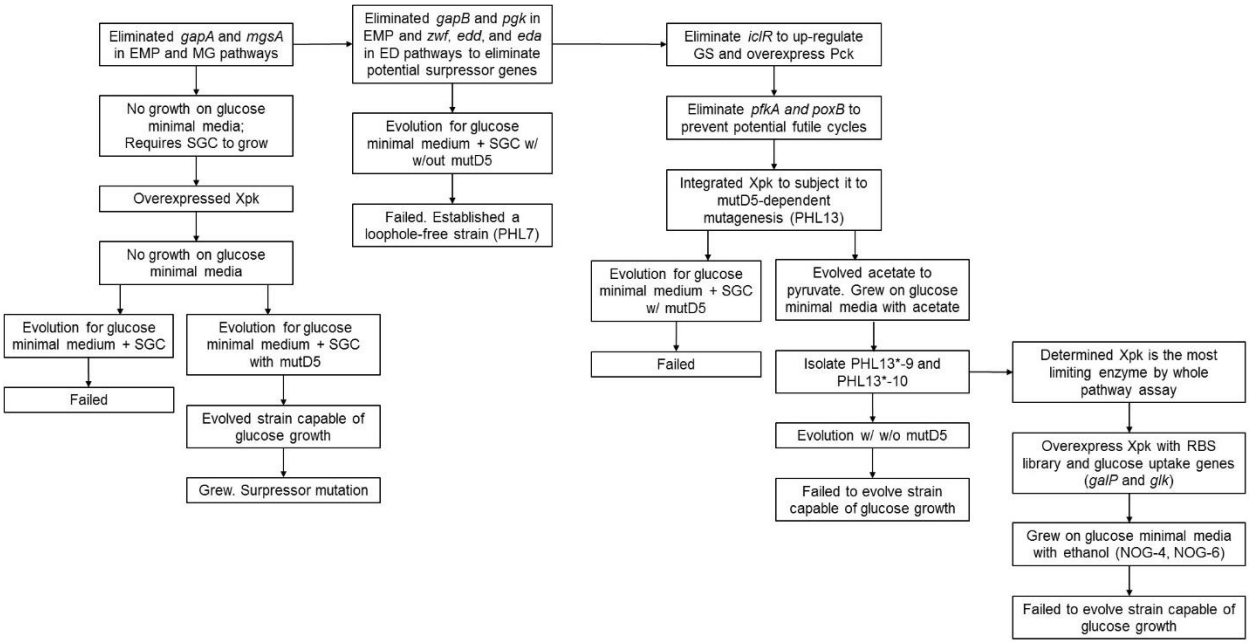

Figure 5-1. NOG strain construction flowchart.

gapA, glyceraldehyde-3-phosphate dehydrogenase; mgsA, methylglyoxal synthase; xpk, phosphoketolase; *gapB*, erythrose 4-phosphate dehydrogenase; *pgk*, phosphoglycerate kinase; *zwf*, glucose-6-phosphate dehydrogenase; *edd*, phosphogluconate dehydratase; *eda*, 2-keto-3-deoxygluconate 6-phosphate aldolase; *iclR*, IclR transcriptional repressor; *pfkA*, 6-phosphofructokinase; *poxB*, pyruvate oxidase. *mutD5*, *E. coli* mutator. SGC, SGC medium (M9 minimal salt with 50 mM succinate, 50 mM glycerol and 3% casamino acid). EMP; Embden-Meyerhof-Parnas. MG, methylglyoxal. ED, Entner–Doudoroff. GS, glyoxylate shunt. RBS, ribosome-binding site.

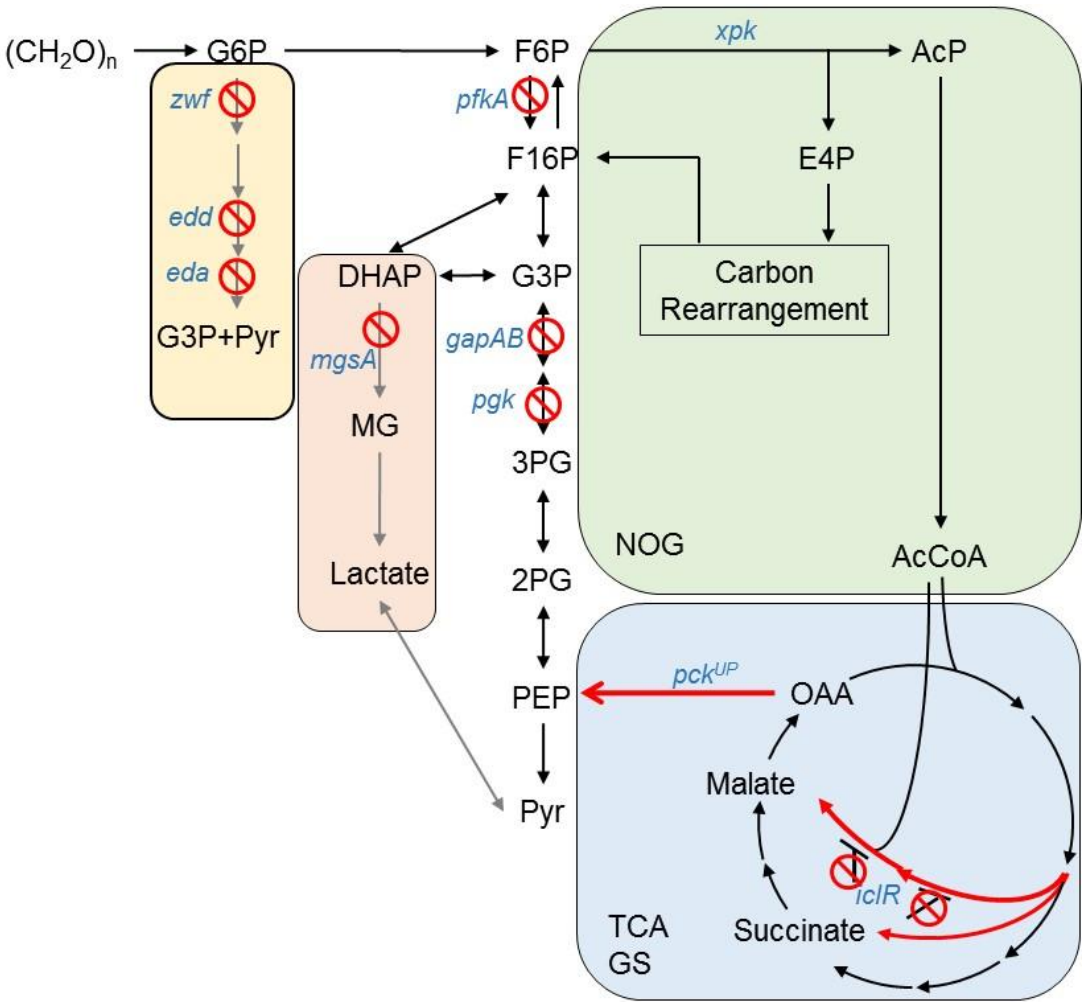

Figure 5-2. NOG strain construction.

Gene knockout are highlighted. Red arrow represents for gene up-regulation. *gapA*, glyceraldehyde-3-phosphate dehydrogenase; mgsA, methylglyoxal synthase; xpk, phosphoketolase; *gapB*, erythrose 4-phosphate dehydrogenase; *pgk*, phosphoglycerate kinase; *zwf*, glucose-6-phosphate dehydrogenase; *edd*, phosphogluconate dehydratase; *eda*, 2-keto-3-deoxygluconate 6-phosphate aldolase; *iclR*, IclR transcriptional repressor; *pfkA*, 6-phosphofructokinase; *poxB*, pyruvate oxidase.

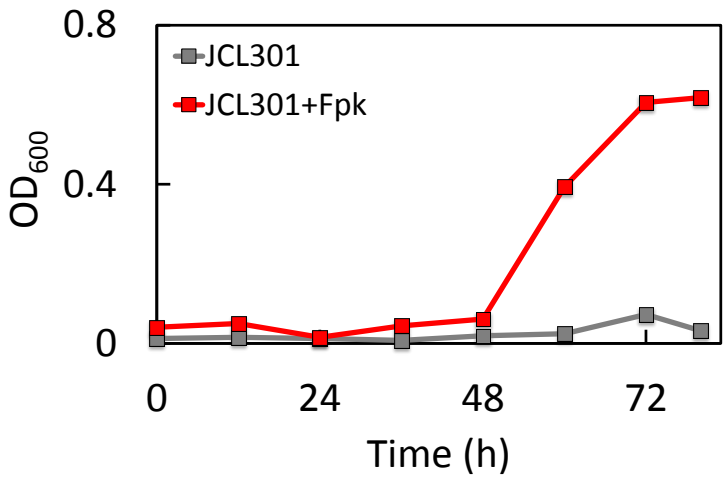

Figure 5-3. Growth curve of an acetyl-CoA auxotroph strain JCL301 (Δ*aceE* Δ*poxB* Δ*pflB*) with and without Xpk overexpressed.

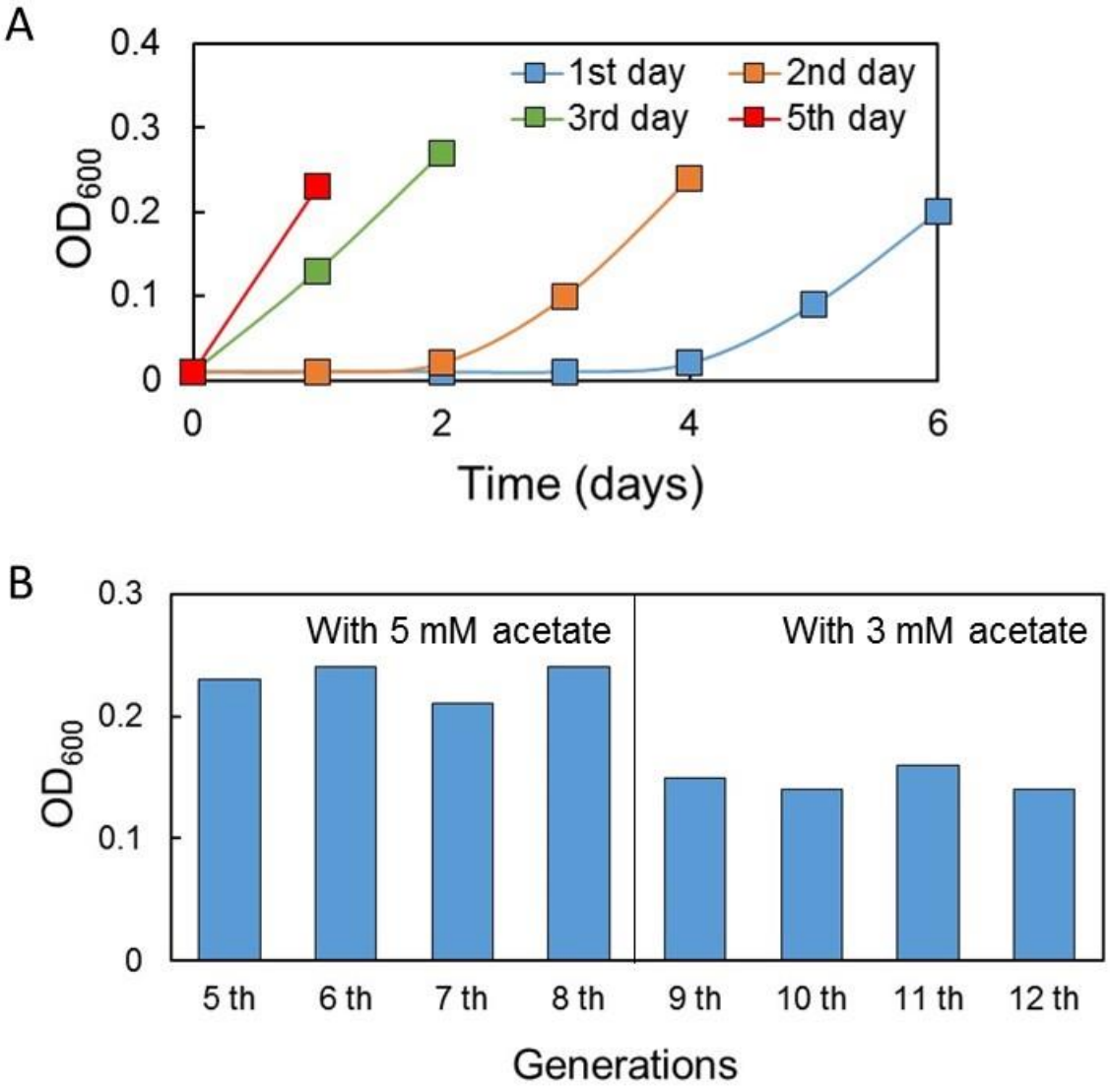

Figure 5-4. (A) Evolution of PHL13 in glucose minimal media with 30 mM acetate and (B) Optical density (OD_{600}) at stationary phase of PHL13* evolved in glucose minimal media with decreased amount of acetate

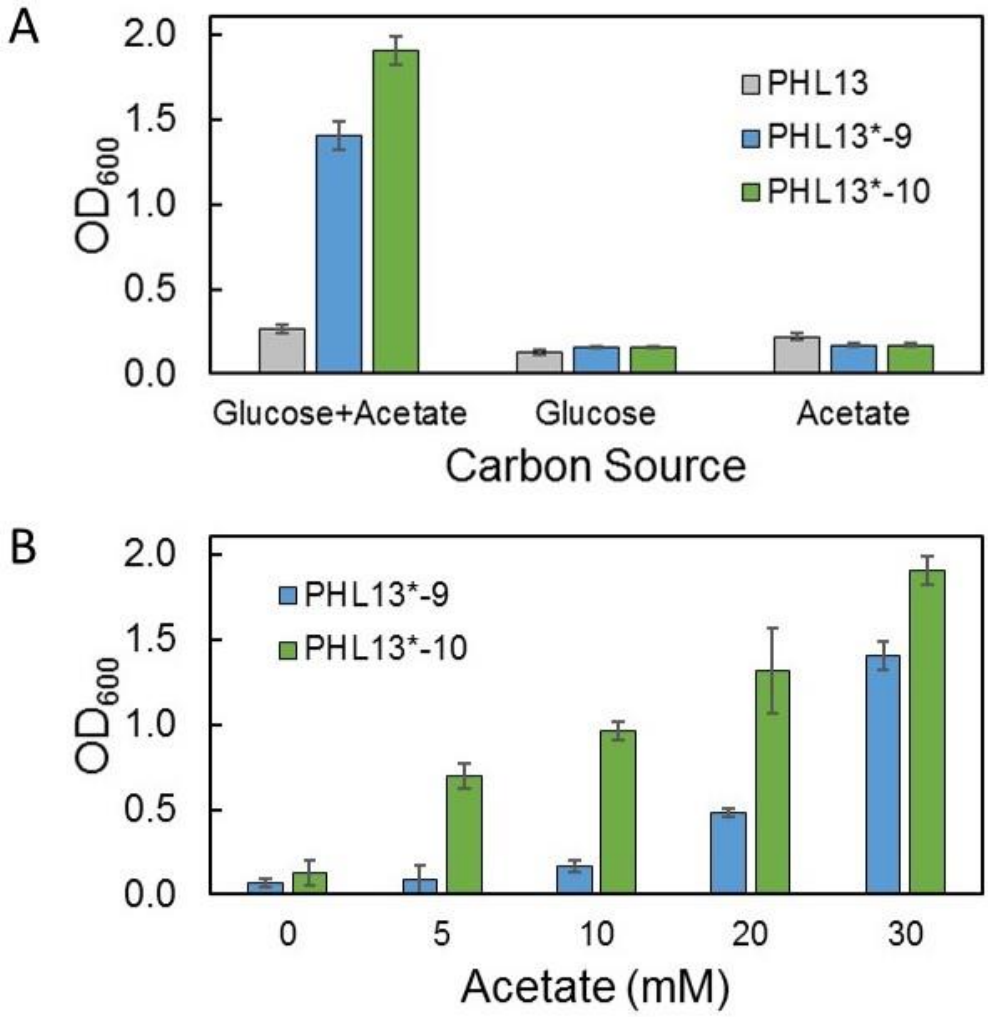

Figure 5-5. (A) Evolution of PHL13 in glucose minimal media with 30 mM acetate and (B) Optical density (OD_{600}) at stationary phase of PHL13* evolved in glucose minimal media with decreased amount of acetate

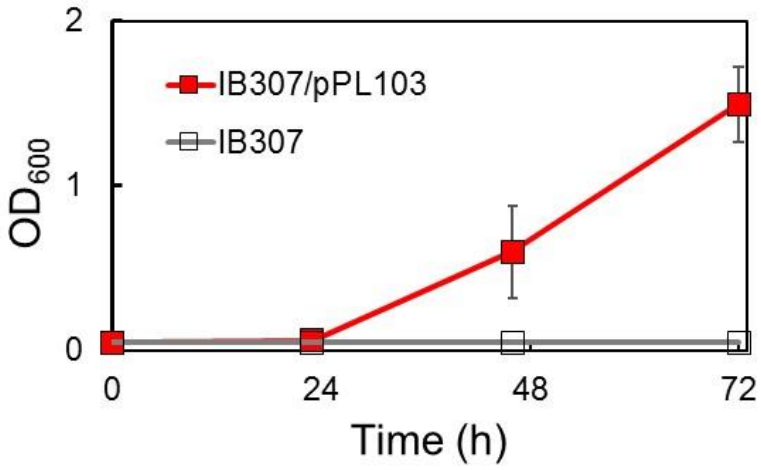

Figure 5-6. Growth curve of IB307 (Δ*ptsI Δglk*) in glucose minimal medium with and without plasmid pPL103 (*galP* and *glk* overexpressed)

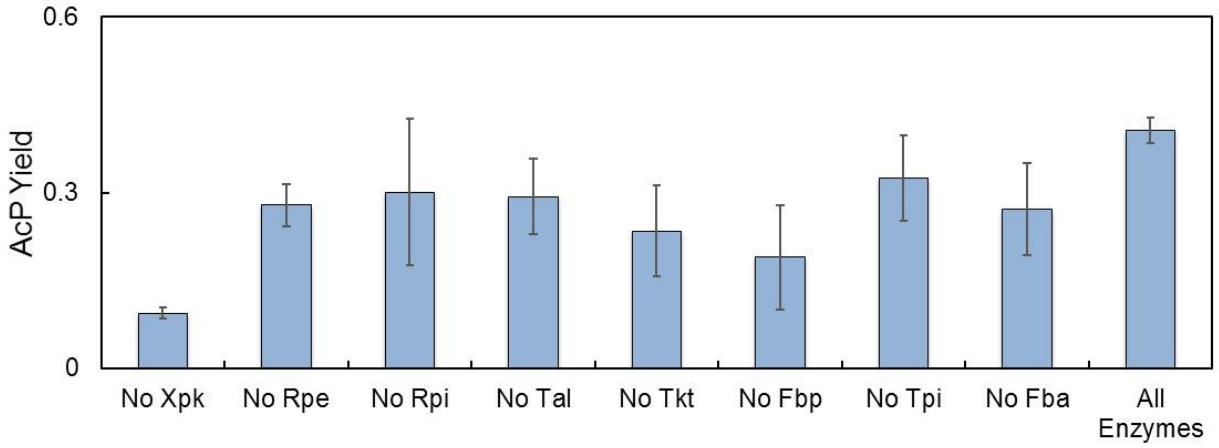

Figure 5-7. Identify limiting enzyme in NOG strain using the whole pathway assay

5.4 Reference

Bogorad, I.W., Lin, T.-S., Liao, J.C., 2013. Synthetic non-oxidative glycolysis enables complete carbon conservation. Nature advance online publication. doi:10.1038/nature12575

Boschi-Muller, S., Azza, S., Pollastro, D., Corbier, C., Branlant, G., 1997. Comparative enzymatic properties of GapB-encoded erythrose-4-phosphate dehydrogenase of Escherichia coli and phosphorylating glyceraldehyde-3-phosphate dehydrogenase. J. Biol. Chem. 272, 15106–15112.

Damagnez, V., Doutriaux, M.P., Radman, M., 1989. Saturation of mismatch repair in the mutD5 mutator strain of Escherichia coli. J Bacteriol 171, 4494–4497.

Irani, M.H., Maitra, P.K., 1976. Glyceraldehyde 3-P dehydrogenase, glycerate 3-P kinase and enolase mutants of Escherichia coli: Genetic studies. Molec. gen. Genet. 145, 65–71. doi:10.1007/BF00331559

Li, H., Liao, J.C., 2015. A Synthetic Anhydrotetracycline-Controllable Gene Expression System in Ralstonia eutropha H16. ACS Synth. Biol. 4, 101–106. doi:10.1021/sb4001189

Martinez-Gomez, K., Flores, N., Castaneda, H.M., Martinez-Batallar, G., Hernandez-Chavez, G., Ramirez, O.T., Gosset, G., Encarnacion, S., Bolivar, F., 2012. New insights into Escherichia coli metabolism: carbon scavenging, acetate metabolism and carbon recycling responses during growth on glycerol. Microb Cell Fact 11, 46. doi:10.1186/1475-2859-11-46

Schaaper, R.M., 1988. Mechanisms of mutagenesis in the Escherichia coli mutator mutD5: role of DNA mismatch repair. PNAS 85, 8126–8130.

Schaaper, R.M., Radman, M., 1989. The extreme mutator effect of Escherichia coli mutD5 results from saturation of mismatch repair by excessive DNA replication errors. EMBO J 8, 3511–3516.

Seta, F.D., Boschi-Muller, S., Vignais, M.L., Branlant, G., 1997. Characterization of Escherichia coli strains with gapA and gapB genes deleted. J. Bacteriol. 179, 5218–5221.

Waegeman, H., Beauprez, J., Moens, H., Maertens, J., De Mey, M., Foulquié-Moreno, M.R., Heijnen, J.J., Charlier, D., Soetaert, W., 2011. Effect of iclR and arcA knockouts on biomass formation and metabolic fluxes in Escherichia coli K12 and its implications on understanding the metabolism of Escherichia coli BL21 (DE3). BMC Microbiol. 11, 70. doi:10.1186/1471-2180-11-70

Yomano, L.P., York, S.W., Shanmugam, K.T., Ingram, L.O., 2009. Deletion of methylglyoxal synthase gene (mgsA) increased sugar co-metabolism in ethanol-producing Escherichia coli. Biotechnol Lett 31, 1389–1398. doi:10.1007/s10529-009-0011-8